Geologic Investigations of the 1988 Tennant Creek, Australia, Earthquakes—Implications for Paleoseismicity in Stable Continental Regions

U.S. GEOLOGICAL SURVEY BULLETIN 2032–A

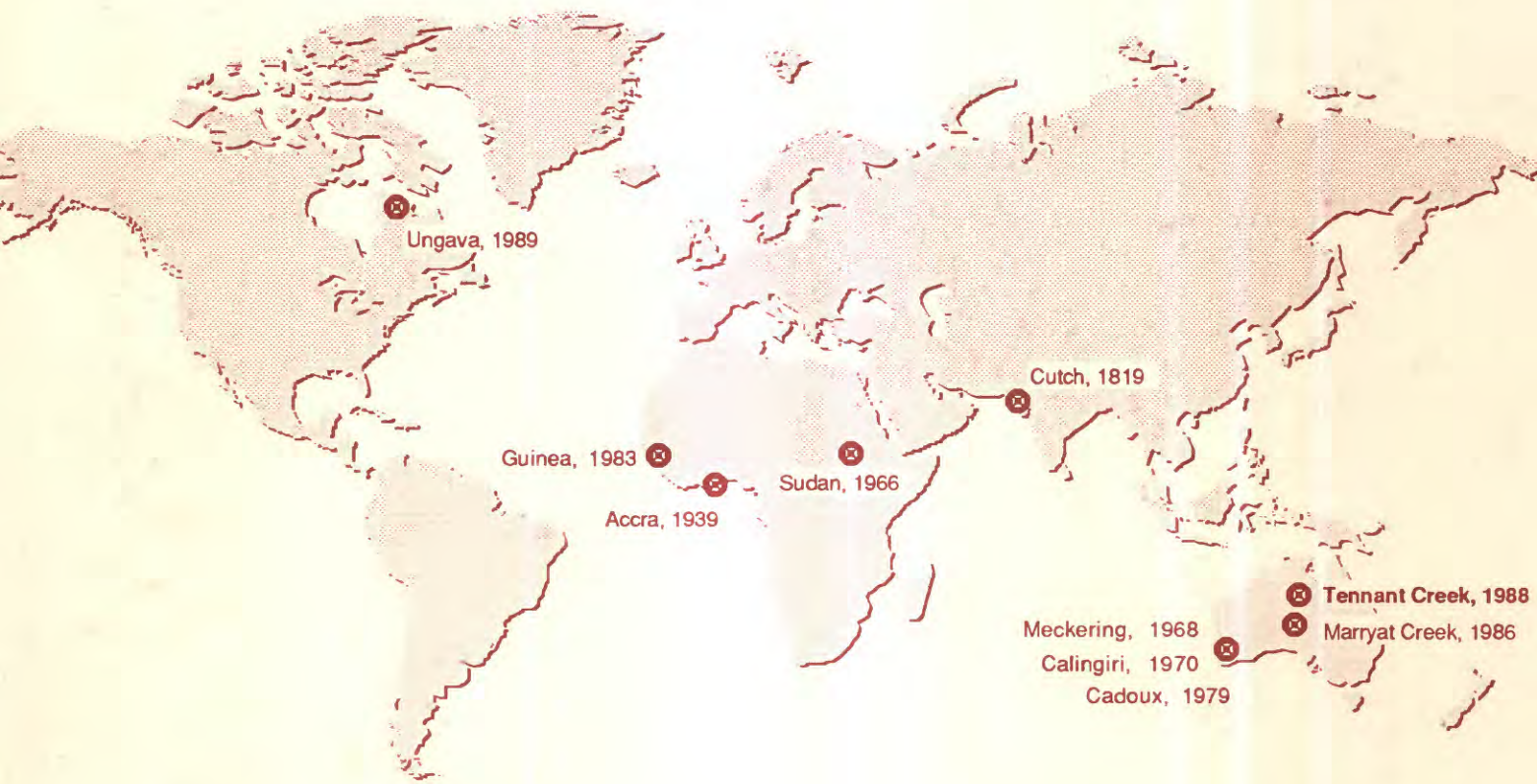

Cover: Global map showing the location of the 10 historical earthquakes that have caused surface faulting in the stable interior of continents.

Geologic Investigations of the 1988 Tennant Creek, Australia, Earthquakes—Implications for Paleoseismicity in Stable Continental Regions

By ANTHONY J. CRONE, MICHAEL N. MACHETTE, *and* J. ROGER BOWMAN

PALEOSEISMOLOGICAL STUDIES IN AUSTRALIA

U.S. GEOLOGICAL SURVEY BULLETIN 2032–A

Investigations of the paleoseismology, deformation, and Quaternary stratigraphy associated with reverse faulting caused by three major earthquakes in the interior of the Australian craton

UNITED STATES GOVERNMENT PRINTING OFFICE, WASHINGTON : 1992

U.S. DEPARTMENT OF THE INTERIOR
MANUEL LUJAN, JR., Secretary

U.S. GEOLOGICAL SURVEY
Dallas L. Peck, Director

For sale by the Books and Open-File Reports Section
U.S. Geological Survey
Federal Center, Box 25286
Denver, CO 80225

Library of Congress Cataloging-in-Publication Data

Crone, Anthony J.
Geologic investigations of the 1988 Tennant Creek, Australia, earthquakes— implications for paleoseismicity in stable continental regions : investigations of the paleoseismology, deformation, and Quaternary stratigraphy associated with reverse faulting caused by three major earthquakes in the interior of the Australian craton / by Anthony J. Crone, Michael N. Machette, and J. Roger Bowman.
p. cm. — (U.S. Geological Survey bulletin)
(Paleoseismological studies in Australia)
1. Faults (Geology)—Australia—Tennant Creek Region (N.T.) 2. Earthquakes—Australia—Tennant Creek Region (N.T.) 3. Geology—Australia—Tennant Creek Region (N.T.) 4. Geology, Stratigraphic—Quaternary. 5. Seismology—Australia—Tennant Creek Region (N.T.) I. Machette, Michael N. II. Bowman, J. Roger. III. Title. IV. Series. V. Series: Paleoseismological studies in Australia. VI. Series: Paleoseismological studies in Australia.
QE75.B9
[QE606.5.A8]
557.3 s—dc20 92-20137
[551.2'2'0994295] CIP

CONTENTS

PLATES

[Plates are in pocket]

FIGURES

TABLES

GEOLOGIC INVESTIGATIONS OF THE 1988 TENNANT CREEK, AUSTRALIA, EARTHQUAKES—IMPLICATIONS FOR PALEOSEISMICITY IN STABLE CONTINENTAL REGIONS

By ANTHONY J. CRONE, MICHAEL N. MACHETTE, *and* J. ROGER BOWMAN[1]

ABSTRACT

Within 12 hours on January 22, 1988, three major earthquakes with surface-wave magnitudes (M_s) of 6.3, 6.4, and 6.7 struck the Tennant Creek area, Northern Territory, Australia. The earthquakes produced surface ruptures along two major fault strands that have a total length of about 32 km (kilometers). Individual ruptures are 6.7 to 16.0 km long and are characterized by north- and south-directed folds and reverse fault scarps. The longest ruptures are along the Lake Surprise scarp, a convex-to-the-north, boomerang-shaped scarp along which the sense of throw changes along strike. The eastern part of the Lake Surprise scarp has a general strike of 115° and a south-over-north sense of throw. In contrast, the western arm of this scarp generally strikes 245° and has a north-over-south sense of throw. Lake Surprise, a 1-km-wide playa, is 3.5 km west-southwest of the apex of the Lake Surprise scarp and is a few hundred meters west of where the sense of throw changes direction. The second fault strand is marked by the Kunayungku scarp, which is about 7 km northwest of Lake Surprise. The Kunayungku scarp is 10.2 km long, strikes 290°, and has a south-over-north sense of throw. The seismological data suggest that the Kunayungku strand ruptured first, and the rupture produced mainly folds with minor scarps. The second earthquake occurred along the western arm of the Lake Surprise scarp, which coincides with a 5-km-long quartz ridge. This scarp has the only evidence of prior Quaternary rupturing. The last and largest of the three earthquakes produced the rupture along the eastern Lake Surprise scarp where the largest scarps formed (about 1.8 m high).

We excavated four trenches across the 1988 ruptures to determine the prehistoric activity of these faults and to characterize the style of the historical near-surface deformation. The trenching shows that the 1988 ruptures are associated with reverse faults that dip 25°±5° in the shallow subsurface. The stratigraphy typically exposed in the trenches consists of Proterozoic bedrock at the base, Miocene(?) to Quaternary(?) ferricrete on the bedrock, and late Pleistocene eolian sand that forms the modern ground surface. The 1.5- to 3-m-thick sand preserves intricate details of the 1988 deformation. Thermoluminescense (TL) dating indicates that deposition of the sand started about 50,000±4,000 yr (years) ago and continued into the Holocene.

Trenches across the Kunayungku and eastern Lake Surprise scarps exposed no stratigraphic or structural evidence of Quaternary movement, whereas two trenches across the western Lake Surprise scarp revealed a buried bedrock scarp that is inferred to be a Quaternary fault scarp. This scarp was buried by eolian sand, and the burial implies that the scarp formed more than 50,000 yr ago. The stratigraphy in the trenches indicates that the last earthquake sequence involving rupture of all three sections of the 1988 scarps occurred more than 50,000 yr ago. Thus, the recurrence of surface-rupturing earthquakes on these faults is at least several tens of thousands of years and could be hundreds of thousands of years or more.

The Tennant Creek earthquakes occurred in the interior of the tectonically stable Precambrian shield of the Australian plate, about 1,500 km from the nearest plate margin. The Tennant Creek earthquakes join a group of only nine other historic intraplate earthquakes in the world that have produced documented surface ruptures in stable continental interiors. These investigations of historical intraplate faulting at Tennant Creek, companion studies of the 1986 ruptures at Marryat Creek, Australia, and limited paleoseismologic data on the Meers fault in the United States suggest that faults in this kind of tectonic setting have long time intervals between surface ruptures. Therefore, the concept of recurrence intervals may not be appropriate in describing these faults. Perhaps hazard assessments in stable continental interiors should be based on a random earthquake that can occur at any time on a suitably oriented fault,

[1]Australian National University, Canberra, ACT, Australia; now at Australian Seismological Center, Bureau of Mineral Resources, Geology and Geophysics, Canberra, ACT, Australia.

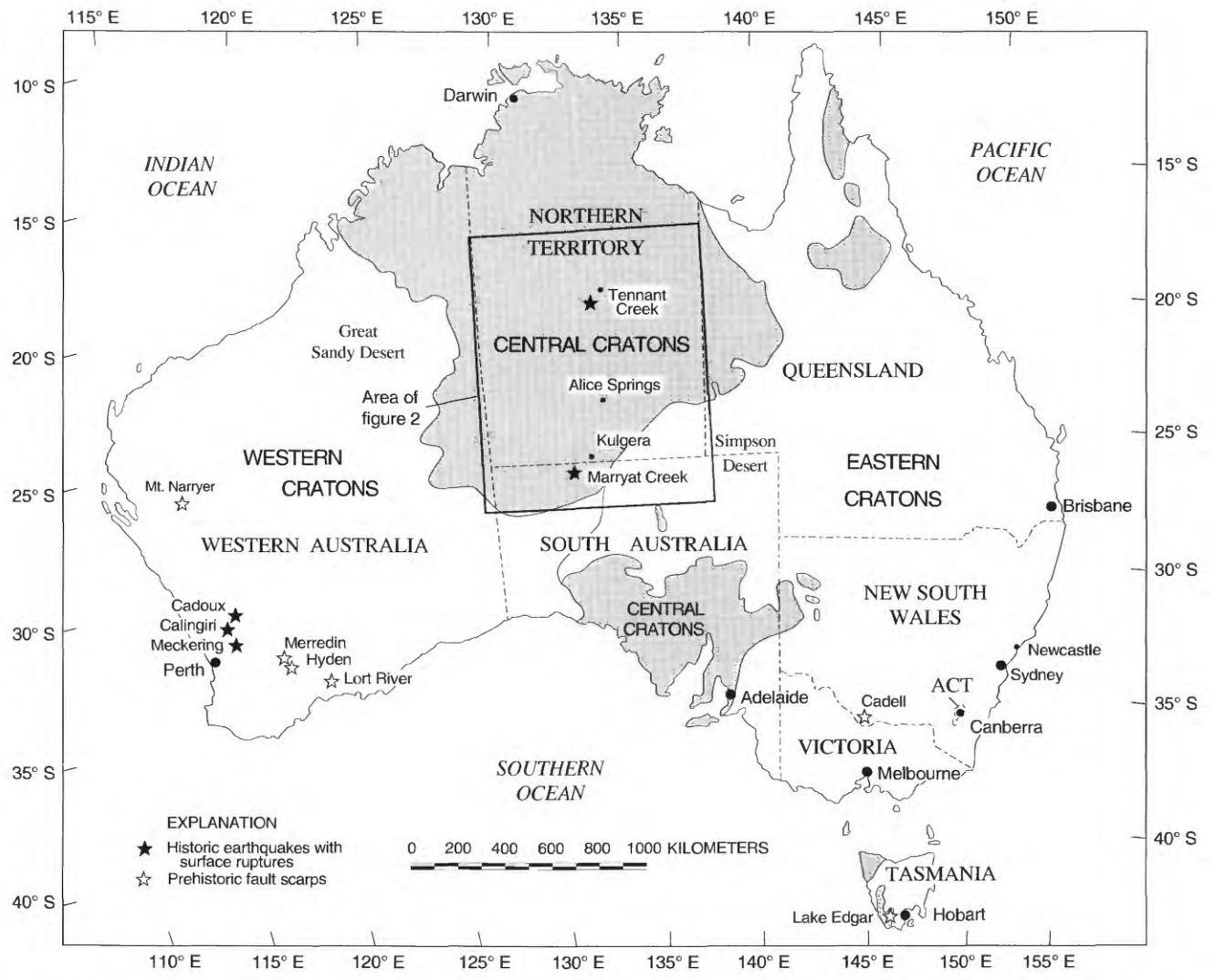

Figure 1. Index map of Australia showing features mentioned in the text and the location of historic earthquakes that produced surface ruptures and prehistoric fault scarps. Shaded areas show extent of the Central Cratons province (modified from Palfreyman, 1984). The map uses the Bonne projection.

rather than only on faults having demonstrable Quaternary movement.

INTRODUCTION

At 10:06 a.m. local time on the morning of January 22, 1988, the remote mining town of Tennant Creek in the Northern Territory of Australia (fig. 1) was shaken by a M_s 6.3 earthquake. In the next 20 hours, two more major earthquakes (M_s 6.4 and 6.7) and a large aftershock (M_s 5.0) rattled the town, continued to alarm the residents, but did little damage. The earthquakes produced about 32 km of surface rupture in an essentially unpopulated area of arid to semiarid rangeland about 30 km southwest of the town of Tennant Creek (fig. 2, pl. 1*A*). Soon after the earthquakes, some trees, bushes, and bunch grass (*Spinifex triodia sp.*) along the ruptures died because their roots were severed by faulting. The 1988 fault scarps are still in pristine condition and have escaped significant cultural modification because of their remote location and the dry climate (459 mm (millimeters)/yr of rainfall in Tennant Creek) (fig. 3). Earthquakes that produce surface ruptures in the interior of continental plates, such as the Tennant Creek earthquakes, are rare, and because of their rarity little is known about the long-term activity of the faults associated with these infrequent earthquakes. This report summarizes the results of our efforts to document the timing of the last prehistoric movement on the faults that ruptured during the 1988 Tennant Creek earthquake sequence, to characterize the style of faulting, and to describe the surficial features produced by the 1988 earthquakes.

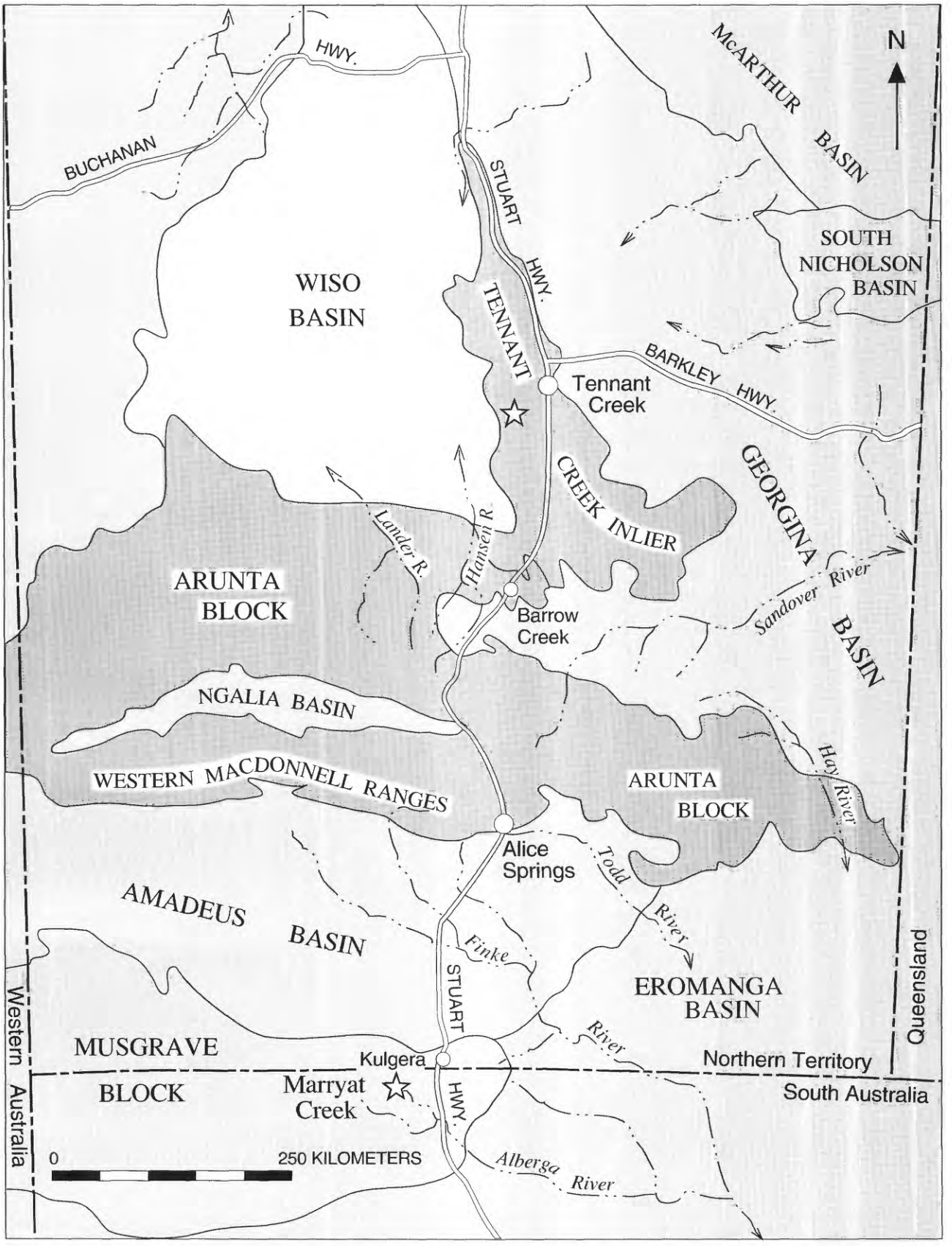

Figure 2. Index map of the Tennant Creek region showing major Phanerozoic basins and basement provinces (blocks) in the southern part of the Northern Territory and adjacent South Australia (modified from Kennewell and Huleatt, 1980). Epicentral locations of Marryat Creek (1986) and Tennant Creek (1988) earthquakes are shown by stars.

Figure 3. Aerial view of fault scarps along the eastern part of the Lake Surprise scarp, Tennant Creek area, showing typical sinuous trace. The single-track road marks the position of the NT Gas pipeline, which is buried a few meters below the surface at this locality. The eastern Lake Surprise trench (ELS) is a few hundred meters to the east (left) of the road. Single-track road is 2–3 m wide. View is to the south-southeast.

INTRAPLATE EARTHQUAKES

The Tennant Creek earthquakes occurred in the interior of the tectonically stable Precambrian shield of the Australian plate (fig. 1), about 1,500 km from the nearest plate margin. The Tennant Creek earthquakes are one of only ten historic intraplate earthquakes in stable continental interiors in the world that have produced documented surface ruptures. The superb preservation of the fault scarps and the excellent seismological data from the Tennant Creek earthquakes offer a rare opportunity to characterize the activity of seismogenic faults in the interior of stable continental plates. In this report we use the term "seismogenic" to describe faults that are capable of generating damaging earthquakes.

Earthquakes are commonly classified into two broad categories based on their general tectonic setting: Interplate earthquakes that occur along or near the margins of lithospheric plates, and intraplate earthquakes that occur in the interior of plates. The concept of plate tectonics provides the broad geologic framework for understanding the general cause and driving forces that produce interplate earthquakes—most interplate earthquakes are a direct result of the differential movement between adjacent lithospheric plates at their boundaries. In contrast, the tectonic framework and causes of intraplate earthquakes are very poorly understood (Sykes, 1978; Johnston, 1987), even though these earthquakes pose a significant threat to lives and property worldwide (Johnston and Kanter, 1990).

Intraplate earthquakes can be further subdivided by whether their tectonic setting is related to plate-margin interactions (for example, backarc basins) or is distant from plate margins (Scholz and others, 1986) and largely isolated from plate-margin interactions. Earthquakes in the latter places are usually considered to occur in the stable interior of continental plates (Johnston, 1989). On the basis of historical records, it is clear that earthquakes occur in stable continental interiors much less frequently than in interplate settings, but these earthquakes can be extremely damaging for several reasons. First, because they occur infrequently, both the general population and manmade structures are poorly prepared to cope with severe ground motion. As a result, modest-size earthquakes can be very damaging. For example, the

Table 1. Historic earthquakes in Australia that have produced surface ruptures

[M_S, surface-wave magnitude of the earthquake; <, less than; WA, Western Australia; SA, South Australia; NT, Northern Territory]

Date	Location	Magnitude (M_S)	Surface rupture length (km)	Maximum scarp height (m)	Reference
Oct. 14, 1968	Meckering, WA.....	6.8.....	37	3.5	Gordon and Lewis (1980).
Mar. 11, 1970.....	Calingiri, WA.....	5.7.....	3	<0.4	Gordon and Lewis (1980).
June 6, 1979	Cadoux, WA.....	6.4.....	28	<1.4	Lewis and others (1981)
Mar. 30, 1986.....	Marryat Creek, SA	5.8.....	13	<0.8	McCue and others (1987).
Jan. 22, 1988	Tennant Creek, NT	6.3-6.7 (3 events).	32	<2.0	Bowman and others (1990).

Newcastle, Australia (fig. 1), earthquake of December 29, 1989, caused 13 deaths and about A$1.5 billion in damage even though it only had a moderate moment magnitude (M 5.6). Secondly, the strong ground motion generated by major earthquakes ($M \geq 7.5$) in the interior of continental plates may affect significantly larger areas than comparable-size plate-margin earthquakes (Hanks and Johnston, 1992; McKeown, 1982; Nuttli, 1973a, 1973b; Nuttli and Zollweg, 1974). Based on intensity data from historical reports, a recurrence of the great earthquakes that struck the New Madrid, Missouri, region in the winter of 1811–12 could cause damage and injury to an area as much as 20 times larger than the 1906 San Francisco, California, earthquake (about 600,000 km^2 in the New Madrid region versus about 30,000 km^2 in the San Francisco region) (Hamilton and Johnston, 1990).

Efforts to understand the hazards and to reduce the risks from intraplate earthquakes are severely hampered by a nearly complete lack of data on the characteristics of the causative seismogenic faults. The historical record of earthquakes, especially in the central and eastern United States, is far too short and incomplete to accurately represent the long-term activity of intraplate faults. The primary reason for the lack of earthquake-recurrence information is the rarity with which large intraplate earthquakes generate surface faulting. Geological investigations of prehistoric earthquakes that have caused surface rupturing can provide valuable information about the location and magnitude of ancient earthquakes and, thus, insight into the long-term activity of seismogenic faults over geologically meaningful periods of time (many thousands of years).

At present, it is unknown if the recurrence of large earthquakes on intraplate faults in continental interiors is measured in hundreds, thousands, tens of thousands, or even hundreds of thousands of years. This kind of basic information is vital to understanding the mechanics of potentially hazardous intraplate faults. Worldwide, 10 historic earthquakes in stable intraplate settings are known to have produced surface ruptures (A.C. Johnston, written commun., 1990; Johnston and Bullard, 1990). Of the 10 events, 5 were in Australia (fig. 1), all of which occurred since 1968 (table 1). The extraordinary occurrence of surface-rupturing earthquakes in Australia presents a unique opportunity to apply paleoseismologic techniques to historic surface ruptures and, thus, to examine the long-term record of movement on recently active seismogenic faults in a stable intraplate setting. Historic ruptures on the respective faults record the most recent surface-faulting event, whereas paleoseismologic data provide information on the timing of prehistoric ruptures. Combining the historical and paleoseismologic data provides a realistic perspective by which one can gauge the recurrence of major earthquakes on intraplate faults.

The Tennant Creek earthquakes are the most recent to have caused surface faulting in Australia, and the seismological data for the earthquake sequence is perhaps the most comprehensive set for any major ($M \geq 6$) intraplate earthquake in the world. The seismological data provide invaluable insight into the characteristics of the rupture process at hypocentral depths and the downdip geometry of the seismogenic faults (Choy and Bowman, 1990). However, the insight derived from the seismological data is limited to the faulting activity that occurred in 1988 and the few preceding decades for which seismological data are available. To develop a more complete geological perspective of the long-term activity of the faults, we used paleoseismologic techniques to investigate the Quaternary history of surface-rupturing earthquakes. Much of our geological data was obtained from four exploratory trenches across the 1988 scarps; the trenches also revealed details about the style and characteristics of the near-surface deformation. This study

and a companion paleoseismologic study of the 1986 ruptures at Marryat Creek, South Australia, (fig. 2) (Machette, Crone, and Bowman, unpub. data, 1990) offer new geological data to characterize the activity of earthquake-generating faults in the interior of continental plates.

ACKNOWLEDGMENTS

Support for this study was provided primarily by a U.S. Geological Survey-sponsored G.K. Gilbert Fellowship to Crone and Machette. We gratefully acknowledge the support provided by this program. Bowman's research was partly supported by the Electric Power Research Institute (EPRI) in Palo Alto, Calif. The cooperation and logistical support offered by the Research School of Earth Sciences of the Australia National University (ANU) were vital to the successful completion of our Australian field studies. Equally important to the success of our fieldwork was the constant cooperation and generous support we received from Peter Robinson, Brian Ferguson, and Cameron Hughes of ANU's Warramunga Seismic Station in Tennant Creek. We greatly appreciate their enthusiastic assistance. We also thank Mick Hayes, manager of the Tennant Creek Station, for allowing us access to the station and for permission to excavate our trenches.

We wish to thank John Prescott of the Department of Physics and Mathematical Physics, University of Adelaide, Adelaide, South Australia, and Kazuhiro Tanaka of the Central Research Institute of Electric Power Industry, Abiko City, Japan, for assisting us in the field and for providing age control using TL and electron-spin resonance (ESR) dating, respectively. Peter MacDonald and Ralph Northy (Water Resources Branch, Australian Water and Power Authority, Alice Springs, Northern Territory), and John Love (consulting geologist, Tennant Creek) participated in helpful discussions and offered observations in the field. We appreciate the thoughtful, perceptive reviews and comments by Arch C. Johnston (Center for Earthquake Research and Information, Memphis State University) and Daniel R. Muhs (U.S. Geological Survey), which improved the clarity and presentation of this report.

THE 1988 TENNANT CREEK EARTHQUAKE SEQUENCE

The Tennant Creek earthquakes on January 22, 1988, consisted of three major shocks (M_s 6.3, 6.4, and 6.7) that struck within a period of 12 hours (Bowman, 1988; Bowman and others, 1990; Choy and Bowman, 1990). The earthquakes produced surface ruptures along two major fault strands that have a total length of about 32 km (pl. 1*A*). The longest strand is the Lake Surprise scarp, a convex-to-the-north, boomerang-shaped scarp that changes sense of throw along strike. The eastern part of the Lake Surprise scarp has a general strike of 115° and a down-to-the-north throw. In contrast, the western part of the scarp generally strikes 245° and has a down-to-the-south throw. Lake Surprise, a 1-km-wide playa, is 3.5 km west-southwest of the apex of the Lake Surprise scarp and is a few hundred meters west of where the sense of throw changes direction. The second strand of the fault (the Kunayungku scarp) is about 7 km northwest of Lake Surprise and consists of a 10.2-km-long scarp that strikes 290° and has down-to-the-north throw.

Prior to 1987, the region around Tennant Creek was virtually aseismic. No instrumentally recorded or historically felt earthquakes of magnitude 5 or greater had occurred within 500 km of Tennant Creek, and only a few local earthquakes of smaller magnitude had been instrumentally recorded in the area (Bowman, 1988). In 1965, the Warramunga Seismic Array, a seismic network operated by the Australian National University, was installed about 30 km southeast of Tennant Creek for monitoring nuclear explosions in the circum-Pacific region. It was strictly coincidence that this high-gain, short-period network was located adjacent to the area that was affected by the 1988 events. In retrospect, the network provided excellent and sensitive records of precursory earthquake activity. However, it is sometimes difficult to distinguish between earthquakes and artificial blasts from mining in the Tennant Creek area. A review of local seismic activity from the network's bulletins and array's seismograms shows that there were only two unequivocal earthquakes (in contrast to mining-related explosions) in the 20 yr of the array's operation preceding the onset of earthquakes in the Tennant Creek area (Bowman, 1988).

Detailed information on the faulting process and the sequence of events for the Tennant Creek earthquakes is mainly derived from seismological data. Much of this information is from focal mechanisms and waveform analyses by the National Earthquake Information Center (1988), Chung and others (1988), McCaffrey (1989), and Choy and Bowman (1990). The seismological data cannot unambiguously relate the first and second main shocks to specific sections of scarps. In the following discussion, we mainly use the sequence of events proposed by Choy and Bowman (1990), but also comment on alternative interpretations proposed by McCaffrey (1989).

The first indication of the impending surface-rupturing events was an earthquake swarm that began on January 5, 1987, in the area struck by the main shocks a year later. The swarm included six events with body-wave magnitude (m_b) of 4 to 5.2 (local magnitude—M_L 4.9–5.4) and about 1,100 aftershocks. This swarm was marked by two peaks of activity, one in January 1987, and a second one 6 months later (Bouniot and others, 1990). The number of aftershocks in this sequence gradually diminished until the first main shock of the 1988 earthquake sequence, which occurred on the morning of January 22. In retrospect, the

Table 2. Parameters for main shocks of the January 22, 1988, Tennant Creek earthquake sequence

[Data from National Earthquake Information Center (1988), Choy and Bowman (1990), and Bowman and Dewey (1991). Rupture lengths as measured from plate 1*A* are inferred from propagation direction, direction of reverse faulting, and mapped trace of faults. M_s, surface-wave magnitude; m_b, body-wave magnitude; UT, Universal time]

Time (UT and local)	Latitude (south)	Longitude (north)	Magnitudes	Seismic moment ($\times 10^{25}$ dyne-cm)	Depth and focal mechanism	Remarks
0036:00 10:06 a.m.	19°49'48"	133°55'37"	M_s=6.3 m_b=6.1	2.9	6.5 km; NNE reverse.	10.2-km-long rupture; unilateral to the northwest.
0357:27 01:27 a.m.	19°48'25"	133°55'12"	M_s=6.4 m_b=6.1	5.2	3-3.5 km; S oblique reverse.	6.7- and 3.1-km-long ruptures; no resolvable directivity.
1205:00 09:35 p.m.	19°50'42"	133°56'53"	M_s=6.7 m_b=6.5	8.3	4.5 km; NNE reverse.	16.0-km-long rupture; unilateral to the southeast.

1987 swarm is now regarded as a precursory sequence to the 1988 surface-rupturing events because the number of earthquakes associated with the 1987 swarm diminished at an anomalously slow rate (Bowman and others, 1990) and because the 1987 earthquakes occurred between two areas that would rupture in 1988 (Bowman and Dewey, 1991). This precursory series is attributed to the failure of small asperities on the eastern margin of the Kunayungku fault (Choy and Bowman, 1990; Bowman and Dewey, 1991), which eventually ruptured during the 1988 events.

The first of the three Tennant Creek main shocks struck at 0036:00 Universal time (UT). It was composed of three subevents, and had an M_s of 6.3 and an m_b of 6.1 (table 2). Of the two focal-mechanism nodal planes, we prefer the plane that indicates north-directed reverse motion on a fault that strikes 100°, dips 35° S., and has nearly pure dip-slip motion. The event nucleated at a depth of 6.5 km near the eastern end of the Kunayungku fault and ruptured to the northwest (pl. 1*A*). This earthquake probably created the Kunayungku scarp, based on its location with respect to all of the 1988 scarps and the directivity of the rupture (Bowman, 1988; McCaffrey, 1989; Choy and Bowman, 1990). The entire scarp is 10.2 km long measured along the trace of the scarp and 9.7 km long measured from end to end (pl. 1*A*). Six minutes before the first major earthquake, a foreshock of duration magnitude (M_D) 3.6 occurred in the gap between the Kunayungku and Lake Surprise scarps.

The second main shock (M_s 6.4; m_b 6.1) occurred about 3.5 hours later (0357:27 UT, table 2) and released almost twice the seismic moment of the first event. The second main shock probably produced the rupture along the western part of the Lake Surprise scarp (pl. 1*A*), which is characterized by south-directed reverse faulting. The southward reverse faulting is associated with a 6.7-km-long scarp, much of which coincides with a prominent quartz ridge (discussed in the following section). In addition, there is a second scarp, 3 km long, parallel to and about 1 km south of the western end of the main scarp (pl. 1*A*). The analysis of broadband wave forms shows that the second earthquake was also composed of three subevents and had a complex rupture process (Choy and Bowman, 1990). Focal mechanisms for the first two subevents show reverse faulting with a moderate component of left-lateral slip on a plane that strikes 051° and dips 32° SE. but does not reach the surface. These subevents nucleated at a depth of only about 3.0–3.5 km. The seismological record of the third subevent is partly obscured by the seismic waves from the preceding subevents.

The seismological data are somewhat ambiguous about which main shock produced the western Lake Surprise scarps. Choy and Bowman (1990) proposed that this scarp was formed by south-directed thrusting on a northwesterly dipping fault plane, which ruptured during the last subevent of the second main shock. However, the focal mechanism for this subevent shows minor right-lateral slip, which is difficult to reconcile with postearthquake field observations that show a consistent pattern of left-lateral displacement (fig. 4, table 3). McCaffrey (1989) offered two explanations for the formation of the western Lake Surprise scarp. One explanation proposes that the scarp formed during the first main shock because the north-dipping nodal plane (with minor left-lateral slip) for this event best fits the attitude of the north-dipping fault. However, the waveforms for the first main shock are better modeled by a south-dipping fault plane (Choy and Bowman, 1990), which is consistent with the morphology of the Kunayungku scarp, not the western Lake Surprise scarp. Thus, we do not favor McCaffrey's

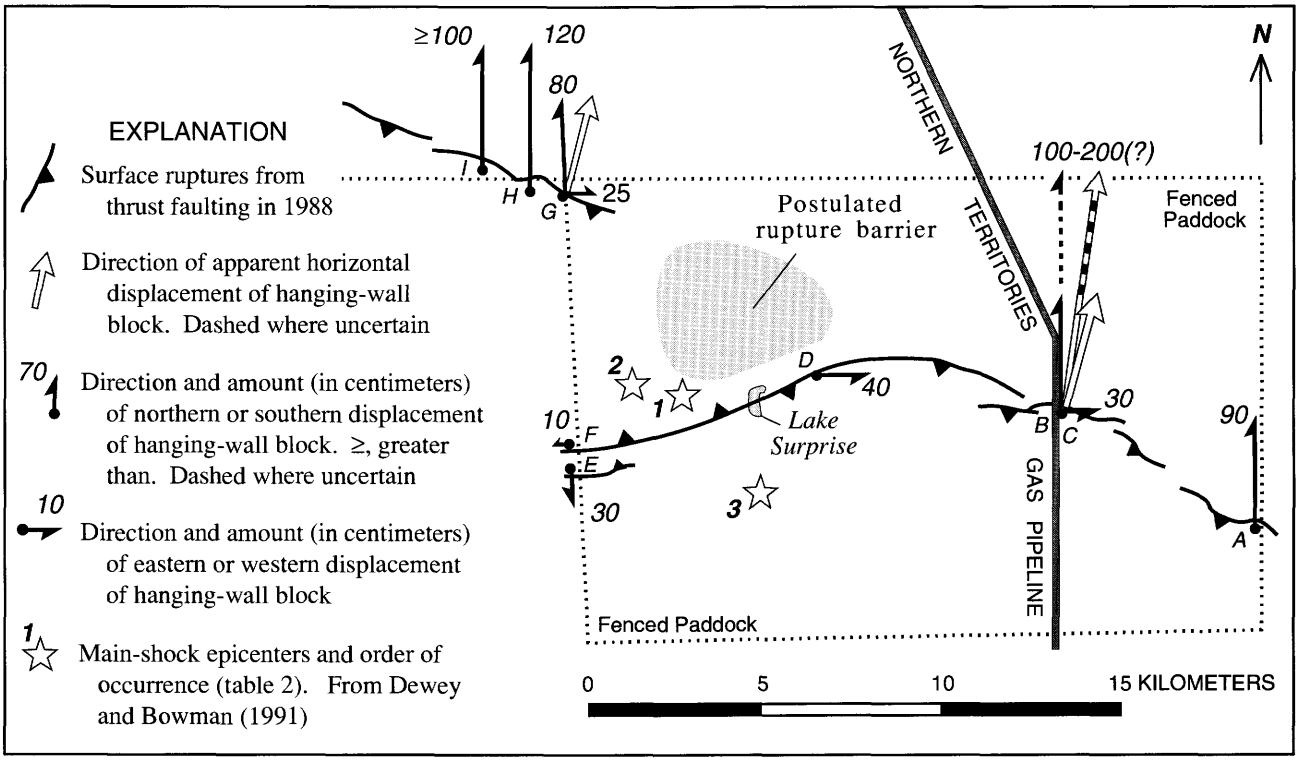

Figure 4. Measured horizontal fault displacements on the Tennant Creek fault scarps. Letters correspond to individual measurements listed in table 3. Displacement values are resolved into north-south and east-west components because measurements were obtained from the offset of cultural features such as fences, which generally trend north-south and east-west.

interpretation. Alternatively, McCaffrey (1989) proposed that the second main shock initiated on a north-dipping fault plane and that the subsequent rupture and the largest moment release occurred on a southeasterly dipping fault plane. This explanation associates the western Lake Surprise scarp with a subsidiary north-dipping fault in the hanging wall of a master south-dipping reverse fault (the Kunayungku and eastern Lake Surprise faults). However, the aftershocks in the central part of the surface ruptures (near the western Lake Surprise scarp) define a northwesterly dipping pattern (Bowman and others, 1990). Other published focal mechanisms (Chung and others, 1988; National Earthquake Information Center, 1988) do not have nodal planes that match the orientation of the western Lake Surprise scarp and the northwestern dip inferred from the distribution of aftershock hypocenters and thus provide little insight about which shock formed the western Lake Surprise scarps. On the basis of the relocated hypocenters (Bowman, 1988), the northwesterly dipping pattern of aftershocks in the central part of the rupture zone (Bowman and others, 1990), and the teleseismic-waveform constraints (McCaffrey, 1989; Choy and Bowman, 1990), we favor Choy and Bowman's interpretation that the western Lake Surprise scarp formed during the second main shock (although it is not clear which subevent ruptured the surface).

The third and final main shock (M_s 6.7; m_b 6.5) had the largest seismic moment of the three shocks (8.3×10^{25} dyne-cm) and was also composed of three subevents. It occurred at 1205:00 UT (table 2), about 8 hours after the second major earthquake. The source parameters for these three subevents are very similar and show reverse faulting on a plane that strikes 100° and dips 45° S. The earthquake nucleated at a depth of 4.5 km and ruptured to the southeast.

The last main shock produced the right-stepping surface rupture along the eastern section of the Lake Surprise scarp, which has a measured length of 16.0 km along its trace (pl. 1*A*). This section of the scarps crosses a 35.6-cm-diameter high-pressure natural-gas transmission pipeline operated by the Northern Territory Gas Proprietary Limited (NT Gas). The surface faulting shortened the pipeline in a north-south direction by nearly 1 m. An aerial survey of the gas transmission line before the third earthquake showed no evidence of surface rupture or damage. Thus, the deformation in the pipeline was related to the third main shock of the sequence.

Collectively, the three main shocks produced three distinctive sections of surface rupture; two sections consist of west-northwesterly trending scarps, the eastern part of the Lake Surprise scarp and the Kunayungku scarp, which are separated by a 7-km-wide gap and which are associated with

Table 3. Estimated horizontal surface displacements for Tennant Creek earthquakes, January 22, 1988

[N, north; S, south; E, east; W, west; LL, left-lateral offset; N.D., not determined; ≥, greater than or equal to; AUSLIG, Australian Surveying and Land Information Group. Sources of data: NT (Northern Territory Gas Proprietary Limited), written commun. to J. R. Bowman, Mar. 14, 1988, and later; JRB, J. R. Bowman, Jan. 25–Feb. 25, 1988]

Symbol on pl. 1A and fig. 4	Location with reference to AUSLIG Station No.	North/south component		East/west component		Source of data
		Feature	Amount (cm) sense	Feature	Amount (cm) sense	
A	At Station 4665	Slack in north-south fence.	90 N	Offset in north-south fence.	N.D.	JRB
B	40 m NE of Station 4655.	Shortening of north-south pipeline.	100-200 N	Bend in north-south pipeline.	N.D.	NT
C	100 m ENE of Station 4655.	Road overthrust	N.D.	Offset in north-south road berm.	30 LL	JRB
D	375 m SW of Station 4900.	Road overthrust	N.D.	Offset in north-south road berm.	40 LL	JRB
E	75 m E of Station 5002	Slack in north-south fence.	30 S	Offset in north-south fence.	N.D.	JRB
F	590 m W of Station 4970.	Offset of cracked termite mound.	N.D.	Offset of cracked termite mound.	10 LL	JRB
G	275 m ESE of Station 4620 (A8).	Slack in north-south fence.	80 N	Offset in north-south road berm.	25 LL	JRB
H	Between Stations 5090 and 2060 (A7).	Offset posts in east-west fence.	120 N	N.D.	N.D.	JRB
I	Near Station 4635 (A6)	Buried tree trunk	≥100 N	N.D.	N.D.	JRB

south-dipping faults (pl. 1*A*). The third section is the southwesterly trending scarp along the western section of the Lake Surprise scarp, which is associated with a north-dipping fault. The largest amount of deformation is along the eastern part of the Lake Surprise scarp where offsets of 1 m are common and are as much as about 1.8 m (fig. 5). In contrast, the surface offset along the Kunayungku and western part of the Lake Surprise scarps is typically 1 m or less. For all three sections of surface rupturing, the predominant style of deformation at the surface is reverse faulting, although some lateral slip was documented locally (fig. 4, table 3).

More than 17,000 aftershocks have been recorded by the Warramunga Seismic Array since the January 22 main shocks (Bowman, in press). The largest aftershock was a m_b 5.8 event that occurred about 9 hours (2054:05 UT) after the third main shock. Other notable large aftershocks occurred on January 29 (m_b 5.5) and September 30, 1988 (m_b 5.2). The aftershock sequence continues, and a magnitude-5.1 aftershock occurred as recently as March 7, 1991. The most abundant aftershocks were near the margins of inferred rupture areas on the faults; the interior of the rupture surfaces was relatively inactive (Bowman and others, 1990). This observation indicates that the coseismic slip largely relieved the accumulated strain energy on the interior parts of the faults and that the stress was transferred to the edges of the rupture areas.

The following hypothesis, which is based largely on the interpretation of Choy and Bowman (1990) and Bowman (in press), summarizes the sequence of events associated with the Tennant Creek earthquakes. The precursory sequence of earthquakes that began in January 1987 was the first indication of the impending release of a large amount of strain energy. The M_D 3.6 foreshock 6 minutes before the first major earthquake signaled the first stages of failure of the Kunayungku fault. The first main shock nucleated about 6.5 km deep near the southeastern end of the south-dipping Kunayungku fault (pl. 1*A*) and ruptured upward and to the northwest. The failure of the Kunayungku fault increased the loading on the ends of the fault and, 3.5 hours later, the increased load stimulated the second main shock, which ruptured the western and central part of the Lake Surprise fault (pl. 1*A*). The second main shock nucleated about 3–3.5 km deep and near the middle of the zone of aftershocks that define a north-dipping fault plane. This earthquake is considered to be the critical event in the series because it had the highest stress drop (136 bars) of the three major earthquakes

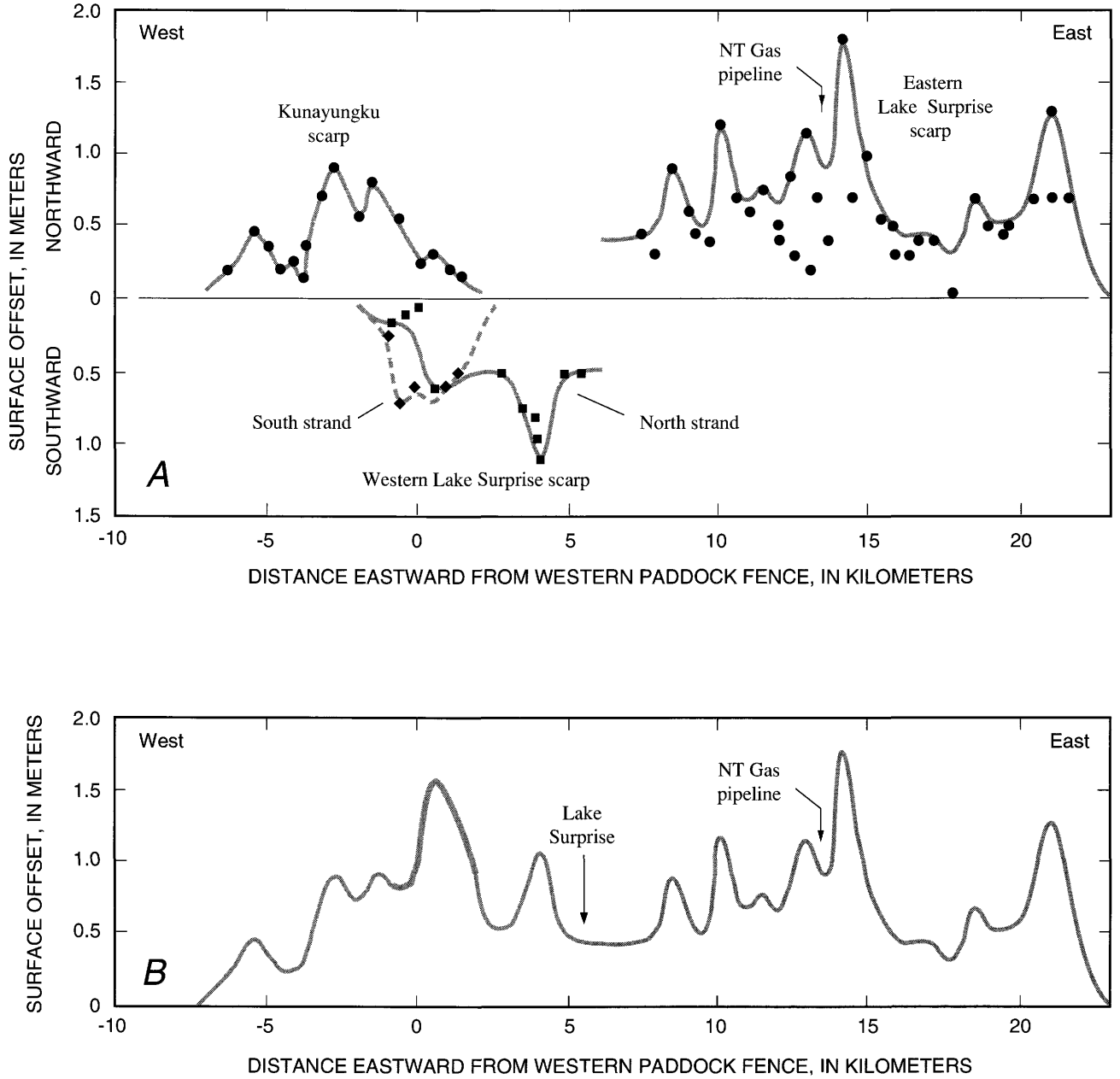

Figure 5. Surface offset on the 1988 Tennant Creek fault scarps versus distance east of the western edge of the paddock. *A*, Surface offset on individual scarps. Solid dots are measurements along the eastern Lake Surprise and Kunayungku scarps, solid squares are measurements along the northern strand of the western Lake Surprise scarp, and solid diamonds are measurements along the southern strand of the western Lake Surprise scarp. Positive values of surface offset indicate offset caused by northward-directed movement, negative values indicate southward-directed movement. See plate 1*A* for map of scarps. Shaded lines show generalized maximum amounts of surface offset. *B*, Net cumulative surface offset of the Kunayungku and Lake Surprise scarps. Values of net cumulative offset were obtained by adding the surface-offset values of north-directed and south-directed scarps together along the Kunayungku and western Lake Surprise scarps. This plot portrays the total amount of surface offset across the system of scarps that was produced by the north-south shortening.

and, therefore, probably ruptured the strongest barrier. If this barrier had not failed, the third earthquake in the series may not have occurred. The failure of the western part of the Lake Surprise fault during the second earthquake shifted stress to the eastern end of the fault, toward the central area between the three scarps. About 8 hours later, the third main shock nucleated at 4.5-km depth at a point about 3 km south of the Lake Surprise fault and ruptured to the east-southeast along the south-dipping fault (pl. 1*A*). The three main shocks were followed by thousands of aftershocks in the immediate area

of the scarps, and moderate-magnitude aftershocks have continued to occur more than 3 yr after the surface faulting. Notably, some of the most recent aftershocks have shifted eastward from the Lake Surprise scarp to the region beneath the Warramunga Seismic Array (Bowman, in press), a shift that probably reflects ongoing adjustments in the surrounding upper crust to the abrupt change in the regional stress field caused by the Tennant Creek earthquakes.

GEOLOGIC SETTING OF THE TENNANT CREEK EARTHQUAKES

The Australian continent is composed of an amalgamation of crustal blocks (Plumb, 1979a) that are broadly grouped into the Western, Central, and Eastern Cratons (fig. 1; Palfreyman, 1984). The Tennant Creek region lies within the Central Cratonic province. The 1988 earthquakes occurred near the border between the Tennant Creek inlier (or block) to the east and the Wiso basin to the west (fig. 2; Palfreyman, 1984; Bowman, in press). The Tennant Creek inlier is composed primarily of Early and Middle Proterozoic marine sedimentary, volcanic, and intrusive rocks. The Wiso basin generally contains less than about 500 m of largely undeformed Middle Cambrian through Devonian shallow marine and continental sedimentary rocks, but locally these Paleozoic rocks might be as much as 2,000 m thick (Kennewell and Huleatt, 1980; Palfreyman, 1984).

Near Tennant Creek, the most widely exposed Precambrian rocks are the Warramunga Group, an interstratified sequence of Early Proterozoic sedimentary and volcanic rocks (Dodson and Gardener, 1978). Poor exposures of the Warramunga Group make it difficult to characterize and subdivide these rocks accurately, but the group is known to contain interbedded graywacke, sandstone, siltstone, shale, hematitic shale, chert with tuff, and acidic volcanic rocks, all having a composite thickness of about 6,000 m. Early Proterozoic granite and small sills and dikes of diorite and lamprophyre intrude the Warramunga Group.

Detailed information about the bedrock geology in the immediate area of the 1988 faulting is limited because the widespread veneer of Tertiary and Quaternary surficial deposits, the low-relief landscape, and the lack of an integrated drainage system result in few bedrock exposures. Much of what is known about the pre-Quaternary geology is based on regional structural and stratigraphic relations, and on subsurface data from exploratory and production water wells drilled for Tennant Creek's public water supply.

Data from water wells adjacent to the eastern part of the Lake Surprise fault and in the area of the Kunayungku fault indicate a generalized stratigraphy of Precambrian granitic basement rock overlain by several tens of meters of Cambrian and Ordovician sandstone and siltstone, which is capped by about 10–30 m of unconsolidated Cenozoic sediments (Verhoeven and Knott, 1980; Verhoeven and Russell, 1981). Locally in the Kunayungku area, the crystalline basement rocks consist of Proterozoic schist. The Cambrian and Ordovician sandstone and siltstone are part of a wedge of Paleozoic sedimentary rocks that were deposited in the Wiso basin but which onlap onto the western flank of the Tennant Creek inlier (Kennewell and Huleatt, 1980).

The major geologic structures in the Tennant Creek area formed in response to three phases of folding and repeated episodes of faulting (Dodson and Gardener, 1978). Major faults in the area trend northwest. Plumb (1979b) noted that west-northwest-trending faults are widespread throughout north-central Australia and are commonly thrust and reverse faults. North-trending strike-slip and oblique-slip faults are also present. Many of the faults show evidence of reactivation both on a local and regional basis (Dodson and Gardener, 1978; Plumb, 1979b). Many fractures and ancient faults are mineralized with quartz, jasper, and, less commonly, dolomite or talc. Faults that have been mineralized with silica are commonly referred to as quartz ridges because they are usually topographically high features, which result from their greater resistance to weathering compared to the surrounding bedrock. About 5 km of the western part of the Lake Surprise scarp coincides with a quartz ridge that presumably marks the location of an ancient mineralized fault or fault zone. The precise spatial coincidence of the scarp with the quartz ridge is evidence that the 1988 earthquakes locally reactivated preexisting ancient faults.

The Mesozoic and Cenozoic history of the interior of Australia is characterized by a prolonged period of tectonic and landform stability, minor deposition of sediment, and deep surficial weathering. In the Tennant Creek area, the characteristics and stratigraphy of Cenozoic deposits is poorly known, in part because these deposits are rarely exposed. However, several small, shallow basins filled with unconsolidated clastic sediment thought to be of Cenozoic age have been recognized from water-well drilling (Dodson and Gardener, 1978; Verhoeven and Knott, 1980).

Much of the Cenozoic in central Australia has been characterized by deep surficial weathering, but in parts of Australia, the subaerial weathering of some presently exposed geomorphic surfaces may have started in the Paleozoic. For example, in the Western MacDonnell Ranges (west of Alice Springs, fig. 2) and in southern and southwestern Australia, some surfaces may have remained exposed since Permian time (Mabbutt, 1966, 1988; Twidale, 1983), and in the Tennant Creek area, some landforms may date to Cambrian time (Stewart and others, 1986). This prolonged episode of surficial weathering, which has continued throughout much of the Cenozoic in many areas, is widely regarded to have produced the iron- and manganese-rich laterites that are common in much of western and north-central Australia. The precise origin, age, and original areal extent of the laterites are still subject to discussion. Stratigraphic and geomorphic evidence in some parts of central Australia indicate that the lateritic profiles began forming in

Cretaceous time (Twidale, 1983; Pickup and others, 1988). In the Wiso basin, the laterite and a slightly younger lateritic conglomerate rest on Lower Cretaceous rocks and may be older than the Miocene Canfield beds (Kennewell and Huleatt, 1980). Dodson and Gardener (1978) reported that locally in the Tennant Creek area, the laterite has been eroded and redeposited in layers that are as much as 15 m thick.

In all of our trenches, we exposed nodular ferruginous deposits that probably correspond to this widespread laterite or lateritic conglomerate (ferricrete and associated materials on pl. 2; see the section on "Description of Units Exposed in the Trenches"). In this report, we choose not to use the term "laterite" because it has a genetic connotation that implies deep surficial weathering under moist, warm (that is, tropical) climatic conditions (Loughnan, 1969; Goudie, 1973). Instead, we use the term "ferricrete" (Goudie, 1973), which we consider to be a nongenetic descriptive term for accumulations of iron- and manganese-cemented surficial materials (Bates and Jackson, 1980). Because we are not absolutely certain about the origin and parent material of the ferricretes in our trenches, we prefer to use the more generic term.

For our purposes, the time when ferricrete formation essentially ceased is important because it defines a time marker to use in evaluating rates of tectonic deformation. The best estimates of the cessation of ferricrete development seem to favor Miocene to early Pliocene time. These estimates are based on paleoclimatic reconstructions of a climatic change from warm, relatively wet conditions to progressively drier conditions (Bowler, 1976; Twidale, 1983; Mabbutt, 1988) and on the geomorphology of ancient valleys in the interior of central Australia (Pickup and others, 1988). In the absence of more specific data from our study, we consider the ferricretes that we describe to be no more than mid-Tertiary in age.

Eolian sand is ubiquitous throughout most of the interior of Australia. More than 1.3 million km^2, or about 20 percent of the continent, is covered by well-developed dune fields (Ash and Wasson, 1983). In the Tennant Creek area, a widespread blanket of unconsolidated late Quaternary eolian sand mantles virtually all of the lowland surfaces in depths that commonly range from 2 m to as much as 5 m. The sand has buried the preexisting topography and produced the essentially flat, nearly featureless landscape. These sands are typically fine to medium grained and light reddish brown, and are both well sorted and well rounded. On the basis of grain-size analyses, they are categorized as sand, loamy sand, and sandy loam (fig. 6); the less sandy samples (sandy loams) are probably altered from sands (see the following discussion of soil formation and weathering of eolian sand).

Quaternary climatic studies in semiarid parts of Australia document multiple episodes of aridity and associated eolian activity in the past 300,000 yr (Bowler, 1976), but the most recent period of major eolian activity began about 25,000 yr ago and ceased about 13,000 yr ago. Thus, the bulk of the eolian sand in the Tennant Creek area is probably late

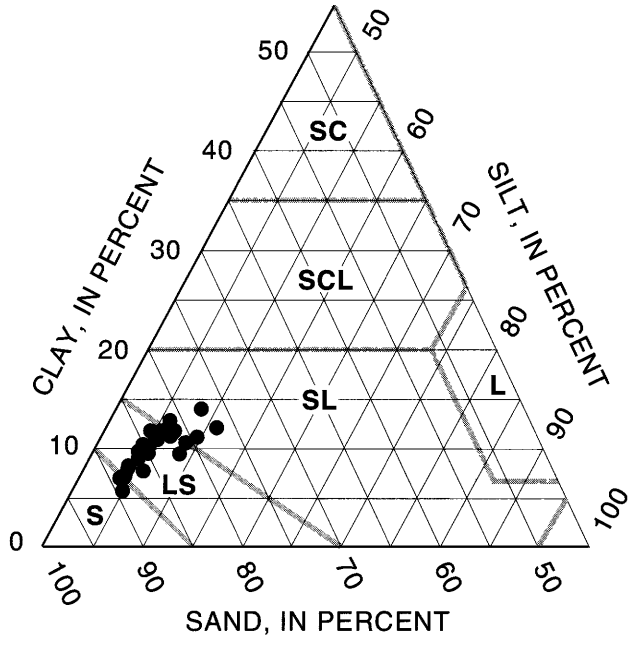

Figure 6. Grain-size data for samples of eolian sand from the four trenches excavated across the 1988 Tennant Creek fault scarps. Textural classes are: S, sand; L, loam; LS, loamy sand; SL, sandy loam; SCL,sandy clay loam; SC, sandy clay.

Pleistocene in age. However, the lack of significant soil development on the sand at some of our trench sites is evidence that the sand may have been locally remobilized and reworked during the mid- to late Holocene (Bowler, 1976).

Samples from the trenches were collected for dating by radiocarbon (^{14}C), TL, ESR, and uranium-trend analysis. The ^{14}C and TL analyses are complete, but the final analyses of the ESR samples are in progress (1992), and only preliminary results are available for a few samples (tables 8 and 9 in the section on "Description of Units Exposed in the Trenches"). A preliminary analysis of the uranium-trend samples by D.R. Muhs (U.S. Geological Survey, Denver, Colo.) indicated a low chance that this dating technique would yield reliable results; therefore, further analysis of these samples was not undertaken.

The only radiocarbon sample we collected was from the basal part of the eolian sand (unit **es**) in the eastern Lake Surprise trench (pl. 2*A*). The sample consisted of carbonized wood collected from stratigraphically equivalent horizons in the west wall (sample ELS–3, pl. 2*A*) and the east wall (sample ELS–2, pl. 2*A*) of the trench. The sample yielded an AMS (accelerator mass spectrometry) uncalibrated radiocarbon date of 1,474±44 yr before present (Geochron Laboratories, sample GX–16282–AMS). Although the sample appeared to be detrital, we conclude that the date is geologically unrealistic. The sample is probably a young carbonized root fragment or it is detrital wood that has been severely

contaminated by young carbon. We regard the date as useless for determining the age of the sand and do not discuss it further.

The TL age determinations of samples from our trenches show that locally eolian-sand deposition began about 50,000 yr ago. The TL age determinations of 13 samples of eolian sand from our trenches (unit **es**, pl. 2) range from 6.6±0.5 ka to 71±5.4 ka and are generally in correct stratigraphic order; that is, the ages are progressively older with increasing depth below the top of the sand (fig. 7, table 9). The thickest and presumably most complete section of eolian sand was exposed in the eastern Lake Surprise trench. The deepest sample of eolian sand in this trench was about 2.5 m below the surface (TC2S/2.5a, table 8) and yielded a TL age of 52±4 ka (table 9). We believe that this age approximates the time when the eolian sand stabilized sufficiently to accumulate as a discrete Quaternary deposit. Shallower samples of the eolian sand in this trench yielded progressively younger TL ages except for a sample 2.25 m below the top of the sand (TC2S/2.25, table 8), which yielded an age of 71±5.4 ka (table 9). We believe that this age is anomalously old because it is not in proper stratigraphic order and it is significantly older than any of the other 12 TL ages. This anomalously old age could be caused by several factors including incomplete bleaching of the sample when it was deposited (Berger, 1988). In the western Lake Surprise trench 1 (TC3S/1.7, table 8), a sample of the basal part of the eolian sand (unit **es**) about 1.9 m below the surface yielded a comparable TL age of 46±3.5 ka (table 9). In the Kunayungku trench, the eolian sand was thin compared to the sand at our other sites; the basal sample of eolian sand from this trench was only about 1.1 m below the surface. This basal sample (TC1S/1.1, table 8) yielded a TL age of 30±2.3 ka (table 9), which suggests that the eolian sand here stabilized 10,000–20,000 yr later than the sand at the eastern Lake Surprise and western Lake Surprise sites. On the basis of these TL data, we conclude that the eolian sand in the Tennant Creek area is late Pleistocene in age, and that deposition began about 50,000 yr ago and continued into the Holocene.

The TL data suggest that the eolian sand has been accumulating gradually at an average rate of about 4.0 cm per 1,000 yr (fig. 7). The maximum and minimum deposition rates are 3.2 and 4.8 cm per 1,000 yr (fig. 7). The similarity of these rates, which are based on samples from localities that are as much as 17 km apart, indicates that the depositional rates are relatively uniform throughout the study area. The uniformity in the rates implies that the sand deposition was probably controlled by regional factors such as climatic conditions rather than local factors such as proximity to sources of sand. The evidence of gradual, generally continuous accumulation of the sand is consistent with our observations that no major depositional hiatuses are present in the sand as indicated by (1) the absence of significant soils (either at the surface as relicts or buried in section), (2) the lack of stonelines or obvious textural changes in the sand, and (3) the subdued development of soil horizons and the moderate amount of clay accumulation deep within the sand.

Our estimate of the onset of eolian-sand deposition about 50,000 yr ago corresponds to the time when gypsiferous dunes were forming in the playas of the Lake Amadeus area (Chen and others, 1990) about 650 km southwest of Tennant Creek. Chen and others (1990) bracketed this dune-forming episode between 45 ka and 60 ka and attribute the dune formation to semiarid but slightly wetter climatic conditions than the present conditions. They believe that the gypsiferous dunes formed when the regional water table was high enough to intermittently flood the playas but not so high to permanently fill the lakes. We speculate that a slight increase in precipitation in the Tennant Creek area might correlate with the onset of the eolian-sand deposition. More precipitation in the Tennant Creek area would probably stimulate the growth of more vegetation, which would tend to partly stabilize the previously mobile eolian sand. The partly stabilized sand could then accumulate to form the permanent deposit than now mantles the landscape.

The preliminary ESR age determinations, which are available only for samples from the Kunayungku trench, are consistently about 1.5 to 2.5 times greater than the ages of companion TL samples (fig. 7, table 9). The cause of the substantial age differences between these methods is unknown, but it may be related to different techniques used to measure the dose rate for each method or to incomplete bleaching of the ESR traps. A detailed discussion of these differences is beyond the scope of this report.

Deciphering the paleoseismology of faults requires at least a rudimentary understanding of the local Quaternary stratigraphic framework. The published literature contains very little information on the Quaternary stratigraphy in the Tennant Creek area, in part because studies are hampered by the lack of natural exposures and suitable materials for dating the deposits. Our observations in the area of the Tennant Creek scarps indicate that the Quaternary deposits are typically thin; they are probably less than 10 m thick and commonly 2–5 m thick. The deposits are dominated by a blanket of red eolian sand that buries most of the preexisting topography and produces the modern low-relief landscape. The lack of relief is exemplified by the fact that only about 30 m of total relief is present within the fenced paddock that surrounds most of the Tennant Creek fault scarps.

The sand lies on units that we describe as ferricrete gravel, massive ferricrete, or altered ferricrete. We consider all of the ferricrete deposits to be largely in-place weathering products. The ferricrete gravel may be a locally mobilized facies of the massive ferricrete. Where the base of the ferricrete is exposed in our trenches, it typically lies directly on weathered bedrock in the shallow subsurface.

Widely separated mounds of calcium carbonate, mapped as calcretes by Dodson and Gardener (1978), are scattered across the landscape near the Tennant Creek scarps. The mounds are typically composed of massive to

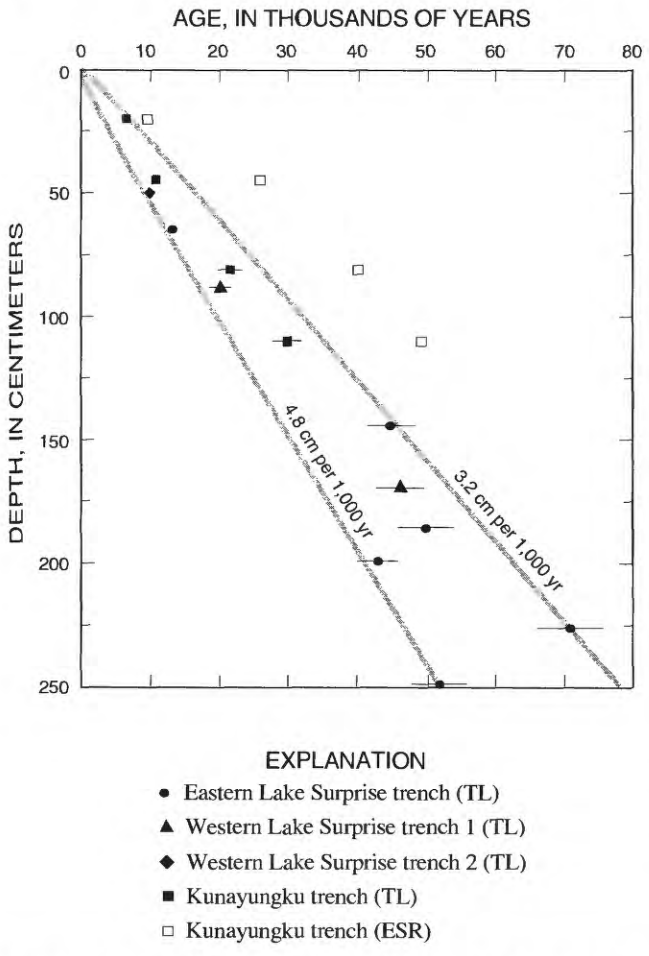

Figure 7. Thermoluminescense (TL) and electron-spin-resonance (ESR) age determinations for eolian sand from the four trenches excavated across the 1988 Tennant Creek fault scarps. The shaded lines indicate maximum and minimum deposition rates (4.8 cm per 1,000 yr and 3.2 cm per 1,000 yr, respectively) for the eolian sand based on the TL data. The average deposition rate based on these data is 4.0±1.0 cm per 1,000 yr. Detailed information on sample locations and age estimates are shown in tables 8 and 9. Horizontal bars show error limits (1σ).

porous calcium carbonate, which contains fragments of chalcedony and, in places, is covered by thinly laminated calcium carbonate. Individual calcrete mounds are generally about 20–40 m in diameter and form small hills and ridges that commonly rise from less than 1 m to 10 m, at most, above the low surrounding landscape (fig. 8). They commonly have a central 1- to 2-m-deep depression that is filled by a thin, discontinuous mantle of eolian sand. Several of the depressions near Lake Surprise are not clogged by eolian sand and appear to be open to a depth of much more than 1 m, which seems to indicate that the mound-formation process might still be active, at least on an intermittent basis.

The origin of these unusual mounds is uncertain, but several origins have been proposed to us by Australian geologists and hydrologists. One hypothesis considers the mounds to be pedogenic features even though modern soils in the area are not calcareous. If the mounds are pedogenic, they must have formed under climatic and aerosol-influx conditions that are considerably different than the modern conditions. Furthermore, if the mounds are remnants of an old soil, then exposures should be more widespread and uniform on the landscape, in contrast to their occurrence as rather small, isolated, widely separated features. We do not believe that their present distribution supports the existence of a thick, formerly widespread calcareous soil.

Another hypothesis considers the mounds to be residual ground-water deposits associated with a former landscape (perhaps an ancient valley) whose topography is now inverted. The central depression in the mounds is attributed to partial dissolution of the ground-water calcretes by infiltrating surface waters (that is, karst solution). However, the mounds are everywhere topographically higher than the surrounding landscape, and concentrating adequate amounts of surface water to dissolve the carbonate would be difficult. In addition, the annual precipitation in the Tennant Creek region is only 459 mm, which is very low compared to other regions where surficial dissolution is currently active (for example, the southeastern United States).

Our favored interpretation for the origin of the mounds, particularly those adjacent to Lake Surprise, is that they are paleospring deposits. We favor this explanation because of the morphology, dimensions, and wide separation of the mounds. The areal distribution of the mounds may be related to shallow subsurface features that interfere with the ground-water flow and force carbonate-laden water to the surface. The source of the hydrostatic head for the springs remains unclear.

Lake Surprise (fig. 9), a small playa in the center of the study area, is filled by water from overland flow every few years. Frequent monsoonal rains occur during the hot austral summer months of December through February, and it is not uncommon for most of the annual precipitation to fall in this short period. After a decade of dry playa conditions, Lake Surprise refilled during the unusually wet austral summer of 1991. Deep soil wetting can occur, but a large part of the rainfall probably runs off because of the intensity of the storms and the sparse vegetative cover. The historical high stand of Lake Surprise covers about ⅛ km^2, but the modern lake is surrounded by a series of higher paleoshorelines (sandy beach ridges) that define its areal extent during higher lake levels in late Pleistocene(?) and Holocene time. These shorelines show that the lake has been as large as 1 km^2 in the recent geologic past.

The interior of Australia is known for its long history of tectonic stability and the resulting low-relief landscape. Several major, largely unmodified but old geomorphic surfaces are considered to be present in the northern part of the Northern Territory (Kennewell and Huleatt, 1980). In the Tennant Creek area, the highest of these surfaces is a pediment thought to be Cretaceous in age, but it might be as old as

Figure 8. Calcrete mounds about 150 m east of Lake Surprise. Mounds are typically 20–40 m in diameter, have a central depression, and form isolated hills that rise from less than 1 m to about 10 m above the surrounding landscape. The origin of the mounds is unknown.

Cambrian (Stewart and others, 1986). The great antiquity of the regional landscape and the absence of a significant range of hills or low mountains associated with the 1988 scarps indicates that recurrent movement on these faults has not occurred regularly enough in the Tertiary to generate fault-related topography. Thus, the general geomorphology of the landscape indicates that the average recurrence time for surface ruptures on these faults during the last several million years must be very long.

At all of our trench localities, the land surface in the immediate vicinity of the scarps is nearly featureless and essentially planar (fig. 9, pl. 1*A*). We saw no geomorphic evidence of pre-1988 fault-scarp topography. Thus, the absence of scarps in the late Pleistocene eolian sand is consistent with the evidence of a long recurrence interval for surface-rupturing earthquakes throughout the Tertiary.

In contrast to the lack of geomorphic evidence of faulting, we do note a subtle and perhaps significant correlation between the gross topography along the Lake Surprise fault (as expressed by the contour lines on pl. 1*A*) and the sense of throw on the scarps produced by the 1988 earthquakes. On the south side of the eastern Lake Surprise scarp, the 320-m contour has a prominent westward deflection, which indicates a broad topographic area 10–15 m higher on the south side relative to the north side of the fault. This topographic relation is the same as the sense of throw on this part of the fault during the 1988 earthquakes. In contrast, on the south side of the western Lake Surprise scarp, the 300-m contour is deflected eastward, which indicates a topographic low on the south side relative to the north side of the fault. Here again, the topography mimics the 1988 throw, even though the throw direction on the fault has reversed. We recognize that this topographic expression is subtle and inconclusive. Nevertheless, it might reflect the influence of earlier faulting on the topography.

TRENCHING INVESTIGATIONS

As we have noted, earthquakes in stable continental interiors are rare, and the recurrence time between successive events on the same fault is much longer than the length of time encompassed by historical records, which, at most, span a few thousand years. Therefore, geologic investiga-

Figure 9. Panoramic view of Lake Surprise showing the low-relief, featureless topography that typifies the area of the 1988 Tennant Creek fault scarps. The modern bed of Lake Surprise extends from the trees in the foreground (3–4 m high) to the trees in the distance. View is to the south.

tions of prehistoric surface-rupturing earthquakes can provide valuable information about the location and magnitude of ancient earthquakes and supply insight into the long-term activity of seismogenic faults over geologically meaningful periods of time (many thousands of years). As a result, these investigations can improve our understanding of the hazards posed by faults in plate interiors that might generate damaging earthquakes. These kinds of geologic investigations are part of a relatively new discipline known as paleoseismology, which is rapidly becoming an important component of earthquake investigations (Crone and Omdahl, 1987). Exploratory trenching is commonly a key part of most paleoseismic investigations because trenches can reveal critical stratigraphic relations between faulted and unfaulted deposits, and can also expose materials that will help establish the time of prehistoric surface-rupturing events.

METHOD OF STUDY

In this study, we combined geologic field studies and exploratory trenching to determine the rupture history of the faults associated with the Tennant Creek earthquakes and to evaluate this history with respect to the sequence of events in 1988. Our initial step was to reconnoiter the 1988 ruptures to locate suitable trenching localities. To obtain data on the prehistoric faulting on each of the three sections of the 1988 scarps (eastern Lake Surprise, western Lake Surprise, and Kunayungku), we intended to excavate at least one exploratory trench on each section. The primary goals of the trenching studies were to determine the rupture histories for the different sections of the scarps and to document significant differences in these rupture histories.

An important aim of trenching prehistoric fault scarps is to expose colluvial deposits that are generated by the degradation of a fault scarp (Crone and Omdahl, 1987). Dating the Quaternary deposits and soils associated with a degraded scarp can bracket the time of an ancient surface-rupturing event(s) and thus the time of the causative earthquake(s). In addition, the thickness and dimensions of scarp-derived deposits can yield general estimates of the size of prehistoric scarps, which can serve as a guide to estimating the amount of slip and thus the magnitude of the prehistoric earthquake.

The two primary criteria we applied in selecting our trenching localities were to choose locations (1) where the 1988 scarps were the largest, and (2) where the style of deformation was simple and was confined to a relatively narrow zone. Trenching sizable scarps has important advantages because the degradation of a larger scarp is likely to produce a more distinct and interpretable stratigraphic record than the degradation of a small scarp. Furthermore, paleoseismic studies of other faults have shown that the location of the largest historical displacements commonly coincides with large displacements during past ruptures (Schwartz and Crone, 1985; Schwartz, 1988) and, thus, the likelihood of detecting prior movement is greater at locations of large historical displacements. Most of the 1988 scarps are in geomorphically stable settings where they are virtually unmodified and are not visibly affected by recent, localized erosion or deposition, factors which could complicate the interpretation of the stratigraphy or tectonic history.

Four trenches were excavated using a tire-mounted backhoe that had a maximum excavation depth of about 5 m. With the exception of the eastern Lake Surprise trench, the 5-m-depth limit was adequate to expose weathered bedrock on at least one side of the fault. At the eastern Lake Surprise locality, the trench did not reach bedrock but did reach moderately indurated ferricrete on both sides of the 1988 fault zone. After excavation, the trench walls were carefully scraped with mason's trowels and brushed clean to remove

blade marks and sediment smeared by the backhoe. Important stratigraphic contacts and structural features were identified and marked with multicolored flagging (that is, different-color flags for contacts, faults, fractures, and soil horizons). A grid of string lines at 1-m intervals was constructed to provide vertical and horizontal control for the mapping. The positions of stratigraphic contacts and structural features were transferred directly to metric-gridded mylar sheets at a scale of 1:25. After mapping was completed, we described the mapped units and collected samples for laboratory analyses and age determinations.

TRENCHING OF THE EASTERN LAKE SURPRISE SCARP

The eastern part of the Lake Surprise scarp is the longest of the three surface ruptures that formed in 1988. The surface ruptures along this scarp have a general trend of 105°–115° and are the result of northward-directed reverse faulting. This section of scarps extends from the eastern side of Lake Surprise to just beyond the eastern fence line of the paddock (pl. 1*A*). The eastern Lake Surprise scarp is arcuate with a convex-to-the-north bend that is about 3 km east of Lake Surprise. The scarp is nearly continuous from the east side of Lake Surprise to near the NT Gas pipeline; the eastern part of the scarp is composed of a series of right-stepping echelon ruptures. The highest scarps (about 1.8 m) are between the bend and the area 1–2 km east of the NT Gas pipeline (Bowman, 1991; pl. 1*A*, fig. 4). East of this area, the scarps are generally less than 1 m high.

CHARACTERISTICS OF FAULT SCARPS NEAR THE TRENCH

The eastern Lake Surprise (ELS) trench locality is about 600 m east-southeast of NT Gas pipeline road (pl. 1*A*). The nearest Australian Surveying and Land Information Group (AUSLIG) survey station (No. 4795; labeled Sta. 9500 in the field) is 181 m east-southeast of the trench along a bearing of 122°.

The largest surface offsets that occurred in 1988 are near the ELS trench (fig. 4). At the trench, the scarp is 0.85 m high, but this height represents only the amount of deformation from brittle failure, which is about one-half of the 1.7 m of surface offset that we measured on the scarp profile (pl. 1*C*). The remainder of the offset is from nonbrittle deformation in the hanging-wall block, which is expressed as a monocline, a syncline, and an anticline, each of which have a few tens of centimeters amplitude.

The 1988 scarp typically has minimal deformation in the footwall (north) block; virtually all of the ground deformation is confined to the hanging-wall (south) block. The ground surface of the footwall block slopes gently to the northeast (its original gradient) and is nearly planar all the way to the toe of the free face (pl. 1*C*). Minor cracking and warping are present locally in the footwall and are probably related to reverse drag on the fault. The surface deformation in the hanging-wall block is commonly expressed as a single, abrupt scarp where the main fault zone intersects the surface, and as broad, gentle folds within 10–20 m south of the main scarp (pl. 1*C*). Where a single main rupture is present, the ground surface of the hanging wall is progressively warped adjacent to the rupture. As the warping increases, the sediments fail brittlely and a free face forms. The free face is typically 10–35 cm high along this reach of the eastern Lake Surprise scarp. Where a free face is present, the ground surface of the footwall block is locally buried by relatively intact blocks of the soil from the upper surface that have broken away and collapsed onto the lower surface. South of the free face, the hanging-wall block is gently warped into a broad, low-amplitude arch and trough (pl. 1*C*). In map view (pl. 1*B*), the trough is expressed as a subtle, elongate depression subparallel to the scarp, which is accentuated by a relatively dense growth of *Spinifex triodia sp.* (bunch grass).

The general trend of the scarp in the immediate area of the trench is 115° (pl. 1*B*); the trench was oriented nearly perpendicular to the scarp along a trend of 016°. In map view, the trace of the scarp is sinuous. Along strike, the height of an individual scarp commonly diminishes, and the scarp loses its free face and gradually grades into a monoclinal warp (pl. 1*B*). Where two or more subparallel scarps are present locally, the northernmost strand commonly has the greatest throw. Typically, where the throw on one scarp decreases, the deformation increases on an adjacent en echelon strand.

STRATIGRAPHY IN THE TRENCH

The eastern Lake Surprise trench exposed two primary stratigraphic units: (1) an upper, 2- to 3-m-thick blanket of eolian sand (unit es, pl. 2*A*), and (2) a lower assemblage of ferricrete units (units fcg, fcm, and fca, pl. 2*A*) whose base was not exposed in the 4-m-deep excavation. The eolian sand is composed of 81–89 percent medium- to fine-grained sand that is loose to weakly cemented and contains as much as 11–19 percent silt and clay (see the section on "Description of Units Exposed in the Trenches," fig. 20, and table 4). The individual grains are pervasively coated with iron oxide, which gives the unit its strong red to dark-red color and which probably acts as a cementing agent. The upper part of the sand contains a slight accumulation of organic matter (soil A horizon) and an underlying transitional zone that contains both organic matter and more clay (A/B horizon). Particle-size data for a series of samples from the surface to the base of the sand show a slight, progressive increase in clay and, to a lesser extent, silt (fig. 20). We refer to this thick

zone of clay accumulation and reddening as a cambic B (Bw) horizon. This increase in silt and clay suggest that most of the clay may be forming from in-place weathering, soil formation, or diagenetic alteration. However, the profile does not contain evidence of a prominent Bt horizon (argillic B horizon), which would be expressed as a well-defined bulge (increase and decrease) in the clay content. Such a clay concentration would indicate that the deposit had remained stable for a significant period of time during which pedogenesis could form a well-defined clay-rich horizon.

We have no specific data on soil-formation rates in this part of Australia, but gross similarities in the climate and soil characteristics of central Australia and the southwestern United States suggest that soil-formation rates in the southwestern United States may approximate rates in central Australia. In the southwestern United States, argillic B horizons commonly are incipient on 10,000-yr-old deposits and are moderately well developed on 100,000-yr-old deposits (Birkeland, 1984). The thickness of the sand, the progressive increase in clay from 7 to 12 percent with increasing depth, the pervasive oxidation of iron, and the lack of distinct horizonation all indicate that the eolian sand accumulated gradually and relatively continuously. If the TL age estimates are accurate, then the time needed to generate a modest 5-percent clay increase in a quartz-rich eolian sand under this climate or late Pleistocene climates in central Australia is on the order of 50,000 to 60,000 yr.

The eolian sand lies on ferricrete at this and at all of our other trench localities. The ferricrete in this trench was subdivided into three units (pl. 2*A*), an upper pebbly ferricrete gravel (unit **fcg**), a middle massive ferricrete (unit **fcm**), and a lower altered ferricrete (unit **fca**). In some places, the middle unit, **fcm**, is in direct contact with the eolian sand because faulting has removed the overlying pebbly ferricrete gravel (unit **fcg**), which is normally present. About 90 cm of ferricrete is exposed in the footwall block at the base of the trench, but we suspect that there may be an equal amount of altered ferricrete below the trench, which would make the ferricrete about 2 m thick. We suspect that bedrock is shallow (4–5 m deep) at this locality, assuming the ferricrete is 1–3 m thick, which is what we observed in the other trenches.

STRUCTURAL FEATURES IN THE TRENCH

The most spectacular structural feature in this trench is a network of north-directed (south-dipping) reverse faults that dip an average of 28°–30° to the south (fig. 10). The north-directed reverse faulting is concentrated in a 3-m-wide zone that comprises a set of parallel major faults that dip 20°–28° to the north and a set of conjugate shear planes and minor faults (pl. 2*A*). The pattern of deformation within the main fault zone indicates that transport initially began on a south-dipping shear plane near the southern margin of the fault zone, and, with increasing compression, the brittle failure shifted to adjacent fault planes that are progressively farther north. The amount of displacement on the shear plane that was initially activated was insufficient to rupture the surface; near the surface, much of this deformation was distributed among myriad miniscule shears that terminate in the upper part of the eolian sand near the base of the soil. Apparently, the soil and its meager root system were resistant enough to rupturing that it confined the small amount of deformation to the subsurface in the eolian sand. As the cumulative amount of throw increased on the master fault at depth, shear planes developed that eventually ruptured the surface and transported the hanging wall over the footwall to the north. As a result, the pre-1988 ground surface on the footwall was overridden and buried by the soil horizon in the hanging wall (pl. 2*A*).

In the hanging wall 8 to 10 m south of the main fault, a network of subvertical, near-surface extensional fractures formed where the ground surface is arched into a broad, low-amplitude anticline. In cross section, these secondary features define a crude radial pattern that may indicate the position where the attitude of the master fault changes from a relatively shallow (25°±5°) dip in the poorly consolidated surficial deposits to a steeper dip (35°–45°) (from Bowman and others, 1990; Choy and Bowman, 1990) in subjacent bedrock.

The net dip-slip displacement of the reverse faults in the trench can be estimated from two lines of evidence. The first estimate is based on at least 0.65 m of overthrusting of the soil at the surface. This value is a minimum because the pre-1988 soil has probably been shortened by compression and minor folding. The second line of evidence is based on measuring the cumulative displacement on faults that would be needed to restore formerly continuous stratigraphic contacts. The best stratigraphic relations for this restoration were exposed on the east wall of the trench where the displacement was confined to a few strands in a narrow fault zone (inset map, pl. 2*A*). The contact between the eolian sand and ferricrete gravel (units **es** and **fcg**) was displaced about 1.88 m across the fault zone. This displacement is determined by summing the amount of displacement across individual fault strands to restore the contact between units **es** and **fcg** to its original nearly planar configuration.

The slip on the main fault at depth produced both brittle and nonbrittle deformation at the surface. The amount of brittle deformation is recorded by faults exposed in the trench, and the nonbrittle deformation is expressed by the warped ground surface in the hanging wall. If the main fault at depth along this section of scarps dips 45° (Choy and Bowman, 1990), then about 2.4 m of dip slip is required to produce the 1.7 m of vertical offset measured on the scarp profile (pl. 1*C*). This estimate of the net dip slip is consistent with a dip slip of about 2.5 m calculated from the leveling data along the NT Gas pipeline road and elsewhere (Bowman, 1991).

Figure 10. Western wall of eastern Lake Surprise (ELS) trench showing faults and sets of conjugate shears and fractures that form a pattern of rhombohedral blocks in eolian sand (unit **es**, pl. 2*A*). Pieces of flagging on the string line are 1 m apart. Map of trench wall is on plate 2*A*.

OBSERVATIONS PERTINENT TO PREHISTORIC RUPTURING

The geomorphology in the vicinity of the eastern Lake Surprise trench and stratigraphic relations in the trench offer no evidence of prehistoric rupturing along this part of the Lake Surprise fault. We saw no geomorphic expression of a pre-1988 scarp in the surrounding, virtually featureless landscape. The 1988 scarp is now a conspicuous topographic feature, despite its modest size.

The relatively planar contact between the eolian sand and the ferricrete near the ends of the trench indicate that most of the near-surface deformation associated with the 1988 rupture at this locality was exposed in the trench. However, we could not be certain if the locus of deformation from past ruptures coincided with the location of the 1988 deformation. To be sure that there was no nearby ancient deformation that had not been exposed in the main trench, we extended the trench in both directions and measured the depth of the eolian sand-ferricrete contact (fig. 11). The total length of the extended trench was about 82 m; it continued 54 m north and 28 m south of the 0.0-m mark on the trench log. The extended trench shows that the elevation of the sand-ferricrete contact has a natural variability of about 1 m, which is expressed as broad-wavelength undulations. In contrast, the 1988 faulting created an abrupt step in the contact adjacent to the scarp. The schematic diagram of the extended trench (fig. 11) shows that the net throw on the sand-ferricrete contact at the main fault zone is slightly more than 1 m (after compensating for the natural variability), which is similar to the amount of 1988 surface deformation. Thus, the sand-ferricrete contact has been deformed only by the 1988 event, and any prehistoric ruptures on this fault predate deposition of the basal part of the eolian sand.

We attribute all of the faulting and deformation in the Quaternary units exposed in the trench to the 1988 earthquakes. We found no stratigraphic evidence of colluvial deposits from previous faulting events. In addition, the overall similarity between the amount of displacement on the eolian sand-ferricrete contact (fig. 11) in the extended trench and the 1988 displacement on the ground surface indicates that the 1988 earthquakes are the only events that have

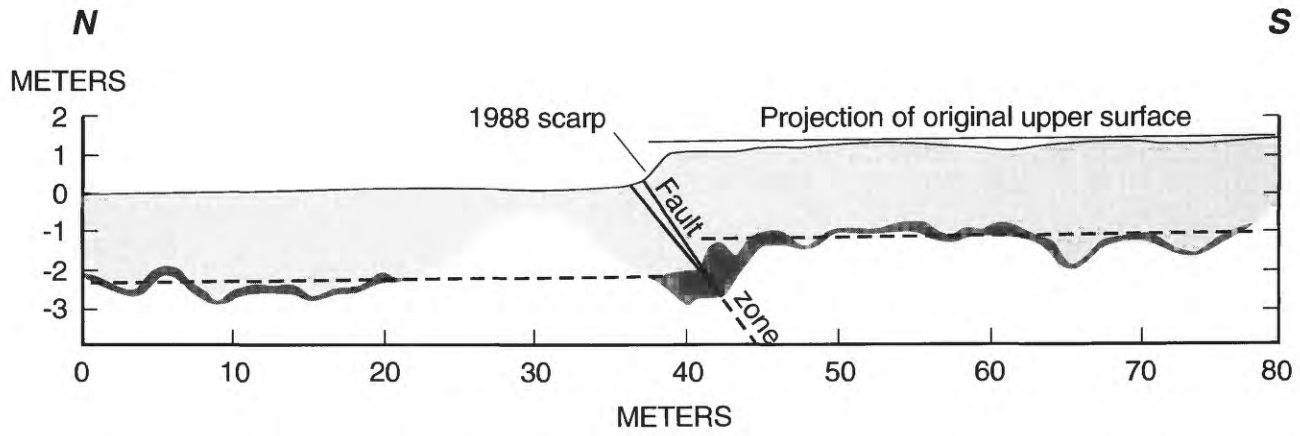

Figure 11. Schematic diagram of the extended eastern Lake Surprise (ELS) trench. Light stipple is eolian sand; dark stipple is ferricrete as exposed by backhoe. Area where no ferricrete is shown spans the north end of the original trench, which could not be deepened. Heavy dashed line is the projection of the average top of the ferricrete, which has slightly more than 1 m of vertical offset at the fault zone. The offset on the top of the ferricrete is comparable to the offset on the ground surface caused by the 1988 earthquakes. Vertical exaggeration is 2.5×; the fault zone has a true dip of about 25°.

displaced the eolian sand-ferricrete contact. In the absence of geologic or geomorphic evidence of a pre-1988 rupture in Quaternary deposits, we use the oldest Quaternary deposits in the trench to establish the minimum amount of time since the previous surface rupturing on this part of the Lake Surprise fault. We conclude that any significant prehistoric deformation must have predated deposition of the basal part of the eolian sand, which is about 52,000 yr old (pl. 2*A*, tables 8 and 9). Thus, surface deformation comparable to that produced by the 1988 faulting has not occurred at the eastern Lake Surprise locality in at least the past 52,000 yr.

TRENCHING OF THE WESTERN LAKE SURPRISE SCARP

The 1988 surface ruptures along the western part of the Lake Surprise fault trend about 065° and have a north-over-south sense of throw, which is opposite to the throw direction along the eastern part of the fault. The scarps with north-over-south throw begin a few hundred meters east of Lake Surprise and extend westward for a distance of slightly more than 6 km to just beyond the western fence of the paddock (pl. 1*A*). A secondary scarp about 3 km long and less than 1 m high is subparallel to the main scarp and is about 1 km south of the western end of the main Lake Surprise scarp. This small scarp commonly consists of a gentle but pronounced steepening of the ground surface across a 20- to 50-m-wide zone and, locally, as discontinuous mole-track furrows. ("Mole track" is an informal but commonly used term to describe the linear but sinuous trace of disturbed ground caused by echelon fractures and small compressional mounds.)

From Lake Surprise westward to beyond the trench localities, the ruptures are generally well-defined, continuous, simple reverse-fault scarps that are about 1 m high. Along this section of the fault, the deformation is typically expressed as a 10- to 20-m-wide planar slope that connects nearly horizontal upper and lower surfaces (fig. 12, pls. 1*E*, 1*G*). Locally, a free face, as high as 10–15 cm, may be present. Extensional fractures are common in the hanging wall 3–8 m north of the scarp. The fractures are 10–40 cm wide, and some were still open to more than 0.5-m depth at the time of our field study in September, 1990 (fig. 13).

One of the most prominent topographic features in the area surrounding the 1988 ruptures is the elongate quartz ridge, which is about 0.5 km west of the westernmost trench (WLS–2, pl.1*A*). The ridge rises about 10–15 m above the surrounding landscape and is about 1.6 km long and 30–150 m wide. It is composed of dark-red to maroon hematitic quartzite that is intensely fractured and mineralized with vein-filling, milky quartz. Small, isolated outcrops of bedrock are present on the ridge, and the ground surface is littered with angular fragments of the fractured quartzite. Along the crest and southern flank of the ridge, most of the 1988 deformation is seen as a network of discontinuous open cracks and fractures, some of which are 20–30 cm wide and more than 1 m deep. In Australia, quartz ridges such as this one are commonly considered to be mineralized ancient faults.

We excavated two trenches (WLS–1 and WLS–2) on the section of the 1988 scarps between Lake Surprise and the quartz ridge. Trench WLS–1 was about 1.6 km west-southwest of Lake Surprise, and trench WLS–2 was about 375 m west-southwest of the first trench (pl. 1*A*). These trenches at two adjacent sites allowed us to compare the characteristics of shallow faulting that formed a scarp expressed as a

Figure 12. Western Lake Surprise fault scarp adjacent to western Lake Surprise trench 1. Scarp is about 1.1 m high. The scarp, which is best seen in the grassy area in the background, is expressed as a planar, gently sloping surface that connects the nearly flat upper slope on the left with the topographically lower slope on the right. Open extensional cracks (in mid ground) are typical of the faulting along much of the western part of the Lake Surprise scarp. Note the lack of relief in the area. A detailed view of cracks is shown in figure 13. A detailed map and profile of the scarp are shown on pls. 1*D* and 1*E*. View is to the east.

monoclinal slope (WLS–1) versus a scarp that has a small free face (WLS–2).

WESTERN LAKE SURPRISE TRENCH 1

CHARACTERISTICS OF FAULT SCARPS NEAR THE TRENCH

The scarp at western Lake Surprise trench 1 (WLS–1) is 1.1 m high (pl. 1*E*) and has a local strike of 067°. It is characterized by a prominent southward-sloping surface that has a generally uniform gradient and separates the nearly flat surfaces above and below the scarp (fig. 12). At the trench, the gentle slope of the scarp is interrupted by a pronounced bulge where a 13-cm-high north-directed backthrust reaches the surface (23-m mark on pl. 1*E*). A network of extensional fractures is present along the upper part of the scarp, close to the inflection point between the flat surface above the scarp and the southward-sloping surface that defines the scarp. Between the extensional fractures and the toe of the scarp, the ground surface is littered with angular fragments of massive silicious, ferruginous rock, 5–8 cm in diameter, which indicates that bedrock is close to the surface (fig. 13).

Trench WLS–1 is the easternmost of the two trenches on this section of scarps and was located about 91 m east-northeast of AUSLIG survey station 4935 (labeled Sta. 23500 in the field) on a bearing of 250°. The AUSLIG station is marked in the field by a 1.5-m-high steel stake. Overall, the local landscape near the trench locality has a very subtle eastward slope toward Lake Surprise (pl. 1*D*).

STRATIGRAPHY IN TRENCH WLS–1

The western Lake Surprise trench 1 exposed extensively sheared, fractured, and weathered iron-rich quartzite capped by ferricrete, gravel, and sand on the north side of the

Figure 13. Closeup view of open fissures and extensional fractures in the hanging wall of the fault adjacent to the western Lake Surprise trench 1. Note the angular to subrounded fragments of ferruginous bedrock exposed in the fractures beneath the thin veneer of eolian sand. Upper part of bar scale is divided in inches and the lower part in centimeters. View is to the east.

fault scarp and about 2 m of eolian sand and gravelly sand on the south side of the scarp (pl. 2*B*). Bedrock was not exposed south of the fault zone in the trench.

The eolian sand (unit **es**) is composed of 85–90 percent medium to fine quartz sand and is dark red from iron oxide coatings on the grains. On the south side of the fault, the basal part of the sand (unit **esr**) and the underlying mixed ferricrete gravel and sand (unit **esr+fcgr**) have a drab gray to white color that we attribute to localized geochemical reducing conditions. We discuss the possible implications of these reducing conditions in the following section on "Observations Pertinent to Prehistoric Rupturing."

The eolian sand (unit **es**) is unstratified and weakly cemented, and it contains a few isolated lenses of granule gravel. The thick sequence of sand and sandy gravel south of the fault progressively thins to the north, and, on the north side of the fault, the veneer of eolian sand and sandy gravel that buries the ferricrete is only 15–20 cm thick. The upper few centimeters of the sand contain a slight accumulation of organic matter that defines a soil-A horizon. Particle-size analyses from a vertical sequence of samples in the sand unit show a gradual but noticeable increase in clay with depth that probably indicates clay enrichment from weathering and soil formation (see the section on "Description of Units Exposed in the Trenches," fig. 21, and table 5). As we noted in the discussion of the eastern Lake Surprise trench stratigraphy, the absence of a well-defined clay bulge in the profile implies that the sand has accumulated gradually and continuously during a period of probably many thousands of years. A sample of the basal part of the sand from 1.9 m deep yielded a TL age of 46±3.5 ka (sample TC3S/1.7, table 9), which approximates the time when unit **es** began to accumulate at this locality.

A thin layer of angular gravel (unit **ag**) is present beneath the eolian sand only on the north side of the fault zone. The gravel is poorly sorted and contains about equal amounts of medium-grained sand, ferricrete nodules, and angular 3- to 8-cm-size quartzite fragments. The gravel pinches out, and the overlying eolian sand thickens to the south. The origin of the angular gravel is uncertain and difficult to determine because only a small amount of the unit was exposed. It may be a thin layer of colluvium that collected on the ground surface prior to deposition of the eolian sand. Alternatively, the poor sorting and the presence of unusually large, angular clasts in a finer grained matrix could be evidence for a debris-flow origin, although the deposit lies on a surface that has a very gentle slope.

The ferricrete in this trench was exposed only on the north side of the scarp. We divided the ferricrete into a gravel unit (**fcg**) and a massive unit (**fcm**). Both the gravel and the massive ferricrete are present as a reddish-brown oxidized facies and as a drab, whitish-gray reduced facies (units **fcgr**, **fcmr**).

The ferricrete gravel consists of clast-supported ferrous nodules in a matrix of medium to coarse sand (see the section on "Description of Units Exposed in the Trenches" for detailed information). The cores of the nodules are commonly composed of maroon hematitic clay that contains about 20–40 percent angular, sand-size quartz grains. The smaller nodules (1–2 cm in diameter) are typically maroon throughout, whereas the larger ones (3–6 cm in diameter) commonly contain manganese oxides on fracture surfaces in the nodules' interiors.

In parts of the trench, the ferricrete gravel rests on a densely cemented, massive, oxidized ferricrete (unit **fcm**)

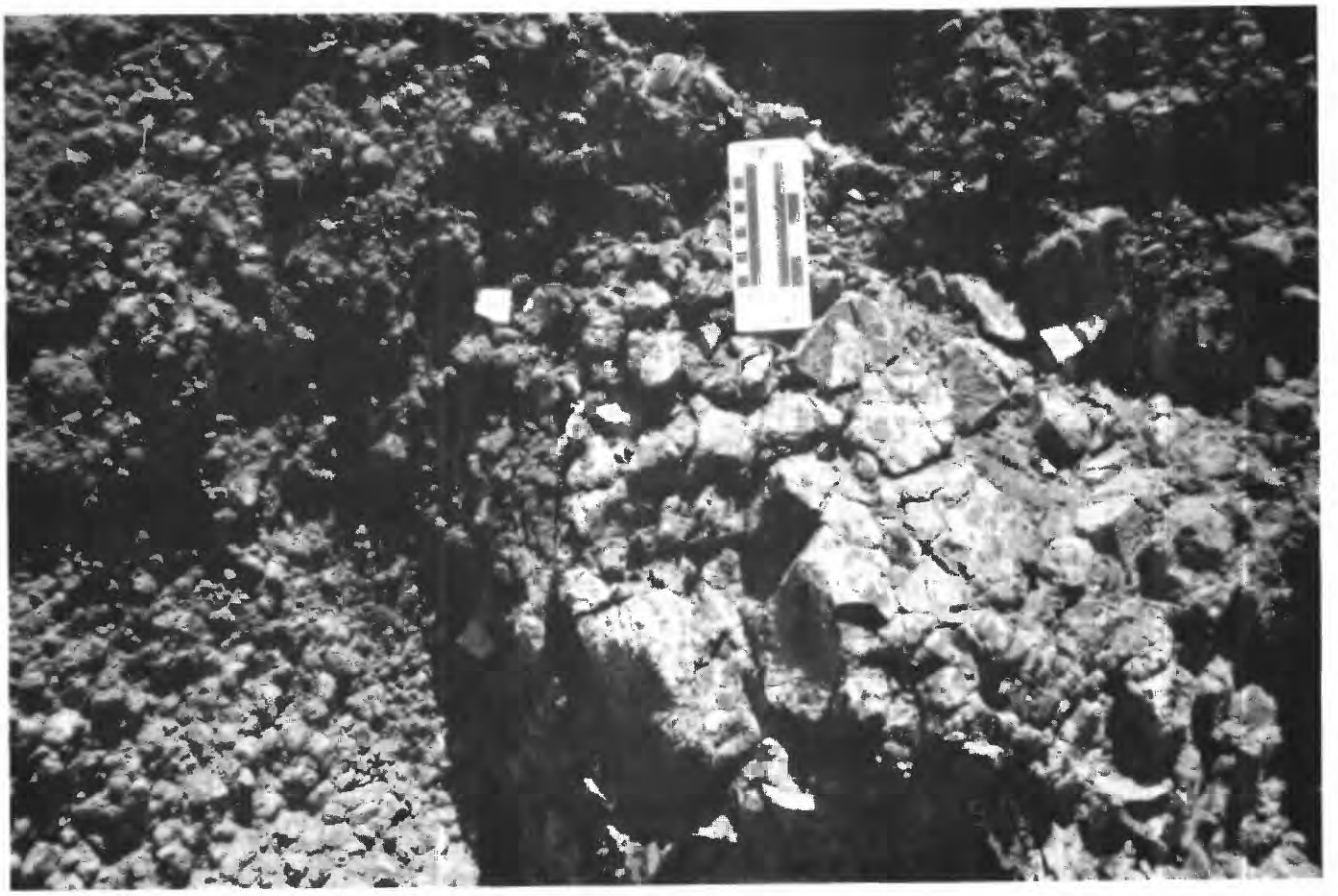

Figure 14. Hematitic quartzite (unit **rq(f)**, pl. 2*B*), which is fractured into roughly rhombohedral blocks 4–6 cm in diameter. A map of the wall of western Lake Surprise trench 1 is shown in pl. 2*B*. Photograph shows quartzite block at x=16 m, y=2.5 m on trench map (pl. 2*B*). Right side of bar scale is divided in inches and left side in centimeters. View is to the east.

and reduced ferricrete (unit fcmr). The massive ferricrete is composed of densely packed angular to subrounded fragments of bedrock that contain a minor amount of iron and manganese oxide cement and sand between the fragments. In places, the ferricrete is sufficiently cemented that it appears similar to the intensely fractured bedrock.

The bedrock (unit rq) in the trench is composed of variably fractured and sheared, medium- to coarse-grained hematitic quartzite. It is pervasively oxidized and contains joint sets that divide the rock into roughly rhombohedral blocks about 4–6 cm on a side (fig. 14). The blocks have a 1- to 5-mm-thick yellow-white rind that is probably the result of reduction of iron oxide. The open joints between the blocks are partly filled with aggregates of iron and manganese oxides that typically are slightly more than 1 mm thick. These aggregates are patchy and do not completely surround the blocks. We interpret these aggregates to be products of the modern near-surface oxidizing conditions, whereas we attribute the yellow-white rinds on the peripheries of the blocks to be the result of an earlier episode of reducing geochemical conditions.

STRUCTURAL FEATURES IN TRENCH WLS–1

The Quaternary deposits in WLS–1 show little evidence of brittle deformation from the 1988 earthquakes (pl. 2*B*). The topographic relief across the western Lake Surprise scarp indicates a net down-to-the-south throw (pl. 1*E*). Both geodetic data (Bowman, 1991) and the distribution of aftershocks (Bowman and others, 1990) indicate that south-directed reverse slip occurred on a north-dipping fault plane along this section of the 1988 scarps. However, the most conspicuous faults in this trench are associated with shear zones in the fractured bedrock that span a range of dips from gently (25°) southward to nearly vertical. Reverse slip on these faults would produce a sense of throw that is opposite to net topographic relief of the scarp. Thus, the south-dipping shear zones are not a direct expression of the main seismogenic fault at depth, but rather, they accommodate shortening at the surface.

We believe that the only near-surface expression of slip on the main north-dipping fault is the network of subtle fractures that dip 20°–25° north in the thick eolian sand between

meters 7 and 12.5 (pl. 2*B*). These fractures strike 060°, which is within a few degrees of the local strike of the scarp. The fractures probably mark the location where deformation in the Quaternary deposits was concentrated, but the amount of deformation was insufficient to cause displacement in the poorly consolidated deposits at the surface. The contacts between units **es** and the underlying unit **fcg** are not displaced by the fractures. The presence of bedrock, which was already extensively fractured and thus contained numerous potential slip planes, probably allowed the slip at depth on the main fault to be distributed among a network of shears and small faults within the brecciated, near-surface bedrock. Because the slip was not concentrated on a single shear zone, brittle deformation is very poorly expressed in the Quaternary deposits.

Other than the net relief on the scarp, the greatest amount of ground deformation in the trench was at the 19.4-m mark on the trench map (pl. 2*B*). At this point, a small (about 15 cm high), north-sloping monocline formed as a result of movement on a prominent, south-dipping shear zone in the bedrock that strikes 069°. The amount of slip on this shear was insufficient to rupture the surface and create a scarp with a free face, although it did cause a bulge in the ground surface.

OBSERVATIONS PERTINENT TO PREHISTORIC RUPTURING

Several lines of evidence show that repeated movement has occurred on faults associated with the western Lake Surprise scarp. The fractured bedrock in the trench is most likely a shallow eastward extension of bedrock that is part of the quartz ridge. Ancient faults are commonly mineralized with quartz or jasper (Dodson and Gardener, 1978) to form quartz ridges; thus the western Lake Surprise scarp is probably associated with an old fault zone that was reactivated in 1988. The time when these old fault zones formed and were subsequently mineralized is poorly known, but in the Tennant Creek area, both are thought to have occurred in Precambrian time (Dodson and Gardener, 1978). Several sections of the surface ruptures from the 1968 Meckering earthquake in Western Australia coincide with small quartz reefs that correspond to old, mineralized faults (Gordon and Lewis, 1980). Similarly, some of the surface ruptures from the 1979 Cadoux earthquake in Western Australia are adjacent to or coincide with quartz dikes in areas where bedrock is shallow (Lewis and others, 1981). Likewise, the southern part of the ruptures from the 1970 Calingiri, Western Australia, earthquake coincides with a 20-m-wide band of quartz float that is thought to mark the trace of a mineralized but concealed fault (Gordon and Lewis, 1980). Thus, parts of the ruptures coincide with probable mineralized old faults in four of the five historical surface-rupturing earthquakes in Australia.

The well-developed shear fabric and thickness of the south-dipping shear zones in trench WLS–1 and the fracturing and brecciation in the quartzite bedrock are so pervasive that it is unlikely that this fracturing and brecciation is solely the result of the small amount of 1988 movement. This shearing and fracturing is clear evidence of pre-1988 movement on the fault zone after the rock in the quartz ridge was mineralized. The relations between the 1988 fractures and Quaternary deposits show that most of the ancient shear zones were not reactivated in 1988. The Quaternary deposits in the trench contain no direct evidence that they had been deformed by prehistoric faulting. In the absence of direct evidence (such as scarp-derived colluvium or faulted Quaternary deposits), we cannot decisively demonstrate prior Quaternary movement on this fault zone.

However, the stratigraphic relations in the trench do offer indirect evidence that can be interpreted as favoring Quaternary movement. Quartzite bedrock was exposed only on the north side of the fault scarp even though the trench was as much as 2.5 m deep on the south side of the scarp (pl. 2*B*). This relation shows that the relief on the bedrock is at least twice as great as the 1.1 m of topographic relief generated by the 1988 ruptures. Thus an old bedrock scarp is present at this locality that was at least as high as the 1988 scarp. The eolian sand (unit **es**), which is about 2 m thick south of the scarp compared to 10–15 cm thick north of the scarp, began to bury this scarp about 46,000 yr ago (table 9). Near the 15-m mark, a lens of angular gravel (unit **ag**, pl. 2*B*), which contains anomalously large clasts, is present along the upper part of this buried scarp (fig. 15). We interpret this deposit as a lag gravel that was being transported down the slope of the scarp as it was being buried. The strike of the buried scarp is subparallel to the 1988 scarp; the ferricrete gravel (unit **fcg**)-eolian sand (unit **es**) contact near the 15-m mark strikes 081° compared to a strike of 067° for the 1988 scarp.

The origin of this bedrock scarp is uncertain. It could be (1) an ancient fault scarp related to prior movement on the Lake Surprise fault, (2) a fluvial scarp related to an eastward-flowing paleodrainage system, or (3) a combination of these two features. If it is an ancient fault scarp, then, by definition, it is evidence of prehistoric surface rupturing on the fault. The bedrock scarp clearly predates the upper Pleistocene eolian sand. We speculate that the scarp is no older than latest Tertiary based on our belief that topography older than latest Tertiary is unlikely to have survived as a physiographic feature for several million years. Such an ancient scarp would likely have been either buried or eroded long before the eolian sand was deposited starting about 46,000 yr ago.

Alternatively, the scarp could be a fluvial feature that was formed by preferential erosion south of the fault zone where the bedrock of unknown lithology might be more easily eroded than the resistant quartzite north of the fault zone.

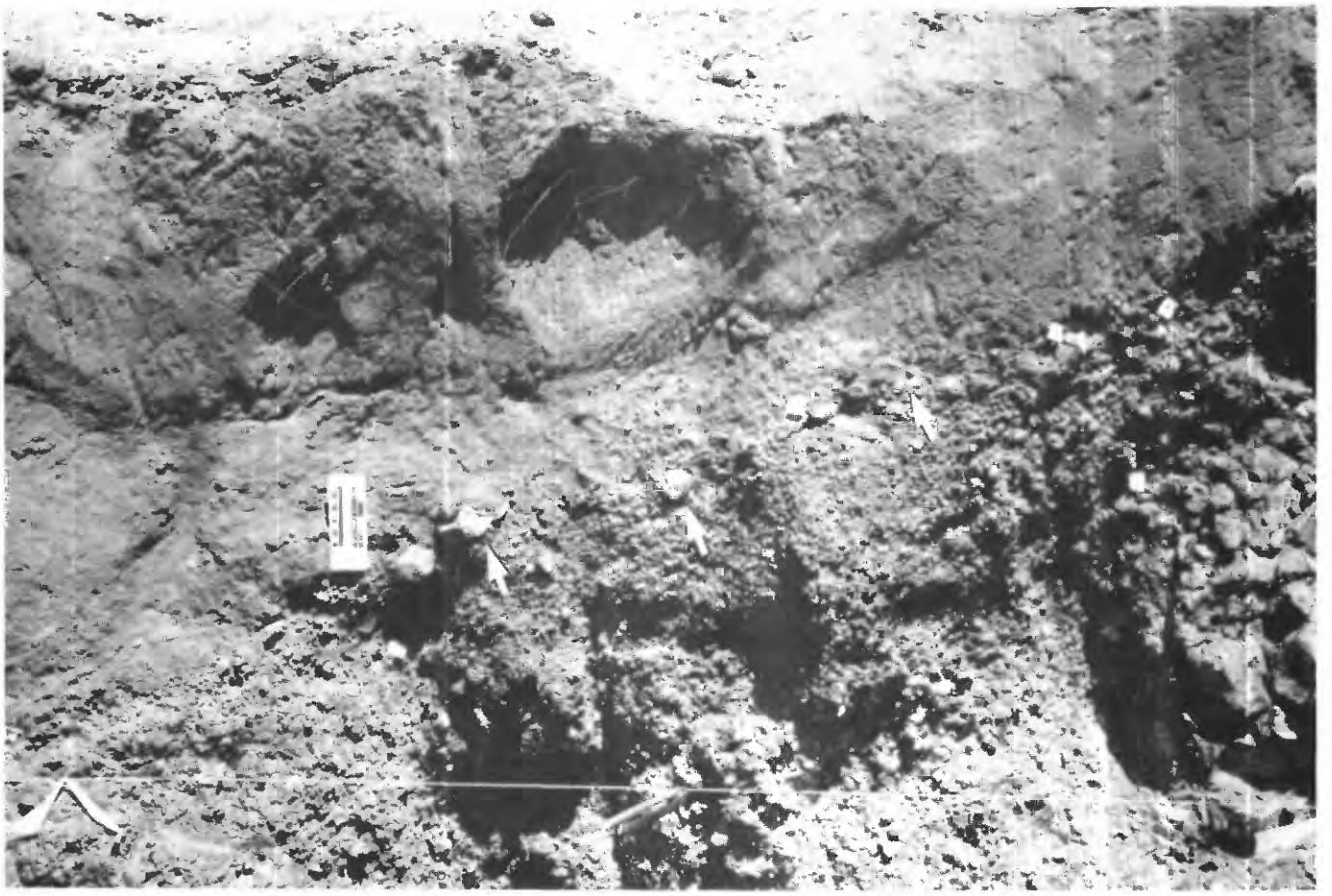

Figure 15. Angular gravel (unit **ag**, pl. 2*B*) that separates eolian sand and ferricrete gravel at the 15-m mark in western Lake Surprise trench 1. The gravel layer, indicated by arrows, contains anomalously large clasts and is interpreted as a lag deposit on the slope of an ancient scarp. Right side of bar scale is divided in inches and left side in centimeters. Base of scale is close to downslope (south) end of unit **ag**, as mapped on pl. 2*B*. Pieces of flagging on the string line at bottom left and bottom center of photograph are 1 m apart. Fractured bedrock shown in figure 14 is partly visible in lower right corner.

The modern topography immediately east and southeast of the quartz ridge and the 1988 scarp is marked by a broad (hundreds of meters wide), low-relief (several meters deep) swale that slopes gently eastward toward Lake Surprise. The swale, which is subtle but is apparent mainly because of the area's extremely flat topography, might mark the location of an old stream channel. However, we note that none of the modern streams in the adjacent area seem to be capable of incising a significant channel in Quaternary deposits or underlying ferricrete. Thus it is possible that there may not have been adequate relief in the area to cause streams to vigorously incise and form erosional escarpments in resistant bedrock.

However, the geometry of the reduced eolian-sand (unit **esr**), and the reduced sand and ferricrete gravel (unit **esr+fcgr**) in WLS–1 (pl. 2*B*) tend to support the interpretation of a fluvial channel. The upper contact of the reduced sand and ferricrete gravel has a shape like a fluvial channel, and the overlying reduced eolian sand has the configuration of a channel-filling deposit. We suspect that the drab colors of the reduced ferricrete gravel and sand are the result of localized geochemical reducing conditions similar to those that might develop in a water-saturated depression like a paleochannel.

Even though we cannot conclusively demonstrate that an ancient fault scarp existed at this locality, the trench does show that a bedrock escarpment was present before it was buried by late Quaternary eolian sand. The escarpment strikes subparallel to the 1988 scarp and has more than twice as much relief as the 1988 scarp. The evidence we cite favoring the presence of a paleochannel does not preclude the possibility that the bedrock scarp was originally the product of faulting. An ancient fault scarp that has resistant quartzite in the hanging wall would probably exert a strong control on the local drainage system, especially in a low-relief landscape. The development of a stream channel along the base of such a scarp would not be unusual or unexpected. We favor a polygenetic origin for the bedrock escarpment and suspect that it is an ancient fault scarp that was subsequently modified by fluvial processes.

WESTERN LAKE SURPRISE TRENCH 2

CHARACTERISTICS OF FAULT SCARPS NEAR THE TRENCH

We excavated a second trench (WLS–2) on the western Lake Surprise scarp to compare a locality where near-surface faulting produced a small but distinct surface rupture (WLS-2) to a locality where the 1988 deformation produced a generally unbroken, sloping surface (WLS–1). The stratigraphy exposed in trenches WLS–1 and WLS–2 is similar, in terms of both the bedrock and the surficial units. Trench WLS–2 was about 375 m west-southwest of WLS–1 and 208 m east-northeast of AUSLIG survey station 24000 along a bearing of 251°.

Overall, the scarps at both localities are morphologically similar—they consist mainly of a planar surface sloping uniformly southward. The scarp at WLS–2 is 0.8 m high and has a surface offset of 0.8 m (pl. 1*G*). The most significant difference between the two localities is that at WLS–2, a south-directed reverse fault ruptured the ground surface and produced a 15-cm-high scarplet (fig. 16). The toe of the scarplet is partly buried by post-1988 eolian sand and colluvium. The ground surface of the hanging wall immediately upslope of the scarp is littered with angular 2- to 10-cm-size fragments of milky quartz that are pervasively stained orange red with iron oxide. These rock fragments are anomalous in a region where the land surface is almost universally mantled by eolian sand.

In plan view, the scarp in the vicinity of the trench has a simple trace and a generalized local strike of about 061° (pl. 1*F*). Northeast of the trench, the scarp is essentially linear, but southwest of the trench, its trace is slightly more sinuous, and the ground on the hanging wall is warped into small-amplitude anticlines and synclines.

Along this section of the western Lake Surprise scarp, a series of prominent, discontinuous extensional fractures run subparallel to but about 5–15 m north-northwest of the reverse-fault scarp (pl. 1*F*). The fractures are typically 20–30 cm wide, and some are open to depths of as much as 1 m, whereas others are almost completely filled with collapse debris and eolian sand. The fractures are generally arranged in a right-stepping en echelon pattern, which could be evidence of a minor component of left-lateral slip.

About 12 m west-southwest of the trench, a roughly 1-m-deep exploratory pit was dug into the fault scarp by mineral prospectors (pl. 1*F*). Based on the degradation of the spoil pile and the size of the vegetation growing on it, we think that the pit was dug before the 1988 earthquakes. This pit shows that there was some evidence of shallow bedrock at this locality before the earthquakes; this evidence may have simply been the presence of quartz float on the surface. The exact location of the pit on the trace of the 1988 rupture may simply be fortuitous, or alternatively, the pit may have been dug into an anomalous topographic feature such as a small subdued fault scarp that could have existed before the 1988 earthquakes. Although we attach little significance to the presence of the pit, its coincidence with the 1988 rupture is noteworthy in terms of possible evidence of prior faulting at the surface.

STRATIGRAPHY IN TRENCH WLS–2

Trench WLS–2, as trench WLS–1, exposed fractured bedrock capped by Quaternary deposits north of a main fault zone and primarily eolian sand and angular gravel south of the zone (pl. 2*C*). The bedrock in WLS–2 is massive, pervasively fractured and jointed hematitic quartzite (unit **rq(f)**) that is typically broken into orthogonal blocks 5–10 cm in size. In places, the bedrock is pervasively altered (unit **rf**) and it grades into a massive ferricrete breccia (unit **fcm**) composed of angular blocks. Individual blocks in unit **fcm** contain a core of iron oxide surrounded by an interior rim of manganese oxide and an outer rind of iron oxide. The quartzite and ferricrete are overlain by 15–30 cm of ferricrete gravel (unit **fcg**) that is composed of ferrous nodules 0.5–1.5 cm in diameter. Between the 1.25- and 2.25-m marks in the trench (pl. 2*C*), a pocket of mixed angular gravel and ferricrete gravel (unit **ag+fcg**) is present at the stratigraphic level of the ferricrete gravel. This pocket contains ferricrete gravel mixed with 5–10 percent subrounded to angular fragments of quartzite, 3–8 cm in size. The quartzite fragments are distinctive because they are several times larger than the few fragments of bedrock in the adjacent ferricrete gravel unit (**fcg**). The geometry of this pocket, its limited size, and its presence directly over a cluster of near-vertical faults and fractures in the bedrock suggest that the pocket might be fill in an ancient graben.

The ferricrete gravel unit is overlain by an angular gravel (unit **ag**), which is composed of about equal parts of eolian sand, ferricrete gravel, and angular fragments of quartzite, 3–15 cm in size. The quartzite fragments in unit **ag** are distinctive because of their large size, which is comparable to the fragments in the pocket of unit **ag+fcg**. Initially, one might be inclined to interpret the angular gravel as simply a residual deposit composed of fractured bedrock (unit **rf**) and ferricrete gravel (unit **fcg**) mixed with the overlying eolian sand (unit **es**) but, when carefully examined, this explanation is unsatisfactory. The distinctive quartzite fragments are good evidence that the angular gravel is a transported deposit rather than a residual deposit because, except for the small pocket of unit **ag+fcg** between meters 1 and 2, the gravel is isolated from the underlying fractured bedrock by 15–30 cm of ferricrete gravel. No obvious weathering mechanism can move the large pieces of quartzite upward through the ferricrete gravel without leaving quartzite fragments in the gravel. Furthermore, the shape of the angular

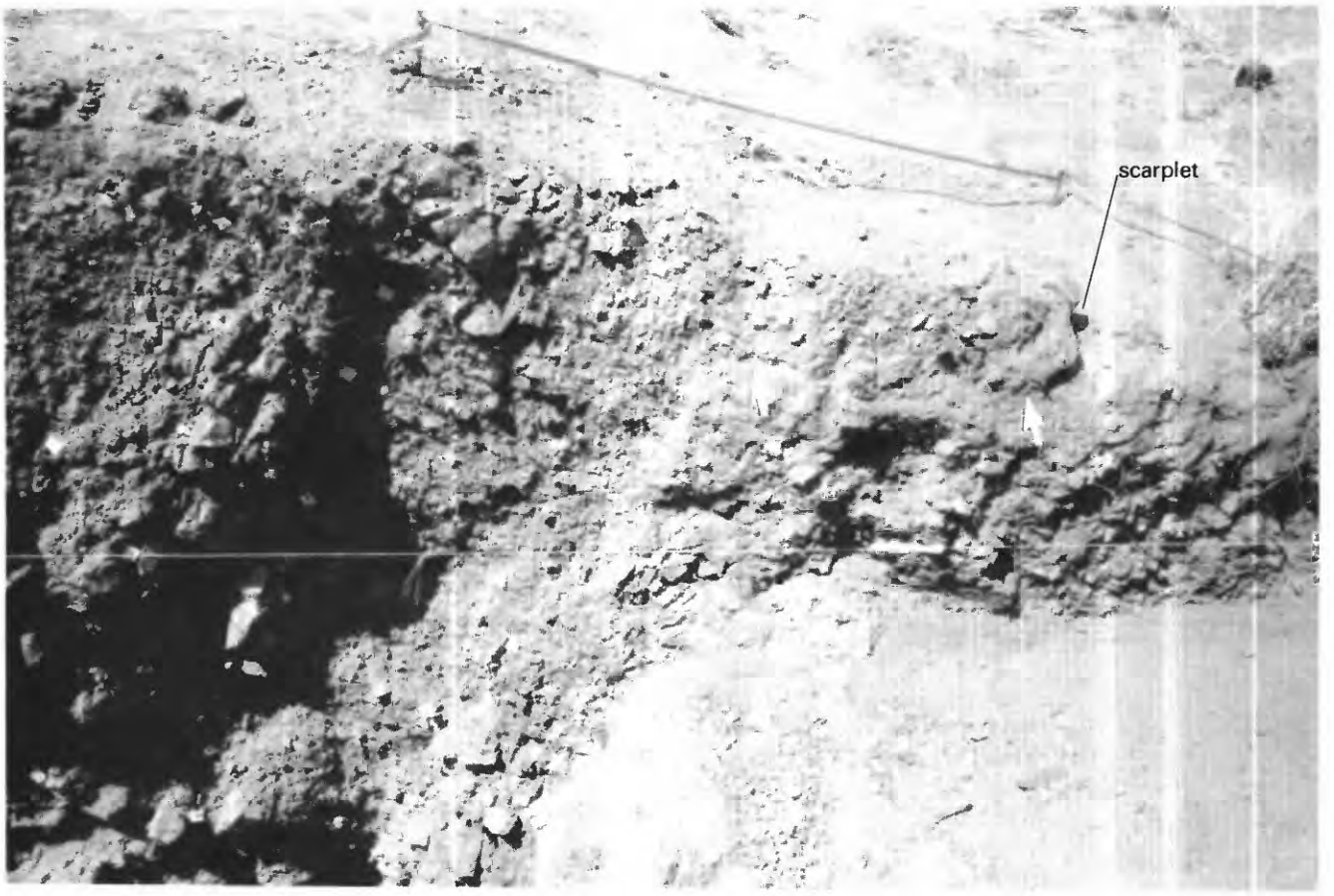

Figure 16. East wall of western Lake Surprise trench 2 showing scarplet that formed during 1988 earthquakes. Maps of the wall are shown on pl. 2*C*. Arrows indicate base of collapse blocks (unit csb, pl. 2*C*) of eolian sand and ferricrete gravel that fell onto the pre-1988 ground surface from the hanging wall of the fault. View spans about 2.5 m of trench wall.

gravel's basal contact supports a depositional origin. The gravel thins slightly to the south and pinches out against unit fcg near the fault zone. The geometry of the angular gravel indicates that the pinchout is the result of nondeposition rather than truncation by faulting. Apparently, the gravel was deposited against a small topographic bulge, which would be directly above the main fault zone. This bulge could be the result of past ground deformation at the fault zone. We prefer to interpret the angular gravel as a thin debris-flow deposit that may have originated on the nearby quartz ridge during an episode of intense rainfall, which is common under modern climatic conditions in this area. The angular gravel is covered by a thin mantle of eolian sand that is slightly darkened in the upper part by soil organic matter. Post-1988 erosion has stripped the sand from the crest of the fault scarp and exposed the underlying sheared ferricrete gravel (unit fcg(s)) at the scarp.

Directly south of the fault zone, the trench exposed a small area of very loose, iron-rich, brecciated quartzite (unit rf) capped by ferricrete (unit fcm), but, to the south, these units project well below the bottom of the trench. Next to the fault zone, the bedrock and ferricrete are buried by a lens of angular gravel (unit ag). Downslope the angular gravel grades into a mixture of angular and ferricrete gravel (unit ag+fcg) that is capped by eolian sand (unit esr). The interfingering, gradational transition between the angular gravel (unit ag) and the mixed angular and ferricrete gravel (ag+fcg) downslope indicate that these units are facies of a single depositional group. The angular gravel is a coarse-grained proximal facies of debris eroded from the bedrock, and the mixed gravel is a finer grained, more distal facies. The mixed gravel contains at least two distinct stone lines defined by aligned large rock fragments (pl. 2*C*). The stone lines converge upslope (to the north) and probably represent either temporary pauses during deposition of the mixed gravel or brief episodes of accelerated deposition when coarse debris was moved unusually far downslope. The facies relations and the stone lines indicate that, prior to deposition of the eolian sand, a bedrock escarpment existed at the fault zone.

The eolian sand is subdivided into three units on the basis of color and cementation: A basal unit that has a

slightly reduced color (unit esr), a middle unit that is moderately indurated (unit esm), and an upper unit that is slightly stained with organic matter (unit es). Each unit except the eolian sand (unit es) thins to the north and onlaps the underlying gravel units. As the eolian sand was deposited across the landscape, it buried and completely concealed the bedrock escarpment associated with the fault.

Where the 1988 rupture reached the surface, small blocks of eolian sand and sheared ferricrete gravel (unit csb) from the hanging wall were thrust onto the pre-1988 ground surface of the footwall (fig. 16; inset, pl. 2*C*). Some blocks were probably emplaced directly by thrusting along the ground because the uppermost part of the pre-1988 surface is deformed into two small chevron folds presumably formed by compression of moist sediment. However, some individual blocks are overturned and probably collapsed from the free face as the scarp became oversteepened. The collapsed blocks have been partly buried by recently deposited eolian sand.

STRUCTURAL FEATURES IN TRENCH WLS–2

The near-surface faulting and deformation at this locality is confined to a 3- to 4-m-wide zone of fractured quartzite in the hanging wall of the fault, and the most intense shearing and fracturing is confined to within 1 m of the 1988 rupture plane. Virtually all the 1988 slip occurred on a narrow, well-defined fault zone along the southern edge of the quartzite (unit rq(f)) that dips 65°–84° to the north in the trench and strikes 062°. The quartzite north of this main fault zone contains numerous fractures and shears that are subparallel to the 1988 fault, but none showed evidence of significant movement in 1988. The Quaternary deposits in the footwall of the fault are completely undeformed, and those in the hanging wall are slightly fractured but otherwise undeformed.

A set of fractures and small-displacement faults that we interpret as mainly pre-1988 (between 1.5–2.0 m in the hanging wall, pl.2*C*) do show some evidence of minor reactivation in 1988. Small void spaces between the walls of these faults and fractures indicate that a small amount of extension or differential slip occurred recently. The trend of these fractures and faults (056°–058°) projects into a 2- to 30-cm-wide open fissure that is about 15–20 m east of the trench. The minor reactivation of these faults and fractures in 1988 is also indicated by the slight sag at about 59 m on the WLS–2 scarp profile (pl. 1*G*). These faults and fractures are visible only in the quartzite and cannot be traced upward into the mixed gravel and ferricrete (unit ag+fcg) or overlying units, which shows that they formed before 1988.

Two shears that dip steeply to the north also show evidence of pre-1988 movement. A near-vertical shear at about 3.6 m (pl. 2*C*) was obvious in the ferricrete (unit fcm) near the bottom of the trench. Upwards, it defines the contact between iron-rich bedrock (unit rf) and ferricrete gravel (unit fcg). A weak fabric in the ferricrete gravel (unit fcg) above the contact indicates that the last movement on this shear postdates formation of unit fcg, but we saw no indication that this shear extends into the overlying angular gravel. The second shear is a prominent reverse fault that is parallel to, but about 50 cm north of the 1988 fault plane. Movement on this fault has transported a large block of fractured quartzite (unit rq(f)) up and over a wedge of sheared ferricrete gravel (unit fcg(s)). The fault can be traced to the top of the gravel but not into the overlying eolian sand. The sheared ferricrete gravel in the footwall block of this fault contains abundant rock fragments that could be coarse debris shed from an ancient bedrock scarp.

Between the 3- and 5-m marks in the bottom part of the trench (pl. 2*C*), two moderately steep faults that dip to the north are present in the ferricrete gravel (unit fcg) and adjacent fractured quartzite (unit rq(f)). Even though these faults are subparallel (065°) to the scarp, they had no apparent displacement in 1988.

OBSERVATIONS PERTINENT TO PREHISTORIC RUPTURING

Western Lake Surprise trench 2 exposed our best evidence of prehistoric surface rupturing along the 1988 Tennant Creek scarps. The bulk of the 1988 slip at WLS–2 occurred on a single, well-defined fault plane, yet the adjacent bedrock contains numerous significant faults that were not reactivated in 1988. The strong shear fabric and the quantity of gouge along many of these faults shows that a substantial amount of movement must have occurred in the past. Most of these faults do not extend into the ferricrete gravel (unit fcg) that overlies the bedrock, so the only time limit they establish is that the last movement postdates the bedrock, which is probably Precambrian.

However, three independent lines of stratigraphic evidence provide substantial support for prior Quaternary surface faulting on the western section of the Lake Surprise fault. One line of evidence is the pocket of mixed angular gravel and ferricrete gravel at 1.25–2.25 m (unit ag+fcg, pl. 2*C*), which we interpret as fill in a fissure that developed above the faults and fractures in bedrock. The development of an open fissure obviously implies the occurrence of a prehistoric earthquake. The bedrock faults and fractures beneath the fissure filling probably connect to similar fractures 15 m to the east, where open fissures formed in 1988.

A second line of evidence is the presence of at least two distinct shears and fractures that can be traced from the bedrock and ferricrete into the overlying ferricrete gravel but not upward into the angular gravel and eolian sand. TL data indicate that the sand is late Pleistocene to possibly Holocene; a sample of the sand from 0.5 m below the surface in the footwall yielded a TL age of 10±0.8 ka (sample TC4S/50, table

9). We presume that the angular gravel (unit ag), which lies directly beneath the sand, is also late Pleistocene. The presence of shears in unit fcg that do not extend into the shallower, younger deposits also implies the occurrence of a surface-rupturing paleoearthquake. However, the presence of a fault strand that cannot be traced upward into undisturbed deposits does not necessarily mean that the last movement on that strand predates deposition of the undisturbed deposit (Bonilla and Lienkaemper, 1991).

The third line of evidence is the facies relations between the lens of angular gravel (unit ag) and the mixed angular gravel and ferricrete gravel (unit ag+fcg) south of the fault zone, which show that a significant paleoscarp existed at this locality. The facies relations between the gravels and the onlap of the eolian sand onto these gravels show clearly that a bedrock scarp was present before deposition of the upper Pleistocene sand. More than 1.65 m of relief exists now on the top of the bedrock (highest point of bedrock north of scarp at 3.5-m mark versus low point in trench south of scarp at 11.35-m mark, pl. 2*C*), which is more than twice the size of the 1988 scarp (0.8 m). Thus, the pre-1988 scarp was at least equal in size to the historical fault scarp.

Stratigraphic evidence in this trench does not unequivocally establish whether the pre-1988 scarp was a fault scarp or a fluvial scarp. If the scarp is a tectonic feature, the stone lines in the mixed angular gravel and ferricrete gravel (unit ag+fcg) could indicate times when recurrent faulting renewed the relief on the scarp. Alternatively, if the paleoscarp is a fluvial feature, the stone lines could simply represent brief episodes of accelerated degradation of the scarp, perhaps caused by major storms, or could be lag deposits that mark temporary intervals of nondeposition. The similarities in the stratigraphy in trench WLS–1 and WLS–2 suggest that the pre-1988 scarps at both localities have a common origin. However, independent evidence of a possible fissure fill and upward-terminating faults in WLS–2 favor an explanation of this paleoscarp as originating by pre-1988 movement on the western Lake Surprise fault.

TRENCHING OF THE KUNAYUNGKU SCARP

The Kunayungku scarp is about 10 km long and consists of sinuous, discontinuous surface ruptures that trend about 110° (pl. 1*A*). The scarp is about 6 km north and northwest of the western part of the Lake Surprise scarp. Movement on the Kunayungku fault is south-over-north with a net throw on the order of 0.1–1.0 m (Bowman, 1991; pls. 1*I*–1*L*). The seismological data from the 1988 earthquakes indicate that this scarp formed from a rupture that propagated from east to west and updip (Choy and Bowman, 1990; McCaffrey, 1989) during the first of the three main shocks (Bowman, 1988).

The Kunayungku trench was roughly near the midpoint of the scarp (pl. 1*A*), 58 m southeast of AUSLIG survey station No. 4635 (labeled Sta. A6 in the field) on a bearing of 117° (pl. 1*H*); this bearing intersects the trench wall at the 17.5-m mark on the trench map (pl. 2*D*). The AUSLIG station is identified by a 1.5-m-high steel stake in the field.

CHARACTERISTICS OF FAULT SCARPS NEAR THE TRENCH

Deformation near the Kunayungku trench is typical of the ruptures along the entire Kunayungku scarp. The surface deformation is expressed as a series of broad folds and monoclines that have amplitudes of as much as 1.5 m and wavelengths of several tens of meters (pls. 1*H*–1*L*). The folds are generally aligned in a right-stepping en echelon pattern (pl. 1*H*), and limbs of the folds are commonly ruptured by low-angle faults that dip to the north and south and that have a few tens of centimeters of displacement. Where present, the free face on a rupture is commonly only 10–20 cm high. All of the reverse faults shown on the map of the Kunayungku trench locality (pl. 1*H*) have less than 25 cm of throw. Many of the fault scarps are associated with backthrusts, that is, second-order reverse faults whose transport direction is north-over-south, which is opposite to that of the master reverse fault at depth. Even though the folding has produced as much as 1.5 m of local relief, the net throw on the Kunayungku scarp is typically 1 m or less (pls. 1*I*–1*L*). Folding and the surface deformation from the 1988 earthquakes is conspicuous relative to the very flat terrain surrounding the Kunayungku scarp. The overall width of the zone of surface deformation is commonly 30–50 m, but locally it is more than 70 m wide.

The right-stepping en echelon pattern of the folds is well developed within about 1 km of the trench. The crests of the folds are commonly cracked by a network of anastomosing open fissures and fractures that form a polygonal pattern roughly subparallel to the crest. Along the flanks of many arches, some of the trees and bushes have died because their tap roots have been severed by faulting. In addition, most of the *Spinifex triodia sp.* (bunch grass) on the arches has died owing to their high topographic position and increased elevation above the local water table.

STRATIGRAPHY IN THE TRENCH

The 22-m-long Kunayungku trench began in the nearly flat footwall of the scarp, crossed a prominent bulge and small south-facing scarplet, and extended across the apex of a broad arch (pl. 1*J*). The trench trended 027° and exposed three distinct stratigraphic units: (1) Deeply weathered bedrock (unit ra, pl. 2*D*) that was present along most of the bottom of the trench, (2) an overlying ferricrete unit (fcm) that

is about 40–60 cm thick, and (3) a relatively homogeneous eolian sand (unit es) that extends to the surface.

Bedrock in the Kunayungku trench is soft, massive, light-grayish-green claystone that is mottled with yellowish orange and black stains of iron and manganese oxides. The bedrock is broken into angular prisms 2–3 cm in diameter. Clay coatings on the prism faces show that some differential movement has occurred between individual blocks, but we attribute much of this movement to swelling and shrinking as the clayey rock was wetted and dried. The density of fractures and the intensity of shearing in the claystone increase greatly closer to the main fault (14.5 m, pl. 2*D*). Much of this fracturing and shearing is probably a direct result of the 1988 earthquakes because it was relatively easy to pluck out blocks of the bedrock by hand within 1 m of the main fault, whereas a rock hammer was needed to extract pieces of the normally compact claystone elsewhere in the trench. Thus, both stress cutans (frictionally induced clay coatings) and argillans (shrinkage-induced clay coatings) are probably present in the trench.

The bedrock is so extensively weathered and altered that it is difficult even to speculate on the characteristics of the original parent rock. In the late 1970's, a network of boreholes was drilled near the Kunayungku scarp as part of a regional ground-water evaluation program. The results of the drilling program show that, in places, about 15 m of Cenozoic sedimentary rocks rest on Precambrian metamorphic and igneous rocks and Cambrian sedimentary rocks (Verhoeven and Knott, 1980; Verhoeven and Russell, 1981). Unfortunately, the reports describing the subsurface stratigraphy fail to elaborate on the characteristics of the Cenozoic sedimentary rocks. We speculate that the easily excavated claystone in the trench might be part of these Cenozoic sedimentary rocks, although it could also be very extensively weathered Precambrian or Cambrian rock.

In this trench, the bedrock is overlain by ferricrete (unit fcm) that is composed of rounded to subrounded ferruginous nodules. The ferricrete appears to be a transitional unit between the claystone and the overlying eolian sand. The upper half of the ferricrete contains abundant red sand in the matrix, but downward the sand content diminishes and the clay content in the matrix increases.

The most extensive deposit in the trench is a blanket of dark red, eolian sand (unit es) that ranges in thickness from less than 1 m to more than 1.5 m and is composed of well-sorted, nonstratified fine- to coarse-grained quartz (see the section on"Descriptions of Units Exposed in the Trenches"). The sand has moderately well developed soil that consists of A/B and B/A horizons in the upper 15–20 cm, a cambic (Bw) horizon that is defined on the basis of color change, and a deep argillic (Bt) horizon that is defined by a progressive increase in clay toward the ferricrete (see the section on "Description of Units Exposed in the Trenches," fig. 23, and table 7). The argillic B horizon contains as much as 14 percent clay, extends to more than 1-m depth, and is formed in a parent material of well-sorted eolian sand that probably had only a few percent clay initially. This degree of clay accumulation strongly suggests that the material near the base of unit es is late Pleistocene and is probably at least several tens of thousands of years old. This conclusion is corroborated by TL age determinations on a sequence of four samples from the hanging wall (south) of the fault (pl. 2*D*). The samples were collected from depths of 0.2 m, 0.45 m, 0.8 m, and 1.1 m, and have TL ages of 6.6±0.5ka, 10.7±0.8 ka, 23.0±2.2 ka, and 30±2.3 ka, respectively (table 9).

We mapped a thin unit at the base of the sand between 18 and 20 m (pl. 2*D*) that is identified as unit es and fcm (a mixture of eolian sand and the underlying ferricrete). The mixing that produced this unit appears to be nontectonic and was probably caused by bioturbation or some other surficial process.

STRUCTURAL FEATURES IN THE TRENCH

The 1988 earthquakes caused warping, flexing, and plastic deformation in the weathered claystone and the overlying Quaternary deposits at the Kunayungku trench site (fig. 17). Nearly all of the topographic and structural relief across the scarp results from monoclinal warping; brittle failure on faults is responsible for only a small fraction of the total structural relief.

Two networks of faults were present in the trench: (1) A major, southward-dipping reverse fault and its associated subsidiary fractures that extend down to a small step in the bedrock at the bottom of the trench (14.5-m mark on pl. 2*D*); and (2) a network of low- to moderate-angle, northward-dipping reverse faults and fractures that are concentrated in the footwall of the fault. Some of the northward-dipping faults and fractures in the intensely faulted area between 10 and 12 m (pl. 2*D*) could be conjugate features associated with the main, south-dipping fault. The measurable displacement on individual faults is typically less than 10 cm, regardless of whether they dip to the north or south. The overall pattern of deformation in this trench is remarkably similar to the fold-thrust structures generated in the early stages of rock-deformation experiments to examine the development of fold-thrust structures (fig. 8a of Chester and others, 1991).

The focal mechanism for the first main shock, which is believed to have formed the Kunayungku scarps, the pattern of aftershocks along this section of faulting, and the south-side-up sense of throw on the fault scarp all indicate that the master fault at depth is a south-dipping reverse fault. These observations and the fact that the southward-dipping fault that extends from the surface at the 10-m mark to the bottom of the trench at about 14.5 m coincides with a large step in the bedrock suggests that this fault is the surface expression of the seismogenic fault. In the eolian sand and ferricrete, this fault strikes 146° and has an average dip of about 16°, but in the claystone, the dip increases abruptly to about 58°.

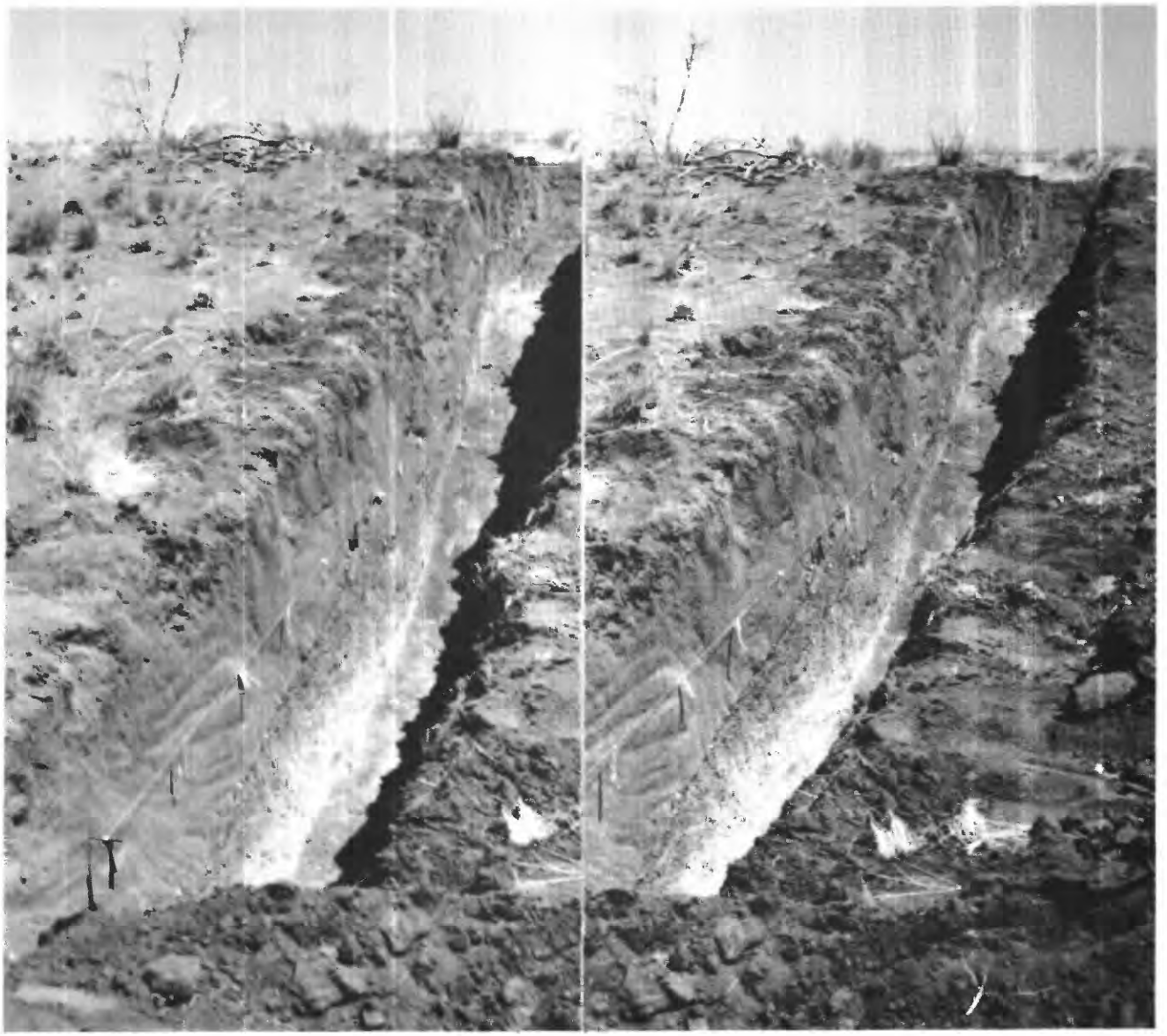

Figure 17. Stereographic photographs of the Kunayungku trench locality showing the morphology of the scarp. The scarp is 1.4 m high, but net throw (surface offset) across the deformed zone is only 0.8 m. A map of the locality and the scarp profile are shown on pls. 1*H* and 1*J*. The light-colored unit in the bottom of the trench is claystone. Pieces of flagging on the string line are 1 m apart. View is to the south.

Reverse movement on this fault has produced a 7-cm offset in the top of the ferricrete. However, along the same fault, the top of the claystone is offset 30 cm in the opposite direction. We discuss possible explanations for these discordant relations in the following section.

The majority of the faults and fractures in the trench dip to the north. These faults were best expressed in the eolian sand, but, when traced downward, they disappear and none could be traced into the underlying claystone. In the eolian sand, the dips of these faults range between 19° and 33°, but in the ferricrete, the dip diminishes to less than 10°. Two of these faults ruptured the surface and created small backthrust scarps. The flattening of these faults with depth and their failure to penetrate the bedrock show that they are minor shallow features that formed in response to near-surface compression caused by the overall horizontal shortening.

A system of extensional fractures formed in the hanging wall near the apex of the antiformal arch that was bisected by the trench (fig. 18). In cross section, the cracks define a crude, semiradial pattern across the crest of the arch, which is similar to the pattern of the extensional fractures we observed in the hanging wall of the eastern Lake Surprise trench. As we noted earlier, the position of the arch and extensional fractures relative to the main fault may identify

Figure 18. Stereographic photographs of extensional fractures aligned subparallel to the crest of the arch that was bisected by the Kunayungku trench. A 3-m-long section of the upper part of the east trench wall is visible in the lower right part of the view. Note dead bushes in foreground that were probably killed because tap roots were severed by the fault and dense growth of *Spinifex triodia sp.* (bunch grass) in the upper right that occupies a synclinal trough. Note also the lack of significant topography in the area. Maps of the locality and the trench wall are shown on pls. 1*H* and 2*D*. View is to the southeast.

the location where the overall geometry and attitude of the main reverse fault zone at depth changes from a moderate dip in competent rock at depth to a shallower dip in unconsolidated deposits or deeply weathered rock near the surface. Many of the extensional fractures along the crest of the arch were still open in September 1990, but the walls of the fractures had been coated with a thin layer of finely laminated silt. This laminated silt shows that the fractures are periodically flooded with meteoric water from surface runoff. A few near-vertical extensional fractures are also present in the footwall of the fault, but these appear to be distributed randomly.

The manner in which faults and shears propagated upward through the stratigraphic section was affected by differences in the physical properties, and thus the mechanical response, of materials in individual stratigraphic units. The effects of contrasts in physical properties was especially pronounced in the footwall of the fault where many of the small-displacement faults and fractures extend upsection through the ferricrete and sand at a low angle. Near the boundary between the ferricrete and sand where the physical properties of the units change, the attitudes of the shears and faults typically flatten and roughly follow or coincide with the boundary. Minor slip on the faults and shears disaggregated the nodules in the ferricrete, especially near the contact with the sand. After carefully examining the geometry of the faults with respect to the ferricrete, we believe that the ferricrete nodules acted almost like ball bearings along the failure planes, thereby decoupling the overlying eolian sand from the underlying ferricrete and bedrock.

The crosscutting relations between the north-dipping network of faults and the main south-dipping fault establish the following chronology for the development of the fault sets. Initially, movement on the main south-dipping fault zone at depth caused primarily plastic deformation in the shallow, weathered bedrock and warping of the overlying deposits. Some of the near-vertical extensional fractures in the footwall began to form at this stage because the fractures at 6, 7.5, and 11 m (pl. 2*D*) are offset 5, 6, and 7 cm (respectively) by younger north-dipping reverse faults. Many of the extensional fractures in the arch could have formed at this early stage or may have developed during a later stage. As

the hanging wall was transported northward, near-surface compression and deformation in the weathered bedrock and Quaternary deposits increased. The strain from this compression was first accommodated by the development of the network of north-dipping faults. Later, as the amount of displacement on the master fault at depth increased, the rupture propagated up through the weathered bedrock, ferricrete, and sand, eventually reaching the surface. Several of the north-dipping faults are offset about 12 cm by the main, south-dipping fault, showing clear evidence of the relative timing of offsets. The last stage of movement on the main fault may have increased the amplitude of the arch and, as a result, stimulated further development of the extensional fractures in the hanging wall.

OBSERVATIONS PERTINENT TO PREHISTORIC RUPTURING

We saw no geomorphic evidence at the Kunayungku locality nor found any compelling structural or stratigraphic evidence in the trench to indicate the presence of a prehistoric scarp. We attribute the extensive fracturing in the upper part of the claystone to the 1988 earthquakes mainly because the fracture surfaces are unoxidized and unstained by iron oxide, which certainly would have migrated down from the overlying ferricrete over a longer time period. The structural relief on the top of the claystone in the trench is 1.35 m, which is virtually the same as the 1.4 m of topographic relief between the crest of the fold and the ground surface north of the scarp. The similarity of these values is strong evidence against a history of repeated late Cenozoic movement on this fault.

The anomalously thick section of ferricrete in the hanging wall immediately adjacent to the main fault is curious; the reason for this difference in thickness remains unknown. In 1988, reverse slip on the main fault offset the top of the ferricrete 7 cm to the north, yet the top of the underlying claystone is offset 30 cm in the opposite direction. The disparity between the sense of slip on the top of the ferricrete versus the top of the claystone could be the result of an unmeasured component of strike-slip movement, which did occur locally in 1988. The generalized right-stepping en echelon pattern of the 1988 scarps might also indicate some strike-slip motion. Finally, the western fence line of the paddock shows 25 cm of east-west-oriented left-lateral offset (and 80 cm of north-south-directed horizontal movement) where it crosses the Kunayungku scarp (*G*, fig.4, table 3). In contrast to these observations, the seismological data show nearly pure reverse-fault motion for the first main shock (Choy and Bowman, 1990) or reverse faulting with a minor component of right-lateral slip (Chung and others, 1988; McCaffrey, 1989; National Earthquake Information Center, 1988).

We offer two hypotheses to explain the apparent change in throw direction between the top of the bedrock and the top of the ferricrete. The first explanation invokes a prehistoric faulting event. Taken at face value, these stratigraphic relations indicate an apparent reversal of slip in which the 1988 earthquakes reactivated a preexisting normal fault (down-to-the-south) with an opposite sense of slip. This normal fault may be the northern edge of a keystone block at the apex of a broad arch that formed during this prehistoric earthquake. We speculate that the low-angle north-dipping normal fault with 22 cm of dip slip at the 19.5-m mark (pl. 2*D*) may bound the southern edge of this keystone block. The normal slip on the main fault would have occurred during, but not after, formation of the ferricrete, because only the base of the ferricrete is offset by normal slip. The age of the ferricrete is unknown, but as discussed earlier, we assume that it is probably late Cenozoic, which implies that the inferred prehistoric event would also be late Cenozoic in age.

The second hypothesis attributes the apparent normal-slip offset to an unusually thick section of ferricrete directly south of the fault. The thick ferricrete is so localized that it appears to be somehow related to its proximity to the fault zone; accordingly, this hypothesis proposes that the unusually thick ferricrete is the result of preferential weathering or ground-water alteration in fractured claystone adjacent to the preexisting fault zone. The claystone near the fault zone is more fractured than the surrounding bedrock and therefore has greater permeability. If the ferricrete is largely a product of intense in-place weathering, as we suspect, then increased fracture permeability near the fault might facilitate formation of the ferricrete. The apparent normal slip on the bedrock could actually be the result of preferential development of the ferricrete immediately south of the fault zone. We recognize that this hypothesis fails to explain why the preferential development is confined to only one side of the fault when the fracturing would certainly have occurred on both sides of the fault.

The extensive drilling program that was part of the regional hydrologic analysis (Verhoeven and Knott, 1980; Verhoeven and Russell, 1981) provides some useful information about the subsurface structure near the Kunayungku scarp. Drilling near the scarp documents a generalized stratigraphic section of Cenozoic sediments that bury Cambrian sedimentary rocks, Proterozoic granite, and Archean schist. The drill-hole data are interpreted to define a complex set of intersecting northwest- and northeast-trending faults, but none of the interpreted faults coincides with the Kunayungku fault scarp. The drill-hole data also are interpreted to show a variable sense of throw on the Precambrian bedrock along the trace of the scarp. Sections across the northwestern end of the scarp show that Precambrian granite is at least 70 m shallower northeast of the scarp versus southwest of the scarp (fig. 9 in Verhoeven and Knott, 1980 (reproduced as fig. 4 in Bowman and others, 1990); figs. 3, 6 in Verhoeven

and Russell, 1981). However, a section across the central part of the scarp infers bedrock to be about 40 m deeper on the northeastern side versus the southwestern side (fig. 4 in Verhoeven and Russell, 1981), a relationship which conforms to the 1988 displacement pattern. The drill-hole data do not allow us to directly relate the historical scarp to a preexisting fault, but they indicate that the distribution of faults and pattern of structures in the subjacent Precambrian rocks is complex.

EVIDENCE OF QUATERNARY FAULTING

Although we did not find definitive stratigraphic evidence of prehistoric surface-faulting earthquakes at any of the trench localities, several lines of indirect evidence favor our interpretation of pre-1988 late Quaternary surface faulting along the western arm of the Lake Surprise scarp. Both of the western Lake Surprise trenches exposed convincing evidence of a preexisting late Quaternary scarp in bedrock that was buried by eolian sand. We cannot unequivocally determine if the buried scarp was actually a fault scarp but, based on the evidence we present, we favor this interpretation. We found no stratigraphic or structural evidence of prehistoric Quaternary events in the Kunayungku or eastern Lake Surprise trenches in either the eolian sand or the underlying ferricrete. In fact, at the Kunayungku locality, the similar amount of relief on the bedrock and the deformation of the ground surface show that virtually all of the deformation of the top of the bedrock at this locality occurred in 1988.

It is noteworthy that our best evidence for late Quaternary faulting was found on the only section of the 1988 ruptures that coincides with exposed bedrock, the quartz ridge. This coincidence is good evidence that the 1988 earthquakes reactivated a fault whose history of movement may extend back to the Precambrian. Based on the geological and seismological factors, Choy and Bowman (1990) regarded the second main shock in 1988, which probably formed the western Lake Surprise scarp, to be the critical event in the Tennant Creek earthquake series. The second main shock had the largest dynamic stress drop (136 bars) of the three major earthquakes, a drop that implies that this earthquake ruptured the strongest barrier. Without the failure of this barrier, the third main shock may not have occurred, and the Tennant Creek earthquakes may have consisted of only one main shock instead of a sequence of three similar-size main shocks. We are unsure about the significance of these various observations, but the geologic evidence of recurrent faulting, the suggestion that this is the only section of the 1988 scarps to rupture in the recent geologic past (late Pleistocene), and the seismologic evidence of a strong barrier associated with this section of the scarps imply that structures related to the western arm of the Lake Surprise fault have had a part in the tectonics of the Tennant Creek area for a long time.

STRUCTURAL CONTROLS OF FAULTING

The spatial coincidence between (1) the location of Lake Surprise, (2) the general area where the sense of throw changes direction on the Lake Surprise fault, and (3) the peculiar concentration of the calcrete mounds suggests that the geological setting of the Lake Surprise area is unique. We speculate that the spatial coincidence of these surficial features is a direct result of structural complexities in the subsurface. Despite its small size, Lake Surprise is a significant physiographic landmark in a generally featureless landscape. In addition, the lake is the center of a local, internal drainage system in a region where the surface drainage is dominated by overland flow rather than runoff that is channeled into an integrated drainage network.

In the area directly east of the lake, the sense of throw on the Lake Surprise fault changes from south-directed reverse slip on the western arm to north-directed reverse slip on the eastern arm. About 3 km east of Lake Surprise, the general strike between the western and eastern parts of the fault (pl. 1*A*) rotates about 40° clockwise within a distance of about 1.5 km. The abrupt change in both the sense of throw and in the strike of the fault is unusual and suggests to us that the subjacent faults in this area interact in a very complex manner. Abrupt major bends are one of several characteristics that identify structural discontinuities in faults or other structural features that can divide faults into individual rupture segments (Aki, 1979; King and Nábelek, 1985; Crone and Haller, 1991; dePolo and others, 1991). The seismological data indicate that the scarps on either side of this bend probably formed during two separate main shocks. Collectively, these observations show that an important structural feature near Lake Surprise affected the propagation of the coseismic ruptures along the eastern and western arms of the Lake Surprise fault.

The juxtaposition of Lake Surprise (a regionally significant depression) with the area of calcrete mounds (a noticeable topographic high on the east shore of the lake) is notable and peculiar. We estimate that there is about 10 m of relief between the lake bottom and the crest of the calcrete mounds across a distance of about 200 m. This amount of relief is remarkable in an area where the topographic relief is commonly a few meters between points several kilometers apart. Although the origin of the mounds is unknown, if our speculation that the mounds are produced by artesian flow is correct, then the concentration of these mounds adjacent to the lake might be evidence that an aquifuge is present in the subsurface near the lake. This aquifuge could abruptly change the local pattern of groundwater flow and force carbonate-bearing ground water to the surface through conduits that are topographically high

relative to the immediately surrounding area. The development of a virtually impermeable clay gouge or the mineralization that sealed ancient faults are possible mechanisms that could create an aquifuge near the lake.

The preceding geologic observations combined with the seismologic data from the 1988 earthquakes constitute strong evidence that a major structural barrier exists near Lake Surprise and that this barrier physically divides the Lake Surprise fault into an eastern and a western segment. This postulated barrier appears to have allowed the two segments to rupture independently, although increased stress on the barrier following the second main shock, combined with the preexisting ambient stress, ultimately exceeded the barrier's strength and led to the third and largest main shock. This barrier separates faults that have significantly different strikes and that probably dip in opposite directions. King and Nábelek (1985) found that major changes in fault geometry, such as that documented along the Lake Surprise fault, may coincide with complex networks of intersecting faults that can affect the initiation and termination of coseismic ruptures. Furthermore, prominent bends in faults can create barriers that are considerably stronger and more resistant to rupturing than adjacent parts of the fault (Andrews, 1989). Thus, the pronounced change in the strike and dip direction of the Lake Surprise fault scarps is probably the surface expression of a structurally complex segment boundary in the subsurface.

It is noteworthy that the topographic low occupied by Lake Surprise coincides with an area where the 1988 net cumulative surface offset is small compared to adjacent areas. A plot of net cumulative surface offset of the 1988 scarps (Fig. 5*B*) was constructed by adding the surface-offset values of north-directed and south-directed scarps together as a function of distance east of the western edge of the paddock along a west-northwest line (strike of about 290°). The resulting plot combines the offsets on the Kunayungku and western Lake Surprise scarps (shown separately in fig. 5*A*) and graphically portrays the total amount of surface offset across the system of scarps that was produced by the north-south shortening. The cumulative surface offset near Lake Surprise is only about 0.5 m compared to surface offsets of about 1 m to the east and west. We speculate that the location of the lake may be, in part, structurally controlled by the segment boundary where the net throw on the faults in 1988 and perhaps from past earthquakes was small compared to other parts of the fault system.

THE RECURRENCE OF SURFACE-FAULTING EARTHQUAKES IN STABLE INTRAPLATE SETTINGS

The stratigraphic and structural data we cite provide only very broad limits on the recurrence of surface-rupturing earthquakes on the faults that ruptured during the 1988 earthquakes. The broad limits established by this study indicate that the recurrence interval of large earthquakes on each of these faults is measured on a time scale of at least tens of thousands of years and perhaps hundreds of thousands of years or longer.

As we stated in the "Introduction," the geologic data on recurrent surface-faulting earthquakes in stable plate interiors are very limited, in part because historic ruptures in these settings are rare. Our conclusion that recurrence intervals on the Tennant Creek faults are on the order of tens of thousands of years or more is consistent with the observations about the recurrence interval of surface-rupturing earthquakes at Marryat Creek, South Australia (Machette, Crone, and Bowman, unpub. data, 1990) and on the Meers fault in southwestern Oklahoma (Crone and Luza, 1990), the only other faults in comparable tectonic settings for which there is any recurrence information. The paleoseismic studies at Marryat Creek conclude that the recurrence interval for surface-rupturing earthquakes on the faults that moved during the 1986 earthquake is at least 100,000 yr and probably much longer. The Meers is a reactivated Paleozoic fault in a part of the United States that is widely regarded to be part of the stable interior of the continent. Along the small section of the Meers fault where Pleistocene deposits are preserved, the amount of offset on middle Pleistocene alluvium is similar to the offset on middle Holocene alluvium. Thus the penultimate surface faulting that preceded the late Holocene rupture occurred more than 100,000 yr ago (Crone and Luza, 1990). A recent investigation of the relations between the 1989 Ungava, Quebec, rupture and preexisting geologic structures concluded that the rupture reactivated a ductile Archean fault but that the fault had not been active any other time in the Phanerozoic (Adams and others, 1992). Collectively these data are meager, yet they consistently indicate that lengthy recurrence intervals of 100,000 yr or more are typical of faults in the stable interior of continents.

Recurrence information on other similar faults that have ruptured historically is virtually nonexistent, so it is impossible to determine whether the pattern implied by paleoseismic studies of the Tennant Creek and Marryat Creek scarps and Meers fault is truly representative of seismogenic faults in continental interiors. If recurrence intervals of tens or hundreds of thousands of years are typical of individual seismogenic faults in stable continental interiors, then the hazard posed by damaging earthquakes on a single fault is very small compared to a human life span. Johnston (1989) noted that the rate of seismicity in stable continental settings is ten to one hundred times lower than it is for plate-boundary settings. Thus, for the stable continental interiors, more realistic and perhaps more meaningful hazard assessments should be based on a regional recurrence interval, which could be determined by statistically combining the recurrence information on individual faults throughout a region. This type of recurrence interval would reflect the likelihood

of a specific locality being affected by a damaging earthquake in the region. Regional perspectives offer a more realistic view of the hazard in stable continental interiors because the collective probability of a damaging earthquake occurring on one of many faults is significantly greater than the hazard posed by a single fault with a recurrence interval of several tens of thousands of years.

The unusual occurrence of surface-rupturing earthquakes in Australia during the past 25 yr has increased concern that unexpected large intraplate earthquakes could occur in more densely populated parts of the world. This concern was further heightened by the Ungava, Quebec, earthquake in December 1989, which is the first known surface-rupturing earthquake in central and eastern North America (Adams, Wetmiller, Drysdale, and Hasegawa, 1991; Adams, Wetmiller, Hasegawa, and Drysdale, 1991) and which occurred in an area that previously had only minor, dispersed historical seismicity (Adams and Basham, 1989). The Ungava earthquake was only the tenth historical earthquake in the world known to produce surface rupture in a stable continental setting, but an increasing number of recent geologic investigations have either documented or cited possible evidence of prehistoric surface ruptures in continental interiors. Of these prehistoric ruptures, the Meers fault is perhaps the most thoroughly studied. The Meers fault was first identified and mapped as a major reverse fault in Paleozoic sedimentary rocks more than 50 yr ago, but the neotectonic significance of the scarp on the fault remained unrecognized until 1983 (Gilbert, 1983a, 1983b). The fact that the scarp remained unnoticed for decades in a thoroughly mapped area underscores the possibility that, worldwide, many other unidentified prehistoric ruptures may exist in stable interiors of continents. For example, recent reconnaissance investigations of newly formed bluffs along the shore of Harlan County Lake in south-central Nebraska have revealed faults in latest Quaternary loess (W.C. Johnson and R.D. Miller, Kansas Geological Survey, written commun., 1991). In Australia, prehistoric fault scarps (fig. 1) are known to exist on the Lort River fault, the Mt. Narryer faults, near Hyden, and near Merredin, all in Western Australia (Gordon and Lewis, 1980; Denham, 1988; McCue, 1990), near Cadell, New South Wales, and near Lake Edgar, Tasmania (McCue, 1990). Along the western flank of the Flinders Ranges, which are about 350 km north of Adelaide in South Australia (fig. 1), a reverse fault displaces alluvial-fan gravels that are thought to be about 30 ka (Williams, 1973). In addition, while in Australia we learned about possible Quaternary fault scarps east of Barrow Creek, Northern Territory (fig. 2) (P. W. Haines, Department of Mines and Energy, Northern Territory, written commun., 1990), in the Simpson Desert area of South Australia, and in the Great Sandy Desert of Western Australia (fig. 1). In Ghana, West Africa, archaeological evidence indicates the possibility of 10 m of Holocene displacement on the Accra fault (Thompson, 1970), which is about 150 km northeast of the epicenter of the 1939 Accra earthquake (M about 6½) that generated about 10 km of surface rupture with a maximum height of 46 cm (Langer and others, 1987; Sykes, 1978; Yarwood and Doser, 1990). These few examples stress the incompleteness of the worldwide inventory of Quaternary scarps in interior continental settings and suggest that prehistoric surface ruptures in the so-called stable continental interiors may be more widespread and common than previously believed. Obviously, a more comprehensive inventory is vital to determining how frequently major intraplate earthquakes occur and thus realistically assessing the hazards they pose.

Earthquake-hazard assessments in continental interiors are hindered by an incomplete inventory of prehistoric scarps, but they are also hindered by the apparently small chances of preserving geologic evidence of prehistoric earthquakes based on the historical examples. For example, despite their modest size (1-m-high scarps are common, 1.8 m high is the maximum size), the long-term preservation potential of the Tennant Creek scarps is low because they are formed primarily on easily eroded eolian sand. As a result, erosional and depositional processes will likely obliterate or conceal the scarps in a geologically short period of time. We judge the preservation potential of the scarps from the 1986 Marryat Creek, South Australia, earthquake to also be low because of their size (less than 1 m high) and because they are formed on easily eroded surficial deposits. Lewis and others (1981) noted the ephemeral nature of the scarps from the 1979 Cadoux, Western Australia, earthquake and, likewise, Adams, Wetmiller, Drysdale, and Hasegawa (1991) and Adams, Wetmiller, Hasegawa, and Drysdale (1991) considered the chances of the Ungava scarp leaving a significant geologic record to be poor. The largest scarps from the 1983 Guinea, West Africa, earthquake are only 5–7 cm high (Langer and others, 1987), which is so small that they will probably be obliterated within a few decades. These examples of historical faulting demonstrate the ephemeral nature of the geologic evidence for many of the prehistoric surface faults in intraplate settings. Because the evidence is so ephemeral, even a comprehensive inventory of fault scarps might underestimate significantly the number of faults that could produce potentially damaging earthquakes and, thus, inaccurately reflect the hazard.

IMPLICATIONS CONCERNING SEISMIC HAZARDS IN CONTINENTAL INTERIOR SETTINGS

Assessing the earthquake hazards in the interior of continental plates is a difficult but important challenge for the earth-science and engineering communities. Hazard assessments in continental interiors are confronted by several difficult obstacles. First, potentially damaging earthquakes in plate interiors are several orders of magnitude less frequent

than those along plate margins, and as a result, the public's awareness and concern regarding earthquake' hazards in plate-interior settings are generally low. However, compared to interplate settings, the relatively low attenuation of seismic energy from large earthquakes in intraplate settings can cause damage in large areas (Hanks and Johnston, 1992). In addition, the data from this study and from the Marryat Creek and Meers fault studies indicate that the recurrence of surface rupturing on most individual faults in continental interiors is probably measured on time scales of at least several tens of thousands of years. With such long recurrence times, the hazard posed by a specific fault is statistically miniscule compared to the intended lifespan of human-made structures. With such long recurrence intervals and low slip rates, potentially hazardous faults can be easily overlooked or ignored. Although the actual hazard posed by a single fault may be very low, the cumulative hazard posed by numerous unsuspected faults could be substantially greater.

The lack of seismicity associated with some potentially seismogenic faults in stable continental interiors is another troublesome aspect of intraplate hazard assessments. Microseismicity is commonly used as a guide to identify potentially hazardous faults, but before the Tennant Creek earthquakes there was no seismicity, and in southwestern Oklahoma today, the Meers fault is aseismic. Thus, microseismicity is an unreliable criterion for detecting all potentially seismogenic faults.

Past hazard assessments for the interiors of continental plates have relied primarily on statistical analyses of the rates of seismicity (Nishenko and Bollinger, 1990). However, recent geological studies demonstrate that the limitations of short historical records of seismicity, the inadequate inventory of potentially seismogenic faults, and the long recurrence intervals for surface-rupturing faults are factors that must be incorporated into hazard assessments in continental interiors. Future hazard assessments need to be based on more comprehensive geologic data on the number and distribution of potentially seismogenic faults, on better knowledge about the paleoseismicity of intraplate faults, and on patterns in the long-term activity of hazardous faults in supposedly stable parts of the continents.

REFERENCES CITED

Adams, John, and Basham, Peter, 1989, The seismicity and seismotectonics of Canada east of the Cordillera: Geoscience Canada, v. 16, no. 1, p. 3–16.

Adams, John, Percival, J.A., Wetmiller, R.J., Drysdale, J.A., and Robertson, P.B., 1992, Geological controls on the 1989 Ungava surface rupture—A preliminary interpretation, *in* Current research, part C: Geological Survey of Canada Paper 92–C, p. 147–155.

Adams, John, Wetmiller, R.J., Drysdale, J., and Hasegawa, H.S., 1991, The first surface rupture from an earthquake in eastern North America, *in* Current research, part C: Geological Survey of Canada Paper 91–C, p. 9–15.

Adams, John, Wetmiller, R.J., Hasegawa, H.S., and Drysdale, J., 1991, The first surface faulting from an intraplate earthquake in North America: Nature, v. 352, no. 6336, p. 617–619.

Aki, Keiiti, 1979, Characterization of barriers on an earthquake fault: Journal of Geophysical Research, v. 84, no. B11, p. 6140–6148.

Andrews, D.J., 1989, Mechanics of fault junctions: Journal of Geophysical Research, v. 94, no. B7, p. 9389–9397.

Ash, J.E., and Wasson, R.J., 1983, Vegetation and sand mobility in the Australian desert dunefield, *in* Jennings, J., and Hagedorn, H., eds., Dunes—Continental and coastal: Zeitschrift für Geomorphologie, Supplementband 45, p. 7–25.

Bates, R.L., and Jackson, J.A., eds., 1980, Glossary of geology (2d ed.): Falls Church, Va., American Geological Institute, 751 p.

Berger, G.W., 1988, Dating Quaternary events by luminescence, *in* Easterbrook, D.J., ed., Dating Quaternary sediments: Geological Society of America Special Paper 227, p. 13–50.

Birkeland, P.W., 1984, Soils and geomorphology: New York, Oxford University Press, 372 p.

Bonilla, M.G., and Lienkaemper, J.J., 1991, Factors affecting the recognition of faults exposed in exploratory trenches: U.S. Geological Survey Bulletin 1947, 54 p.

Bouniot, Emmanuel, Jones, Trevor, and McCue, Kevin, 1990, The pattern of 1987 sequence at Tennant Creek, NT [abs.], *in* Gregson, P.J., compiler, Recent intraplate seismicity studies symposium, Perth, Western Australia: [Australia] Bureau of Mineral Resources, Geology and Geophysics Record 1990/44, [45 p.].

Bowler, J.M., 1976, Aridity in Australia—Age, origins and expressions in aeolian landforms and sediments: Earth-Science Reviews, v. 12, p. 279–310.

Bowman, J.R., 1988, Constraints on locations of large intraplate earthquakes in the Northern Territory, Australia from observations at the Warramunga Seismic Array: Geophysical Research Letters, v. 15, no. 13, p. 1475–1478.

———1991, Geodetic evidence for conjugate faulting during the 1988 Tennant Creek, Australia earthquake sequence: Geophysical Journal International, v. 107, p. 47–56.

———in press, The 1988 Tennant Creek, NT earthquakes—A synthesis: Australian Journal of Earth Sciences.

Bowman, J.R., and Dewey, J.W., 1991, Relocation of teleseismically recorded earthquakes near Tennant Creek, Australia—Implications for midplate seismogenesis: Journal of Geophysical Research, v. 96, no. B7, p. 11,973–11,979.

Bowman, J.R., Gibson, G., and Jones, T., 1990, Aftershocks of the 1988 January 22 Tennant Creek, Australia intraplate earthquakes—Evidence for a complex thrust-fault geometry: Geophysical Journal International, v. 100, p. 87–97.

Chen, X.Y., Prescott, J.R., and Hutton, J.T., 1990, Thermoluminescence dating on gypseous dunes of Lake Amadeus, central Australia: Australian Journal of Earth Sciences, v. 37, p. 93–101.

Chester, J.S., Logan J.M., and Spang, J.H., 1991, Influence of layering and boundary conditions on fault-bend and fault-propagation folding: Geological Society of America Bulletin, v. 103, no. 8, p. 1059–1072.

Choy, G.L., and Bowman, J.R., 1990, Rupture process of a multiple main shock sequence—Analysis of teleseismic, local, and field observations of the Tennant Creek, Australia, earthquakes of January 22, 1988: Journal of Geophysical Research, v. 95, no. B5, p. 6867–6882.

Chung, W.-Y., Brantley, B.J., and Johnston, A.C., 1988, Source mechanism, surface rupture, and relative locations of the 22 January 1988 Tennant Creek earthquakes, Central Australia: EOS (American Geophysical Union Transactions), v. 69, no. 44, p. 1301.

Crone, A.J., and Haller, K.M., 1991, Segmentation and the coseismic behavior of Basin and Range normal faults—Examples from east-central Idaho and southwestern Montana: Journal of Structural Geology, v. 13, no. 2, p. 151–164.

Crone, A.J., and Luza, K.V., 1990, Style and timing of Holocene surface faulting on the Meers fault, southwestern Oklahoma: Geological Society of America Bulletin, v. 102, no. 1, p.1–17.

Crone, A.J., and Omdahl, E.M., eds., 1987, Proceedings of Conference XXXIX—Directions in paleoseismology: U.S. Geological Survey Open-File Report 87–673, 456 p.

Denham, David, 1988, Australian seismicity—The puzzle of the not-so-stable continent: Seismological Research Letters, v. 59, no. 4, p. 235–240.

dePolo, C.M., Clark, D.G., Slemmons, D.B., and Ramelli, A.R., 1991, Historical surface faulting in the Basin and Range province, western North America—Implications for fault segmentation: Journal of Structural Geology, v. 13, no. 2, p. 123–136.

Dodson, R.G., and Gardener, J.E.F., 1978, Tennant Creek, Northern Territory Sheet SE/53–14 international index, 1:250,000 geological map series: Canberra, Australian Government Publishing Service, 26 p., 1 oversize plate.

Gilbert, M.C., 1983a, The Meers fault—Unusual aspects and possible tectonic consequences: Geological Society of America Abstracts with Programs, v. 15, p. 1.

———1983b, The Meers fault of southwestern Oklahoma—Evidence for possible strong Quaternary seismicity in the midcontinent: EOS (American Geophysical Union Transactions), v. 64, no. 18, p. 313.

Gordon, F.R., and Lewis, J.D., 1980, The Meckering and Calingiri earthquakes October 1968 and March 1970: Geological Survey of Western Australia Bulletin 126, 229 p.

Goudie, Andrew, 1973, Duricrusts in tropical and semi-tropical landscapes: London, Oxford University Press, 174 p.

Hamilton, R.M., and Johnston, A.C., eds., 1990, Tecumseh's prophecy—Preparing for the next New Madrid earthquake: U.S. Geological Survey Circular 1066, 30 p.

Hanks, T.C., and Johnston, A.C., 1992, Common features of the excitation and propagation of strong ground motion for North American earthquakes: Seismological Society of America Bulletin, v. 82, no. 1, p. 1–23.

Johnston, A.C., 1987, Characterization of intraplate seismic source zones, *in* Crone, A.J., and Omdahl, E.M., eds., Proceedings of Conference XXXIX—Directions in paleoseismology: U.S. Geological Survey Open-File Report 87–673, p. 404–413.

———1989, The seismicity of 'stable continental interiors', *in* Gregersen, Søren, and Basham, P.W., eds., Earthquakes at North-Atlantic passive margins—Neotectonics and postglacial rebound: Dordrecht, The Netherlands, Kluwer Academic Publishers, p. 299–327.

Johnston, A.C., and Bullard, Thomas, 1990, The Ungava, Quebec, earthquake—Eastern North America's first modern surface rupture [abs.]: Seismological Research Letters, v. 61, no. 4–3, p. 152–153.

Johnston, A.C., and Kanter, L.R., 1990, Earthquakes in stable continental crust: Scientific American, v. 262, no. 3, p. 68–75.

Kennewell, P.J., and Huleatt, M.B., 1980, Geology of the Wiso basin, Northern Territory: [Australia] Bureau of Mineral Resources, Geology and Geophysics Bulletin 205, 67 p., 1 oversize plate, scale 1:1,000,000.

King, Geoffrey, and Nábelek, John, 1985, Role of fault bends in the initiation and termination of earthquake rupture: Science, v. 228, p. 984–987.

Langer, C.J., Bonilla, M.G., and Bollinger, G.A., 1987, Aftershocks and surface faulting associated with the intraplate Guinea, West Africa, earthquake of 22 December 1983: Seismological Society of America Bulletin, v. 77, no. 5, p. 1579–1601.

Lewis, J.D., Daetwyler, N.A., Bunting, J.A., and Moncrieff, J.S., 1981, The Cadoux earthquake, 2 June 1979: Geological Survey of Western Australia Report 11, 133 p.

Loughnan, F.C., 1969, Chemical weathering of the silicate minerals: New York, Elsevier Publishing Co., Inc., 154 p.

Mabbutt, J.A., 1966, Landforms of the Western Macdonnell Ranges, *in* Dury, G.H., ed., Essays *in* geomorphology: New York, Elsevier Publishing Co., Inc., p. 83–119.

———1988, Land-surface evolution at the continental time-scale—An example from interior Western Australia, *in* Firman, J., ed., Landscapes of the southern hemisphere: Earth-Science Reviews, v. 25, p. 457–466.

McCaffrey, Robert, 1989, Teleseismic investigations of the January 22, 1988 Tennant Creek, Australia, earthquakes: Geophysical Research Letters, v. 16, p. 413–416.

McCue, K., 1990, Australia's large earthquakes and Recent fault scarps: Journal of Structural Geology, v. 12, no. 5/6, p. 761–766.

McCue, K., Barlow, B.C., Denham, D., Jones, T., Gibson, G., and Michael-Leiba, M., 1987, Another chip off the old Australian block: EOS (American Geophysical Union Transactions), v. 68, no. 26, p. 609, 612.

McKeown, F.A., 1982, Overview and discussion, *in* McKeown, F.A., and Pakiser, L.C., eds., Investigations of the New Madrid, Missouri, earthquake region: U.S. Geological Survey Professional Paper 1236, p. 1–14.

Munsell Color Company, Inc., 1954, Munsell soil color chart: Baltimore, Md., Munsell Color Co., Inc.

National Earthquake Information Center, 1988, Preliminary determination of epicenters—Monthly listing: Washington, D.C., U.S. Geological Survey, January, 1988, 29 p.

Nishenko, S.P., and Bollinger, G.A., 1990, Forecasting damaging earthquakes in the central and eastern United States: Science, v. 249, p. 1412–1416.

Nuttli, O.W., 1973a, The Mississippi Valley earthquakes of 1811 and 1812—Intensities, ground motion and magnitude: Seismological Society of America Bulletin, v. 63, no. 1, p. 227–248.

———1973b, Seismic wave attenuation and magnitude relations for eastern North America: Journal of Geophysical Research, v. 78, no. 5, p. 876–885.

Nuttli, O.W., and Zollweg, J.E., 1974, The relation between felt area and magnitude for central United States earthquakes: Seismological Society of America Bulletin, v. 64, no. 1, p. 73–85.

Palfreyman, W.D., 1984, Guide to the geology of Australia: [Australia] Bureau of Mineral Resources, Geology and Geophysics Bulletin 181, 111 p.

Pickup, G., Allan, G., and Baker, V.R., 1988, History, palaeochannels and palaeofloods of the Finke River, central Australia, *in* Warner, R.F., ed., Fluvial geomorphology of Australia: Sydney, Academic Press, p. 177–200.

Plumb, K.A., 1979a, The tectonic evolution of Australia: Earth-Science Reviews, v. 14, p. 205–249.

———1979b, Structure and tectonic style of the Precambrian shields and platforms of northern Australia: Tectonophysics, v. 58, p. 291–325.

Scholz, C.H., Aviles, C.A., and Wesnousky, S.G., 1986, Scaling differences between large interplate and intraplate earthquakes: Seismological Society of America Bulletin, v. 76, no. 1, p. 65–70.

Schwartz, D.P., 1988, Geologic characterization of seismic sources—Moving into the 1990s, *in* Von Thune, J.L., ed., Earthquake engineering and soil dynamics II—Recent advances in ground motion evaluation: American Society of Civil Engineers, Geotechnical Special Publications, v. 20, p. 1–42.

Schwartz, D.P., and Crone, A.J., 1985, The 1983 Borah Peak earthquake—A calibration event for quantifying earthquake recurrence and fault activity on Great Basin normal faults, *in* Stein, R.S., and Bucknam, R.C., eds., Proceedings of Workshop XXVIII on the Borah Peak, Idaho, earthquake: U.S. Geological Survey Open-File Report 85–290, p. 153–160.

Soil Survey Staff, 1975, Soil taxonomy—A basic system of soil classification for making and interpreting soil surveys: U.S. Department of

Agriculture, Soil Conservation Service Agricultural Handbook 436, 754 p.

Stewart, A.J., Blake, D.H., and Ollier, C.D., 1986, Cambrian river terraces and ridgetops in central Australia—Oldest persisting landforms?: Science, v. 233, p. 758–761.

Sykes, L.R., 1978, Intraplate seismicity, reactivation of preexisting zones of weakness, alkaline magmatism, and other tectonism postdating continental fragmentation: Geophysics and Space Physics Reviews, v. 16, no. 4, p. 621–688.

Thompson, T.F., 1970, Holocene tectonic activity in West Africa dated by archaeological methods: Geological Society of America Bulletin, v. 81, no. 12, p. 3759–3764.

Twidale, C.R., 1983, Australian laterites and silcretes—Ages and significance: Révue de Geologie Dynamique et de Géographie Physique, v. 24, p. 35–45.

Verhoeven, T.J., and Knott, G.G., 1980, Tennant Creek Water Supply—1977–1978 investigation: Northern Territory of Australia, Department of Transport and Works, Water Division unpub. report, 50 p., available from Water Resources Branch, Power and Water Authority, P.O. Box 1521, Alice Springs, NT 0871, Australia.

Verhoeven, T.J., and Russell, P.W., 1981, Tennant Creek Water Supply—1979–1980 source investigation, Report on Water Division Project 91 Tennant Creek West-groundwater: Northern Territory of Australia, Department of Transport and Works, Water Division unpub. report, 22 p., available from Water Resources Branch, Power and Water Authority, P.O. Box 1521, Alice Springs, NT 0871, Australia.

Williams, G.E., 1973, Late Quaternary piedmont sedimentation, soil formation and paleoclimates in arid South Australia: Zeitschrift für Geomorphologie, v. 17, p. 102–123.

Yarwood, D.R., and Doser, D.I., 1990, Deflection of oceanic transform motion at a continental margin as deduced from waveform inversion of the 1939 Accra, Ghana earthquake: Tectonophysics, v. 172, p. 341–349.

DESCRIPTION OF UNITS EXPOSED IN THE TRENCHES

In the following discussion, the surficial units are classified according to the predominant grain size of the material in the deposit. For example, a deposit that contains 25 percent sand and 75 percent gravel is a sandy gravel on the basis of its overall grain size. However the textural description of this deposit is based on the texture of the less-than-2-mm fraction and is named and classified according to the soil terminology of the Soil Survey Staff (1975). For the preceding example of the sandy gravel, if the less-than-2-mm fraction is composed of 25 percent clay, 25 percent silt, and 50 percent sand, then texturally, this sandy gravel is classified as a sandy clay loam, and the deposit is classified as a very gravelly sandy clay loam (fig. 19). The "+" and "-" designations are informal and indicate clay-enriched and clay-depleted (respectively) samples within an individual textural class. Soil-color notations were determined by comparing soil peds to a Munsell Color Chart (Munsell Color Co., Inc., 1954) and are followed by "m" to show the color of a moist sample or "d" to show the color of a dry sample.

EASTERN LAKE SURPRISE TRENCH (ELS)

Eolian sand (unit **es**, pl. 2*A*). Well-sorted, nonstratified, fine- to coarse-grained sand, subangular to subrounded. Thickness 225–275 cm. Divided into two subunits in trench.

1. Organic component of soil (A horizon) in eolian sand (samples ELS–4a through –4c, table 4). Medium- to coarse-grained sand (+) to loamy sand (-) (fig. 20), less than 1 percent gravel (all less than 4 mm); slightly organic (shown by root hairs, darkened color, and weak platy structure); few thin clay films on grains, none on peds; noncalcareous and massive. Iron oxide is primary cementing agent, but deposit is loose to weakly friable. Dark reddish brown to dark red (2.5*YR* 3.5-4/7 d; 2.5*YR* 3/4 m), very slightly sticky to nonsticky, very slightly plastic to nonplastic. Modern land surface has 10–20 percent cover of coarse bunch grass (*Spinifex triodia sp.*), 1–2 percent Mulga trees (commonly dead on hanging-wall block because tap roots were severed), and 75–80 percent barren ground. Undisturbed surface has 1-mm-thick clayey crust. Lower contact is gradational and regular. Thickness is 25–40 cm.
2. Sand (samples ELS–4d through –4h, table 4). Medium- to fine-grained sand to loamy sand (fig. 20), less than 1 percent gravel (all granule size) consisting of 90–95 percent subangular to subrounded quartz and 5–10 percent rounded ferricrete nodules (3–5 mm diameter). Few to common thin clay films on grains, none on peds; noncalcareous, weakly cemented, massive. Red (2.5*YR* 4/8 d) to dark red (2.5*YR* 3/6 m), very sticky grading downward to slightly sticky, slightly plastic throughout. We consider this part of sand to be a Bw (cambic B) horizon. Basal part of unit (sample ELS–4h, table 4) contains more silt but less clay than above. Strength and number of peds increases downward; this increase in strength is probably caused by iron oxide and clay (table 4) acting as cementing agents. Lower contact is sharp and regular. Thickness is 180–205 cm.

Ferricrete gravel (unit **fcg**). Nodular, oblong to well-rounded gravel-size clasts (nodules) composed primarily of iron oxide. Nodules have concentric structure composed of a 2- to 3-mm-thick external rind of dusky-red (10*R* 3/3–3/4 d) FeO, a weak red (10*R* 4/4 d) interior rind of FeO, and a red (10*R* 4/6 d to 2.5*YR* 4/6 d) core. Maximum size of nodules is 3–4 cm, average size is 1 cm, minimum size is 0.3–0.4 cm. Interior of nodules consists of quartz sand (similar to overlying unit **es**), which is cemented with FeO; cementation of nodules is strong enough to break across quartz grains. Gravel is massive and lacks stratification. In lower part, nodules contain greater amounts of MnO, particularly in their cores. Nodules are oxidized, but cores are most intensely oxidized. Nodules have a noncemented matrix of fine to coarse sand similar to overlying unit es. Gravel is clast supported and has about 20–25 percent sand matrix. Lower contact is sharp to abrupt and wavy. In tectonically undisturbed parts of trench, unit **fcg** is as much as 50 cm thick.

Massive ferricrete (unit **fcm**). Unit is composed of coalesced nodules of iron oxide that are similar to those in unit **fcg**, but unit is massive and indurated and contains more black MnO than unit **fcg**. Typically well cemented, massive, and nonstratified. Cementation is adequate to cause individual nodules to break during excavation of trench. Maximum dimension of nodules is difficult to identify because of cementation (that is, nodules have coalesced); average size is 1.0 cm, minimum size is 0.5 cm. Interiors of nodules are primarily dark brown to black, are probably composed of psilomelane or other manganese oxides, and have about 5–10 percent porosity. Ferricrete is clast supported and has about 10 percent sand matrix. Lower contact is gradual and wavy. Thickness is commonly 25–45 cm; base is commonly covered.

Altered ferricrete (unit **fca**). Unit is similar to unit **fcm** in color and lithology, but nodules are generally smaller because diagenetic alteration or weathering has broken down nodules and interstitial cement. Alteration processes probably have formed diagenetic clay. Poorly cemented, nonstratified, but massive. Ferricrete breaks out of exposure as pea- to granule-size gravel, rather than pebble size. Nodules have dark- to dusky-red (10*R* 3/5 d) clay coatings. Thickness is unknown, but at least 60 cm is exposed in trench; base is covered.

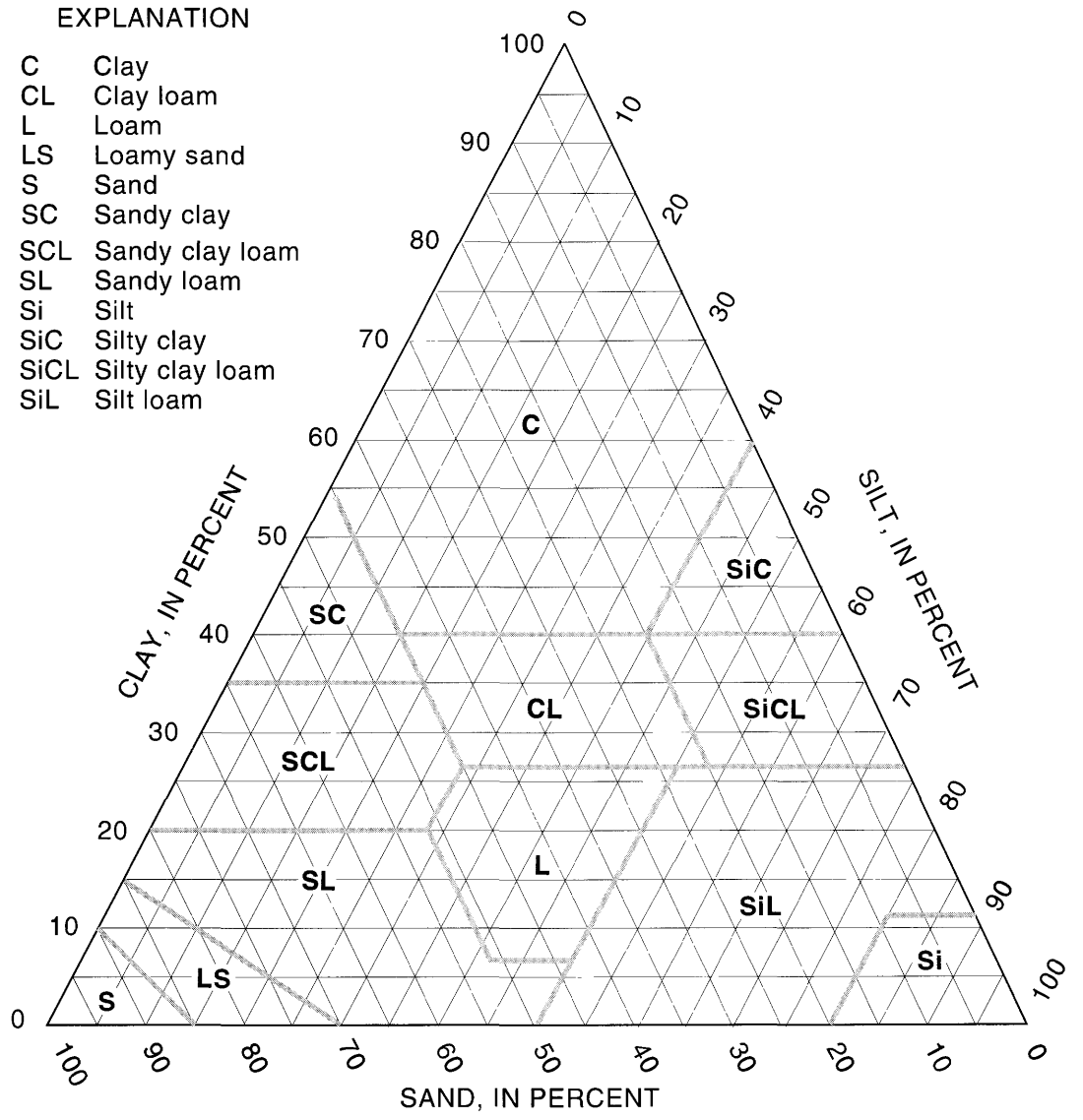

Figure 19. Grain-size distribution for U.S. Department of Agriculture textural classes (Soil Survey Staff, 1975). Sand is defined as material between 2.0 mm and 0.05 mm in diameter; silt is between 0.05 mm (50 micrometers or μ) and 2μ; and clay is less than 2μ.

WESTERN LAKE SURPRISE TRENCH 1 (WLS–1)

Eolian sand (unit **es**; pl. 2*B*, samples WLS1–1a through -1e, table 5). Medium- to coarse-grained sand (+) to loamy sand (fig. 21) containing a trace of gravel (less than 1 percent) composed of roughly equal parts of ferricrete and quartzite; gravel content may increase to 2–3 percent at base. Noncalcareous, massive, and nonstratified, except contains rare lenses of sandy gravel. Red (2.5*YR* 4/8 d; 2.5*YR* 3.5/6 m), nonsticky and nonplastic throughout. Has slightly vesicular structure in upper 5 cm, and coatings on grains are mainly FeO (not clay). Organic component of soil (upper part of unit **es**) not subdivided in this trench. Sand fills a depression shaped like a channel; lower contact is diffuse and regular. Thickness is commonly 10–15 cm in hanging-wall block (north side), 130–200 cm in footwall block (south side).

Eolian sand, reduced phase (unit **esr**; sample WLS1–1f, table 5). Medium- to coarse-grained sandy loam (-) (fig. 21) containing about 6 percent gravel. Gravel is 80–90 percent ferricrete nodules; one-third is less than 1.0 cm in diameter and two-thirds 1.0–2.0 cm in diameter. Sand is noncalcareous and poorly stratified to massive. Reddish yellow (7.5*YR* 6/6 d; 6*YR* 5/4 m), very slightly

Table 4. Particle-size data for samples from eastern Lake Surprise trench (ELS)

[Sand content determined by wet sieving; silt and clay contents determined by pipette method. Iron oxides were removed with 5 percent oxalic acid heated to boiling for 2–3 hours. If present, carbonates were removed with 10 percent HCl, and organic matter was removed with sodium hypochlorite adjusted to a pH of 9.5. (+), at high-clay end of textural field; (-), at low-clay end of textural field]

Sample No.	Sampling depth (cm)	Textural classification	Sand (percent)	Silt (percent)	Clay (percent)
ELS-4a.....	0-5	Sand(+).....	88.7	4.3	7.0
ELS-4b.....	5-15	Sand/loamy sand.....	88.0	4.6	7.4
ELS-4c.....	25-30	Loamy sand(-).....	87.9	4.4	7.4
ELS-4d.....	70-80	Loamy sand.....	85.7	4.4	9.9
ELS-4e.....	110-120	Loamy sand.....	84.5	5.2	10.3
ELS-4f.....	150-160	Loamy sand.....	83.3	5.6	11.1
ELS-4g.....	195-210	Loamy sand/sandy loam...	81.4	6.9	11.7
ELS-4h.....	240-250	Sand.....	88.2	10.3	1.5

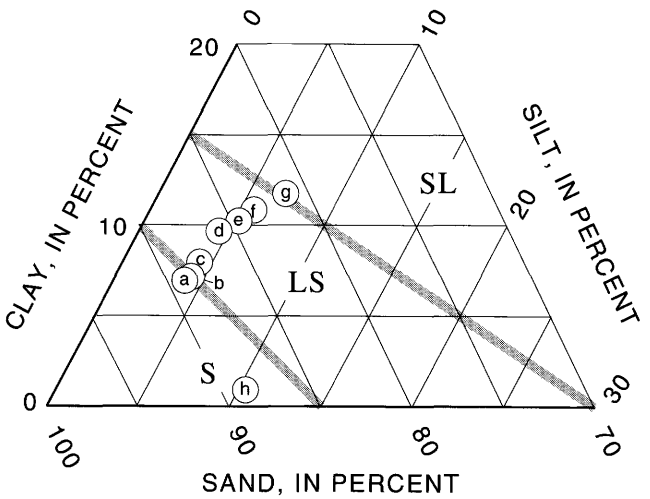

Figure 20. Grain-size data for samples of eolian sand in the eastern Lake Surprise trench (circled letters indicate samples ELS–4a to –4h, table 4). Textural classes are: S, sand; LS, loamy sand; and SL, sandy loam.

sticky, nonplastic. Sand is less oxidized and has a higher color value (lighter tone) than unit **es**; this color change probably results from occasional reducing conditions owing to submergence under high water table. Sand fills channel in underlying unit, lower contact is diffuse and regular. Only recognized in footwall block (south side). Thickness is 0–35 cm.

Eolian sand and ferricrete gravel, reduced phase (unit **esr+fcgr**). Mixture of units **esr** and **fcgr** (see description of unit **es** above and unit **fcgr** below). Maximum size of gravel (nodules) is 1.0–2.0 cm and rare clasts are 3 cm; average size is 0.5–1.0 cm. Cores of some nodules consist of quartzite fragments. Gravel is matrix supported, but gravel content increases downward and becomes clast supported near bottom of trench; poorly stratified. Light color of unit probably results from occasional reducing conditions owing to submergence under high water table. Presence of whitened nodules suggests that nodules are a fluvial lag deposit derived from surface exposures of unit **fcgr**. Although lower contact is generally not exposed, unit rests on unit **fcg** at the south side of the trench (at 4-m mark on map of trench, pl. 2*B*) with a sharp, regular boundary. Thickness is unknown, but at least 30 cm is exposed; base is covered.

Angular gravel (unit **ag**, based partly on unit description from trench WLS–2). Consists of several discrete lenses of sandy gravel that are within unit **es** in the footwall block (south side) and a thin layer of sandy gravel beneath unit **es** in the hanging-wall block (north side). Gravel is composed mainly of angular pebble- to small cobble-size fragments of quartzite (probably derived from units **rq** and **rq(f)**). Maximum size of gravel is about 15 cm; average size is 3–5 cm. Gravel is nonstratified, massive, and has 20 percent matrix of oxidized sand. Lenses are probably relicts of fluvial stream deposits that are interbedded with and underlie unit **es**, whereas thin mantle of unit **ag** in hanging-wall block may be remnant of debris flow. Debris flow predates the most recent episode of unit **es** deposition at this site and pinches out to the south, perhaps as a result of erosion or uplift(?) that formed the sand-filled channel. Upper and lower contacts are sharp and regular, although the lenses have irregular boundaries. Thickness is typically 5–15 cm.

Angular gravel and ferricrete gravel (unit **ag+fcg**, based partly on unit description from trench WLS–2). Mixture of unit **ag** (angular to subrounded fragments of coarse-grained quartzite) and unit **fcg** (described below). Gravel clasts (5–10 percent of the unit) have max-

Table 5. Particle-size data for samples from western Lake Surprise trench 1 (WLS–1)

[Sand content determined by wet sieving; silt and clay contents determined by pipette method. Iron oxides were removed with 5 percent oxalic acid heated to boiling for 2–3 hours. If present, carbonates were removed with 10 percent HCl, and organic matter was removed with sodium hypochlorite adjusted to a pH of 9.5. (+), at high-clay end of textural field; (-), at low-clay end of textural field

Sample No.	Sampling depth (cm)	Textural classification	Sand (percent)	Silt (percent)	Clay (percent)
WLS1-1a.....	0-5	Sand(+).....	89.1	5.0	5.9
WLS1-1b.....	10-20	Sand/loamy sand.....	88.5	4.4	7.1
WLS1-1c.....	40-50	Loamy sand(-).....	87.6	4.4	8.0
WLS1-1d.....	90-100	Loamy sand.....	86.3	4.9	8.8
WLS1-1e.....	140-150	Loamy sand.....	84.9	5.6	9.6
WLS1-1f.....	200-210	Sandy loam(-).....	80.7	6.4	13.0

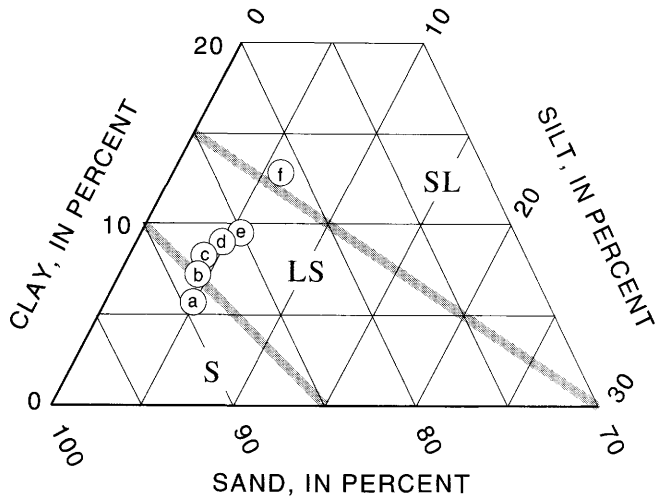

Figure 21. Grain-size data for samples of eolian sand in western Lake Surprise trench 1 (circled letters indicate samples WLS1–1*A* to –1f, table 5). Textural classes are: S, sand; LS, loamy sand; and SL, sandy loam.

imum size of about 6 cm, commonly are 2 cm, and are stained with FeO (hematite and pale-green iron oxide) along fractures. The angular fragments are clearly exotic to the trench site and must have been transported in order to be incorporated into this unit (that is, unit **ag** is not derived from unit **rq** in this trench). Unit restricted to hanging-wall block (north side) and appears to have filled an ancient graben or surface depression. Upper contact is gradual and regular; lower contact is sharp and irregular. Thickness is typically 35–65 cm.

Ferricrete gravel (unit **fcg**, based largely on unit description from trench WLS–2). Composed of rounded to subrounded ferricrete nodules in a matrix of medium- to coarse-grained, subangular to subrounded red (2.5 4/6 d) sand. Maximum size of nodules is 2–3 cm, average size is 0.5–1.5 cm. Gravel is clast supported, noncalcareous, nonstratified, and massive. Nodules are accreted into clusters in places. Upper contact is sharp and regular with a variety of units; lower contact is sharp and wavy to irregular. Thickness is variable, but is commonly 50–100 cm.

Ferricrete gravel, reduced phase (unit **fcgr**). Composed of rounded to subrounded ferricrete nodules in matrix of fine- to medium-grained sand. Maximum size of nodules is 6–8 cm, average size is 3 cm, minimum size is 1–2 cm. Sandy matrix is loose, reddish white in upper part but white in lower part. Nodules form clast-supported gravel having 10–20 percent matrix composed of sand. Cores of nodules are mostly maroon to red hematitic clay with 4–20 percent sand-size angular quartz fragments. Nodules have bleached (whitened) rinds 1–3 mm thick; smaller nodules are commonly red throughout, but larger nodules have MnO on interior fracture surfaces. Upper contact with unit **fcg** is gradational over about 10 cm, although much of boundary defined by transition in color. However, unit **fcgr** generally has larger nodules than unit **fcg**. Exposure of unit **fcgr** restricted to a single fault-bounded block at 14.5-m mark (trench map, pl. 2*B*). Lower contact defined by major south-dipping fault plane that moved in 1988. Thickness is about 100 cm.

Ferricrete (unit **fcm**) (based largely on unit description from trench WLS–2). Massive breccia composed of angular fragments of nodular ferricrete cemented by FeO and MnO. Fragments typically have a core of FeO, a halo of black MnO with irregular boundaries around the core, and an outer rind of FeO that gives the ferricrete its strong red color. Matrix ranges from loose FeO-rich sand to red FeO-rich clay(?). Upper contact is gradational with unit **fcg**, lower contact is a fault. Thickness is at least 110 cm where exposed.

Quartzite (unit **rq**). Hematitic, coarse-grained quartzite with pervasive internal oxidation. Exposed only in lower part of north end of trench, where it is largely unfractured and unjointed because of distance from main

faults. Most quartzite is a strongly jointed and fractured, hematitic quartzite (unit **rq(f)**) with pervasive internal oxidation. The density of fracturing and jointing, which typically depends on proximity to major faults and shears, produces a pattern of angular rhombohedral blocks of rock, commonly 4–6 cm on a side. The surfaces of joint-bounded blocks have 1- to 5-mm-thick yellowish-white rinds probably composed of reduced iron oxides. Oxidized iron-manganese rinds are present between the core fragments; rinds are commonly 1 mm thick and may be largely composed of oxidation products of overlying units **fcg** and **es**. We speculate that the iron-manganese oxides were produced by recent oxidizing conditions, whereas the bleached (yellow-white) rinds probably result from older geochemical conditions. Thickness is unknown, but at least 2 m; base is covered.

WESTERN LAKE SURPRISE TRENCH 2 (WLS–2)

Postfaulting colluvium (unit **csb**, pl. 2*C*). Comprised of locally derived slope debris and moderately coherent blocks shed from the 1988 fault scarp. Contains components from soil, unit **es**, and unit **fcg** exposed in hanging-wall block. As a unit, consists of unsorted, oxidized sand and gravel. Blocks probably deposited by collapse of oversteepened scarp during or soon after faulting. Contains a recognizable block of overturned soil at distal end of deposit (see arrow indicating former upright direction on enlarged part of trench map, pl. 2*C*). Small pocket of postfaulting eolian sand has been deposited against end of colluvium. Colluvium restricted to footwall block, adjacent to fault zone. Lower contact is sharp and irregular, marked by clayey crust on buried unit **es**. Thickness is typically 35–40 cm.

Eolian sand with organic component of soil (unit **es**; sample WLS2–1a, table 6). Fine- to medium-grained loamy sand (-) (fig. 22) that contains less than 1 percent coarse fragments (two-thirds are granules of unit **fcg** and one-third is quartz and angular lithic fragments). Noncalcareous, well sorted, massive. Dark red to dark reddish brown (2.5*YR* 4/6 d; 1*YR* 3/5 m), nonsticky, nonplastic. Soil has clayey, platy surface crust 2–4 mm thick and is slightly organic (as indicated by root hairs and darkened color relative to unit **esm**). Structure becomes moderate, medium, angular blocky and weak, fine, subangular to angular blocky beneath crust; has few thin clay films on grains and pervasive FeO stain on grains. Lower contact is gradual and regular. Base of organic component of soil only shown on hanging-wall block. Thickness is commonly 15 cm.

Slightly cemented eolian sand (unit **esm**; sample WLS2–1b, table 6). Loamy sand (-) (fig. 22) contains 1–2 percent granules and gravel (75 percent rounded ferricrete nodules, 25 percent angular quartzite and lithic fragments). Red (slightly redder than 2.5*YR* 4/7 d; 10*R* 3/5 m), very slightly sticky, nonplastic to very slightly plastic, noncalcareous, friable, slightly harder and more competent than soil above and sand below. Structure is moderate, medium, subangular blocky to weak, fine, subangular blocky; has few thin clay films on grains and pervasive FeO stain on grains. Unit fills channel and pinches out to north against paleoslope formed on unit **ag**. Lower contact is gradual and wavy. Thickness is commonly 15–40 cm.

Eolian sand, reduced (unit **esr**; sample WLS2–1c, table 6). Sand (+) to loamy sand (-) (fig. 22), red (2.5 *YR* 4/7 d; 10*R* 3.5/6 m), contains 2–3 percent granules (80–90 percent lateritic nodules and 10–20 percent angular lithic fragments), loose, noncalcareous, nonplastic, very slightly sticky. Structure is 75 percent weak, medium, subangular blocky to weak, fine, subangular blocky mixed with about 25 percent single grain; has few thin clay films on grains and pervasive FeO stain on grains. Unit fills channel and pinches out to north against paleoslope defined by unit **ag**. Lower contact is sharp and wavy. Thickness is commonly 15–55 cm.

Angular gravel (unit **ag**, described on upthrown block at 3.0 m, pl. 2*C*). Thin layer of gravel (angular to subrounded fragments of quartzite) containing minor amounts of units **fcg** and **es** in about equal proportions. Angular fragments have maximum size of about 15 cm, are commonly 3 cm. Consists of 8- to 15-cm-thick deposit in hanging-wall block, tentatively interpreted as a debris flow (see description of unit **ag** for trench WLS–1). In footwall block, a pod of unit **ag** is present at margin of paleochannel filled with eolian sand. Thickness is at least 40 cm; base is covered.

Angular gravel and ferricrete gravel (unit **ag+fcg**). Mixture of units **ag** and **fcg** (angular to subrounded fragments of quartzite). Quartzite fragments make up about 5–10 percent of the unit (see description of unit **ag** above and unit **fcg** below). Fragments have maximum size of about 8 cm, are commonly 3 cm, and are coarse grained with FeO (hematite and greenish-white iron oxide) along fractures. Fragments are clearly exotic to the trench and must have been transported in order to be incorporated into this unit.

Hanging-wall block (described at 1.6-m mark on trench map, pl. 2*C*). Geometry and restricted distribution of deposit above network of fractures (that are probably contiguous with zone of open fissures 15 m to the east) implies that unit could fill an ancient graben, which was subsequently buried by debris flow (unit **ag**). Upper contact is sharp and regular, lower contact is sharp and irregular. Thickness is 25–30 cm.

Footwall block (sample WLS2–1d, table 6). Contains mixture of sandy pebble gravel (units **esr** and **fcg**) and angular gravel (unit **ag**), estimated to contain 75 percent gravel and 25 percent sand overall. Matrix consists

Table 6. Particle-size data for samples from western Lake Surprise trench 2 (WLS–2)

[Sand content determined by wet sieving; silt and clay contents determined by pipette method. Iron oxides were removed with 5 percent oxalic acid heated to boiling for 2–3 hours. If present, carbonates were removed with 10 percent HCl, and organic matter was removed with sodium hypochlorite adjusted to a pH of 9.5. (+), at high-clay end of textural field; (-), at low-clay end of textural field]

Sample No.	Sampling depth (cm)	Textural classification	Sand (percent)	Silt (percent)	Clay (percent)
WLS2-1a.....	0-10	Loamy sand(-).....	86.3	5.7	8.0
WLS2-1b.....	22-32	Loamy sand.....	85.2	4.6	10.2
WLS2-1c.....	44-55	Loamy sand(+).....	82.0	6.5	11.4
WLS2-1d.....	80-90	Loamy sand(+).....	82.7	5.6	11.7

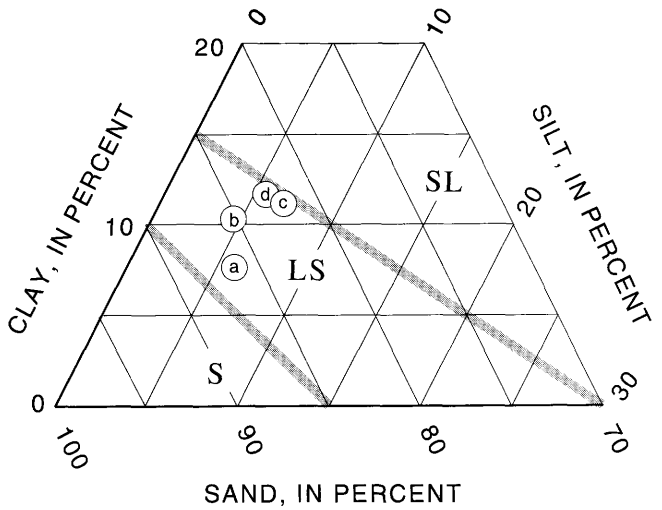

Figure 22. Grain-size data for samples of eolian sand in western Lake Surprise trench 2 (circled letters indicate samples WLS2–1a to –1d, table 6). Textural classes are: S, sand; LS, loamy sand; and SL, sandy loam.

of loose, noncalcareous, loamy sand (+) (fig. 22) having single-grain structure and clay films as in eolian sand units above. Gravel fraction is about 55 percent granules (2–4 mm) and 45 percent pebbles (less than 5 mm). Granules are 80–90 percent ferricrete nodules; pebbles are 75 percent ferricrete nodules (0.8–1.5 cm in diameter) and 25 percent angular lithic fragments having a maximum size of 2–3 cm. Color of less than 2-mm fraction is red (2.5*YR* 4/7 d to slightly redder than 2.5*YR* 3.5/6 m). Unit interfingers with unit **ag** and contains small, isolated lenses of mainly unit **ag**. Grades into unit **ag** towards fault and thus is probably composed, in part, of colluvium shed from ancient fault or fluvial scarp. Contains two stone lines (most conspicuous between 10–12 m on trench map, pl. 2*C*) composed of angular iron-rich quartzite clasts (unit **ag**), one to two stones thick. Clasts are commonly 2–3 cm in size with maximum of 6–8 cm. Upper contact is gradual and regular. Thickness is at least 25–40 cm; base is covered.

Ferricrete gravel (unit **fcg**). Clast-supported gravel-size subangular to subrounded ferricrete nodules. Common size is 0.5–1.5 cm, maximum size is 2–3 cm but may be cemented into clusters as large as 10 cm. Matrix is red (2.5*YR* 4/6 d) medium- to coarse-grained sand derived from unit **es**. Nonstratified, massive, and noncalcareous; abundant root hairs within upper 50 cm. Upper contact is gradual over 10-cm-wide zone, base is sharp but wavy. Thickness is commonly 15–30 cm, locally 60–120 cm where faulted.

Ferricrete (unit **fcm**). Breccia of angular blocky fragments cemented by FeO and MnO. Blocks typically have a core of red FeO surrounded by a rim of black MnO and an outer rind of red FeO; boundary between MnO and outer rind is irregular. Matrix varies from FeO-rich clay to a FeO-rich loose sand (from above). In some places, unit is less blocky and more vuggy, as if it is an accreted (cemented) phase of unit **fcg**. Upper contact is gradual and wavy. Present as 50-cm-thick blocks between shear zones and faults in hanging-wall block, and 10- to 15-cm-thick mantle over unit **rf** in footwall block. Thickness is unknown; base is covered.

Quartzite, fractured (unit **rq(f)**). Hematitic quartzite, massive but pervasively jointed and fractured, which produces a network of rectangular blocks 5–10 cm in size. Major fractures dip about 75° N. and contain red and specular hematite along open and healed joints; some surfaces have coating of reduced iron (as limonite and goethite?). Unit moderately altered but breaks into orthogonal blocks; fracture surfaces not completely filled by iron oxides. Contacts are typically fault bounded. Thickness is at least 2 m in main fault zone; base is covered.

Highly altered iron-rich bedrock (unit **rf**). Large (3 cm to as much as 20 cm in maximum dimension) angular blocks of unidentifiable bedrock that are composed of soft hematitic rock (perhaps containing abundant clay) with minor amounts of quartz. Blocks are moderately porous and fractured, and contain less quartz matrix than units **fcg** or **fcm**. Manganese oxide is present as vein and fracture filling, usually less than 1 mm wide. Contains about 5 percent angular to subrounded quartz of coarse- to very coarse-sand size. Blocks become similar to unit **fcg** upward with less rock fragments, more rounded

fragments that have rinds, and more iron-rich sand in the matrix. At the base, unit rf is more competent but still highly altered. Thickness is at least 1.5 m; base is covered.

KUNAYUNGKU TRENCH (KS)

Eolian sand (unit es, pl. 2*D*). Well sorted, nonstratified, fine- to coarse-grained sand, subangular to subrounded. Although no lithologic or textural divisions were made in this unit, horizons were differentiated for sampling and analysis of soil development. All boundaries are gradual and regular. Thickness is 110–125 cm on axis of fold to as much as 150 cm in footwall block (north side).

1. A/B horizon (sample KS–1a, table 7). Ochric A horizon (surface accumulation of humified organic matter mixed with mineral fraction, which is predominant) in upper part. Organic matter is typically 0.5–1.0 weight percent and is accompanied by slight darkening (increased color value), root hairs, and weak platy structure compared to underlying Bw horizon. Consists of a loamy sand (+) (fig. 23) containing a trace of 2–5-mm size granules (mostly 2–3 mm). Reddish brown (5*YR* 3.5/4 d, 2.5*YR* 3/4 m), very slightly plastic, very slightly sticky. Structure changes from weak, moderate, subangular blocky in upper part to weak, fine, subangular blocky downward (B horizon); noncalcareous. Few thin clay films on grains and weak iron cementation. Surface is characterized by abundant termite burrows and bioturbation. Depth 0–5 cm.
2. B/A horizon (sample KS–1b, table 7). Transitional horizon between A and Bw horizons. Consists of a loamy sand (+) (fig. 23) having a median grain size of medium to coarse sand, 1 percent granules (mainly 2–3-mm rock fragments). Dark red (2.5*YR* 3–6 d; 2.5*YR* 2.5/4 m), very slightly plastic, very slightly sticky; noncalcareous, weakly cemented by FeO. Structure is moderate, coarse, subangular blocky to moderate, medium, subangular blocky. Few thin clay films; mainly FeO on grains. Upper part contains abundant burrows and root holes filled with red sand. Depth 5–18 cm.
3. Bw horizon (sample KS–1c, table 7). Cambic B horizon has illuvial (downward-moving) accumulation of amorphous iron oxide and organic-matter complexes; both color value and chroma are greater than 3 on the Munsell Color Chart (Munsell Color Co., Inc., 1954). Consists of a loamy sand to sandy loam (fig. 23) having a trace (less than 1 percent) of gravel (angular quartz and rock fragments, all 2–3 mm in size). Red to dark red (2.5*YR* 4/6 d; 2.5*YR* 3/5 m), very slightly plastic, very slightly sticky; noncalcareous. Structure is medium, moderate, subangular blocky to medium, fine, subangular blocky. Few thin clay and silt coatings, grains mainly coated by FeO. Depth 18–40 cm.
4. Bt1 horizon (sample KS–1d, table 7). Argillic B horizon has an accumulation of silicate clay (and iron oxide) that either forms in place or is illuvial; hence, it contains more clay-size material than assumed parent material (C horizon) or overlying A horizon. Bt1 horizon is the upper, less well developed part of the thick Bt in unit es. Consists of a sandy loam (-) to sandy loam (fig. 23) containing 10–20 percent nodules (iron-cemented sand) 1.5–3 cm in diameter. Red to dark red (2.5*YR* 4/8 d; 2.5*YR* 3.5/6 m), slightly plastic, slightly sticky; noncalcareous. Structure is medium, moderate, subangular blocky to medium, fine, subangular blocky. Clay films are common and thin on pores and grains; few thin clay films on peds. Depth 40–70 cm.
5. Bt2 horizon (sample KS–1e and -1f, table 7). Bt2 horizon is the lower, better developed part of the thick Bt in unit es. Consists of a sandy loam (fig. 23) having less than 1 percent of 5-mm-size gravel (easily passed through 2-mm screen). Gravel, which increases to about 3 percent at base of horizon, is composed of immature ferricrete nodules (one-third 5–10 mm size, two-thirds 2–5 mm size), angular quartz, and lithic fragments. Red (2.5*YR* 4/8 d; 1*YR* 4/8 m); slightly plastic to plastic, slightly sticky to sticky; slightly more clay than Bt1 horizon. Structure is weak, medium, subangular blocky to moderate, fine, subangular blocky in upper part and strong, medium, angular blocky to strong, fine, angular blocky in lower part. Soil is noncalcareous in upper part to slightly effervescent in lower part, but carbonate is not obvious as a secondary accumulation. Clay films are few and thin on grains, common and thin to medium on pores, not obvious on peds. Lower contact is sharp to gradational (over 5–10 cm interval). Depth 70–120 cm (base of unit es).

Massive ferricrete (unit fcm). Rounded to subrounded nodular ferricrete, nodules commonly 0.5–2 cm in size. Upper half of unit consists of ferricrete nodules in matrix of medium to coarse red sand (similar to unit es). Downward, sand content (as expressed by color of the ferricrete) decreases, and the nodules are surrounded by a matrix of clay that is probably derived from the underlying bedrock (unit ra). Lower half of unit has mottled colors (10*R* red colors, drab ochre, and black MnO staining). Nodules in lower half of unit are typically 2–6 mm in size, which is finer grained than upper half; contains sparse rounded quartz grains, 10–15 mm in size. Lower contact is sharp (1–2 cm) to gradational. Thickness is 30–75 cm.

Altered bedrock (unit ra). Claystone, massive but jointed, breaks into 2–3 cm size angular prisms having thick clay films on faces. Slickensides and grooved surfaces on many prism faces are evidence of differential movement between blocks. Claystone contains 5–10 percent residual, medium-coarse grained, subangular to rounded quartz sand. Drab light gray green but mottled with yellowish-orange and black (MnO) stains. Contains sparse light-gray to white, 3- to 8-mm-diameter, rounded carbonate nodules that are porous and vuggy, massive to laminated, and stained with FeO and MnO. Noncalcareous except nodules. Thickness is at least 50 cm; base is covered.

Table 7. Particle-size data for samples from Kunayungku trench (KS)

[Sand content determined by wet sieving; silt and clay contents determined by pipette method. Iron oxides were removed with 5 percent oxalic acid heated to boiling for 2–3 hours. If present, carbonates were removed with 10 percent HCl, and organic matter was removed with sodium hypochlorite adjusted to a pH of 9.5. (+), at high-clay end of textural field; (-), at low-clay end of textural field]

Sample No.	Sampling depth (cm)	Textural classification	Sand (percent)	Silt (percent)	Clay (percent)
KS-1a.....	0-5	Loamy sand(+)	83.2	4.8	11.9
KS-1b.....	5-15	Loamy sand(+)	82.1	8.5	9.4
KS-1c.....	20-30	Loamy sand/sandy loam...	80.9	8.7	10.5
KS-1d.....	50-60	Sandy loam(-).....	78.6	9.6	11.8
KS-1e.....	80-90	Sandy loam.....	76.6	10.9	12.5
KS-1f.....	105-115	Sandy loam.....	77.7	11.4	14.0

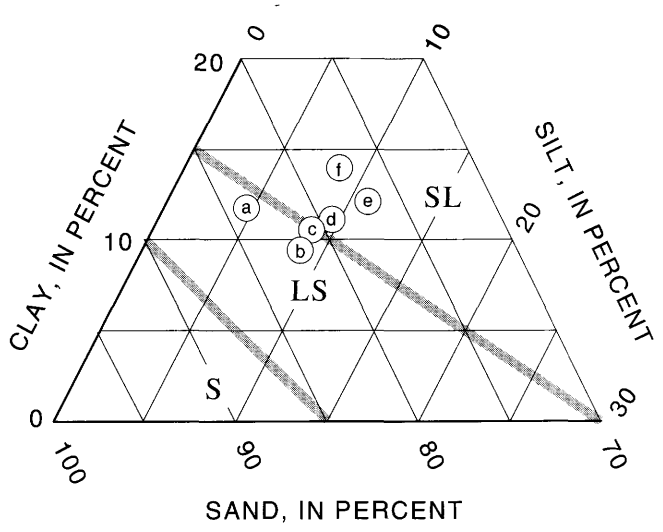

Figure 23. Grain-size data for samples of eolian sand in the Kunayungku trench (circled letters indicate samples KS–1a to -1f, table 7). Textural classes are: S, sand; LS, loamy sand; and SL, sandy loam.

Table 8. Data for samples collected in the Tennant Creek area trenches

[Geologic units are shown on pl. 2. Horizontal and vertical locations are from center of sampling hole or channel shown on pl. 2. Type of analysis: GS, grain size; ESR, electron-spin resonance; TL, thermoluminescence; U-trend and U-series, uranium isotope analyses; ^{14}C (AMS), accelerator mass spectrometry analysis of radiocarbon sample; Chemistry, chemical analysis for ESR age determination. ESR analyses by Kazuhiro Tanaka, Central Research Institute for Electric Power Industry, Abiko City, Japan; TL analyses by J.R. Prescott, University of Adelaide, Adelaide, Australia; uranium isotope analyses by D. R. Muhs, U.S. Geological Survey, Denver, Colo.; ^{14}C determination by Geochron Laboratories, Cambridge, Mass.]

Reference symbol	Field No.	Geologic unit	Horizontal axis (m)	Vertical axis (m)	Type of analysis
Eastern Lake Surprise trench (ELS), hanging wall (south end)					
A	ELS/10	es (soil)	3.1	4.0	ESR
B	ELS-5a	es (soil)	6.5	3.9	U-trend
	ELS/7	es (soil)	6.4	3.9	ESR
C	ELS-5b	es	6.5	3.6	U-trend
	ELS/6	es	6.4	3.6	ESR
	TC2S/65	es	6.5	3.6	TL
D	ELS-5c	es	6.5	3.2	U-trend
	ELS/5	es	6.4	3.2	ESR
E	ELS/9	es	3.3	2.8	ESR
F	ELS-5d	es	6.5	2.7	U-trend
	ELS/4	es	6.3	2.7	ESR
	TC2S/1.45	es	6.5	2.7	TL
G	ELS-5e	es	6.5	2.4	U-trend
	ELS/3	es	6.2	2.4	ESR
	TC2S/1.85	es	6.5	2.4	TL
H	ELS-5f	es	6.5	1.9	U-trend
	ELS/2	es	6.2	1.9	ESR
	TC2S/2.25	es	6.5	1.9	TL
I	ELS-5g	es	6.5	1.7	U-trend
	ELS/1	es	6.2	1.7	ESR
	TC2S/2.5a	es	6.5	1.7	TL
Eastern Lake Surprise trench (ELS), footwall (north end)					
J	ELS-4a	es (soil)	19.8	3.1	GS
K	ELS-4b	es (soil)	19.8	3.0	GS
L	ELS-4c	es (soil)	19.8	2.8	GS
M	ELS-4d	es	19.8	2.4	GS
N	ELS-4e	es	19.8	2.0	GS
O	ELS/8	es (fault zone)	15.8	2.6	ESR
P	ELS-4f	es	16.0	1.7	GS
Q	ELS-4g	es	16.0	1.2	GS
	TC2S/2.5b	es	16.0	1.2	TL
R	ELS-4h	es	17.2	.8	GS
S	ELS/11	es (fault zone)	15.2	2.2	ESR
T	ELS-6a	fcg	15.0	.7	U-series
U	ELS-6b	fcm	13.8	.8	U-series
V	ELS-6c	fca	13.7	.3	U-series
Labeled on pl. 2*A*	ELS-2	es	17.2	1.2	^{14}C (AMS)
Labeled on pl. 2*A*	ELS-3	es	17.7	1.2	^{14}C (AMS)

Table 8. Data for samples collected in the Tennant Creek area trenches—Continued

Western Lake Surprise trench 1 (WLS-1), footwall (south end)					
A	WLS1-1a	es (soil)	6.8	2.6	GS
B	WLS1-1b	es	6.8	2.4	GS
C	WLS1/4	es	6.5	2.1	ESR
	WLS1-1c	es	6.8	2.1	GS
D	WLS1/3	es	6.6	1.7	ESR
	WLS1-1d	es	6.8	1.7	GS
E	TC3S/90	es	6.2	1.6	TL
F	WLS1/2	es	6.6	1.2	ESR
	WLS1-1e	es	6.8	1.2	GS
G	TC3S/1.7	esr	6.5	.7	TL
	WLS1/1	esr	6.8	.6	ESR
	WLS1-1f	esr	6.8	.6	GS
H	WLS1/6	esr	9.1	.8	ESR
I	WLS1/5	esr+fcgr	5.7	.3	ESR
J	WLS1/7	Shear zone in hanging wall (fcgr).	14.9	1.5	ESR
Western Lake Surprise trench 2 (WLS-2), footwall (south end)					
A	WLS2-1a	es (soil)	10.8	2.1	GS
B	WLS2/13	esm	8.8	2.0	ESR
C	WLS2-1b	esm	10.8	1.9	GS
	WLS2/10	esm	11.2	1.8	ESR
D	WLS2-1c	esr	10.8	1.7	GS
	TC4S/50	esr	11.2	1.7	TL
	WLS2/9	esr	11.2	1.7	ESR
E	WLS2/12	esr	9.0	1.7	ESR
F	WLS2-1d	ag+fcg	10.8	1.3	GS
G	WLS2/8	ag+fcg	11.4	1.2	ESR
Western Lake Surprise trench 2 (WLS-2), hanging wall (north end)					
H	WLS2/6	es	3.2	2.8	ESR
I	WLS2/7	rf	2.1	1.9	ESR
J	WLS2/4	Pre-1988 gouge (rq(f)).	4.0	1.0	ESR
K	WLS2/11	rq(f)	4.1	.9	Chemistry
L	WLS2/1,2,3	Pre-1988 gouge (rq(f)).	4.2	.8	ESR
M	WLS2/5	1988 fault zone	4.9	.9	ESR

Table 8. Data for samples collected in the Tennant Creek area trenches—Continued

Kunayungku trench (KS), hanging wall (south end)					
A	KS-1a	es (A/B)	18.3	4.1	GS
B	KS-1b	es (B/A)	18.3	4.0	GS
C	KS-1c	es (Bs)	18.3	3.9	GS
	TC1S/20	es (Bs)	18.3	3.9	TL
	KS/4	es (Bs)	18.3	3.9	ESR
D	KS-1d	es (Bt1)	18.3	3.6	GS
	TC1S/45	es (Bt1)	18.3	3.6	TL
	KS/2	es (Bt1)	18.3	3.6	ESR
E	KS-1e	es (Bt2)	18.3	3.3	GS
	TC1S/80	es (Bt2)	18.3	3.3	TL
	KS/3	es (Bt2)	18.3	3.3	ESR
F	KS-1f	es (Bt2)	18.3	3.0	GS
	TC1S/1.1	es (Bt2)	18.3	3.0	TL
	KS/1	es (Bt2)	18.3	3.0	ESR
G	KS/5	Fault gouge	14.3	1.7	ESR

Table 9. Thermoluminescense and preliminary electron-spin-resonance age estimates for eolian sand in the Tennant Creek area trenches

[Thermoluminescence (TL) analyses by J.R. Prescott, University of Adelaide, Adelaide, Australia. Error limits for equivalent dose are ±6.5 percent, except Ad TL91003, which is ±7.3 percent. Error limits for dose rate are about 5 percent. Error limits for ages are ±1 standard deviation and are based on water contents of 2 percent as determined from samples. Electron-spin-resonance (ESR) analyses by Kazuhiro Tanaka, Central Research Institute for Electric Power Industry, Abiko City, Japan. Age estimates are those reported as of Dec. 31, 1991. No error limits were assigned to the ESR analyses. Sample localities given in table 8]

Laboratory designation (type of analysis)	Field sample designation (depth in cm)	Equivalent dose (Gy)	Dose rate (Gy/ka)	Age and error limits (1,000 yr)
Eastern Lake Surprise trench (ELS)				
Ad TL91001(TL).....	TC2S/65 (65).....	18.3	1.42	13±1
Ad TL91011(TL).....	TC2S/1.45 (145).....	67	1.48	45±3.4
Ad TL91006R(TL).....	TC2S/1.85 (185).....	77	1.54	50±4
Ad TL91012(TL).....	TC2S/2.25 (225).....	111	1.57	71±5.4
Ad TL91002R(TL).....	TC2S/2.5a (250).....	86	1.66	52±4
Ad TL91003R(TL).....	TC2S/2.5b (250).....	64	1.48	43±3
Western Lake Surprise trench 1 (WLS-1)				
Ad TL91008(TL).....	TC3S/90 (90).....	28.5	1.44	20±1.5
Ad TL91013(TL).....	TC3S/1.7 (190).....	73	1.59	46±3.5
Western Lake Surprise trench 2 (WLS-2)				
Ad TL91007(TL).....	TC4S/50 (50).....	17.1	1.70	10±0.8
Kunayungku trench				
Ad TL91004(TL).....	TC1S/20 (20).....	9.5	1.45	6.6±0.5
KS/4(ESR).....	KS/4 (20).....	24	2.483	9.7
Ad TL91010(TL).....	TC1S/45 (45).....	15.6	1.46	10.7±0.8
KS/2(ESR).....	KS/2 (45).....	65	2.483	26.2
Ad TL91009(TL).....	TC1S/80 (80).....	35	1.51	23.0±2.2
KS/3(ESR).....	KS/3 (80).....	100	2.483	40.3
Ad TL91005(TL).....	TC1S/1.1 (110).....	44	1.46	30±2.3
KS/1(ESR).....	KS/1 (110).....	121	2.483	48.9

Published in the Central Region, Denver, Colorado
Manuscript approved for publication April 23, 1992
Edited by Barbara Hillier
Graphics by the authors, Anthony J. Crone and Michael N. Machette
Type composed by Shelly A. Fields

☆U.S. GOVERNMENT PRINTING OFFICE: 1992-774-049/66018